

STUDIES ON VIBRATION AND ACOUSTIC RESPONSE CHARACTERISTICS OF SANDWICH AEROSPACE STRUCTURES

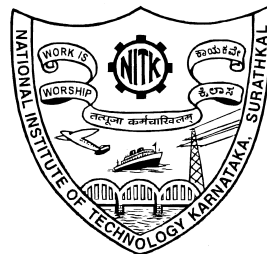
Thesis

Submitted in partial fulfillment of the requirements for the degree of

DOCTOR OF PHILOSOPHY

by

M. P. ARUNKUMAR



**DEPARTMENT OF MECHANICAL ENGINEERING
NATIONAL INSTITUTE OF TECHNOLOGY KARNATAKA
SURATHKAL, MANGALORE - 575025, INDIA**

May, 2018

DECLARATION

I hereby *declare* that the Research Thesis entitled **STUDIES ON VIBRATION AND ACOUSTIC RESPONSE CHARACTERISTICS OF SANDWICH AEROSPACE STRUCTURES** which is being submitted to the *National Institute of Technology Karnataka, Surathkal* in partial fulfillment of the requirements for the award of the Degree of *Doctor of Philosophy* is a *bonafide report of the research work carried out by me*. The material contained in this Thesis has not been submitted to any University or Institution for the award of any degree.

M. P. Arunkumar
Register No.: 138041
Dept. of Mechanical Engg.

Place: NITK - Surathkal

Date:

CERTIFICATE

This is to *certify* that the Research Thesis entitled **STUDIES ON VIBRATION AND ACOUSTIC RESPONSE CHARACTERISTICS OF SANDWICH AEROSPACE STRUCTURES**, submitted by **M. P. Arunkumar** (Register Number: 138041) as the record of the research work carried out by him, is *accepted* as the *Research Thesis submission* in partial fulfillment of the requirements for the award of degree of *Doctor of Philosophy*.

Dr. P. Jeyaraj
Research Guide
Assistant Professor
Dept. of Mechanical Engg.
NITK Surathkal - 575025

Dr. K. V. Gangadharan
Research Guide
Professor
Dept. of Mechanical Engg.
NITK Surathkal - 575025

Chairman - DRPC
(Signature with Date and Seal)

ACKNOWLEDGEMENTS

It is my great pleasure to express my heartfelt gratitude to my research supervisor Dr. P. Jeyaraj, Assistant Professor, Department of Mechanical Engineering, National Institute of Technology Karnataka, Surathkal, Mangalore, for his exemplary guidance and encouragement throughout my research work. Working under him has had a profound effect not only on how research should be carried out at its best, but also on how to develop humbleness and kindness towards students. Without his support and suggestions, achieving this goal would not have been possible.

It is my great pleasure to express my heartfelt gratitude to my research supervisor Prof. K. V. Gangadharan, Professor, Department of Mechanical Engineering, National Institute of Technology Karnataka, Surathkal, Mangalore, for his exemplary guidance and encouragement throughout my research work. Many a times he has guided me on tough terrains with his ever lasting enthusiasm and his charismatic smile. Also I sincerely thank him for providing me an opportunity to work in centre for system design, SOLVE lab, where I have exposed to many real time vibration problems, which helped me to understand the basics.

I sincerely thanks to the RPAC members, Dr. S. M. Murigendrappa, Department of Mechanical Engineering and Dr. A. S. Balu, Department of Civil Engineering for providing valuable suggestion and support extended to me on all occasion.

I wish to express my sincere thanks to Prof. S. Narendranath, Head of the Department, Department of Mechanical Engineering, National Institute of Technology Karnataka, Surathkal, Mangalore for their kind help in providing the facilities.

I wish to express my sincere thanks to Dr. M C Leninbabu, Department of Mechanical Engineering, Vellore university, Chennai campus, for sharing his knowledge, which greatly helped me to carry out my research work.

I wish to express my sincere thanks to Prof. Baburaj, Head of the Department, Department of Mechanical Engineering, Karpagam university, Coimbatore, for his kind support to join as a research scholar in NITK.

I wish to express my sincere thanks to my friend Kirubanidhi jebabalan, Research scholar, Coimbatore Institute of Technology, Coimbatore, for his selfless advice and support to join as a research scholar in NITK.

I would like to thank my friends K. Prasath, G. P. Arunbabu, Nelson, Balakumar, Anbu, A. P. Arunkumar, Bala krishnan, M. Karthikeyan, Hariganesh in Karpagam

Universtiy for their encouragement to carry out the research. I would like to thank my friends Rajasekhara Reddy, Sushil kumar, Praveen shenoy, Niruba, Jagadheesh, Jyothi, Swathi, Resson weldergis, Royson, Arun P parameswaran, Umanath, Harsha, Adhithya, Rohith Rajpal, Shushanth, Rajesh, Vinod Bhagath, Nevis George, Sunil, Madhusudhan, Murali, Vinay, Bharath, Sarath, Vibin, Veereshnayak, Venkatesh, Rahul, Neelesh, Rajees, Subashankar, Praveen in NITK for giving me sweetfull memories in NITK.

I would like to immensely thank my brother M. P. Vinoth kumar for his explanation towards various engineering problems, which is not found in most of the books. His teaching helped me in many ways to complete this work. I would like to thank my sister M. P. Vasantha priya for her underlying love, and support throughout my life. I would like to thank my wife S. Swetha for her encouragement during the downhearted time in research and her prayer to Almighty God to achieve this goal.

I would like to thank God for giving me the strength, knowledge, ability and opportunity to undertake this research study and to persevere and complete it satisfactorily.

Last but not least, I would like to thank my father M. Prabakaran and mother M. Chandra, for their massive love and support throughout my life. Without them, achieving this goal would not have been possible.

(M. P. Arunkumar)

ABSTRACT

Numerical investigation carried out on vibration and acoustic response characteristics of structures used in aerospace application is presented. Sandwich panels are used as structural members in aircraft due to their high stiffness to weight ratio. Vibro acoustic characteristics of sandwich panels with honeycomb, truss and foam filled truss core are analysed in this work. Equivalent 2D finite element model is used to obtain the free and forced vibration response of sandwich panels using commercial finite element solver ANSYS. Further, vibration response of the sandwich panel is given as an input to the Rayleigh integral code built-in-house using MATLAB to obtain the acoustic response characteristics. Initially, influence of important geometrical parameters on vibration and acoustic response characteristics of sandwich panels which are typically used as aerospace structures are investigated. Different types of sandwich panels analysed are (a) Honeycomb core (b) Truss and Z core and (c) Foam core. It is found that for a honeycomb core sandwich panel in due consideration to space constraint, the better acoustic comfort can be achieved by reducing the core height and increasing the face sheet thickness. It is also observed that, triangular core gives better acoustic comfort for the truss core sandwich panel compared to other types of core. Further, a sandwich panel with fibre reinforced plastic (FRP) facing and aluminium honeycomb core is investigated to analyse the effect of inherent material damping associated with FRP facing on vibro-acoustic response characteristics. The result reveals that FRP panel has better vibro-acoustic and transmission loss characteristics due to high stiffness and inherent material damping associated with them. It is observed that resonant amplitude of the vibro-acoustic response is significantly controlled by modal damping factors which is calculated based on modal strain energy. It is also demonstrated that FRP facing can

be used to replace the aluminium panel without losing acoustic comfort with nearly 40 % weight reduction. Effect of foam filling in empty space of the truss core sandwich panel on sound radiation and transmission loss (STL) characteristic is also studied. Results revealed that polyurethane foam (PUF) filling in empty space of the truss core, significantly reduces resonant amplitudes of both vibration and acoustic responses. It is also observed that foam filling reduces the overall sound power level by about 12 dB. Similarly, sound transmission loss studies revealed that, at resonance frequencies nearly 20 dB is reduced. In order to validate the accuracy of results, free and forced vibration response of a honeycomb core sandwich panel made of aluminium is obtained experimentally. The experimental results are compared with the proposed numerical results. From the results, it is observed that numerical and experimental results are in good agreement.

KEYWORDS: Honeycomb, truss and, foam core, Equivalent 2D finite element model, Rayleigh integral, Vibration and acoustic response, Sound transmission loss.

TABLE OF CONTENTS

ACKNOWLEDGEMENTS	ii
ABSTRACT	iv
LIST OF TABLES	xi
LIST OF FIGURES	xv
1 INTRODUCTION	1
1.1 Introduction	1
1.2 Literature Review	3
1.2.1 Equivalent Stiffness Properties of Sandwich Panels	3
1.2.2 Vibration Response of Sandwich Panel	7
1.2.3 Acoustic Response of Sandwich Panels	11
1.3 Closure	16
1.4 Research objectives	17
2 METHODOLOGY AND VALIDATION STUDIES	19
2.1 Introduction	19
2.2 Methodology for Numerical Studies	19
2.3 Validation Studies	24
2.3.1 Experimental Validation	25
2.3.2 Validation for Element Type SHELL 181	28
2.3.3 Validation of Free Vibration of Truss Core Sandwich Panel Nu- merical Results	31
2.3.4 Validation of Sound Transmission Loss Numerical Results .	34

2.3.5	Validation for Sound Power level Evaluation	36
2.4	Closure	37
3	STUDIES ON HONEYCOMB CORE SANDWICH PANEL	38
3.1	Introduction	38
3.1.1	The Effect of Face Sheet Thickness	39
3.1.2	The Effect of Core Height	41
3.1.3	The Effect of Cell Size	46
3.2	Closure	57
4	STUDIES ON HONEYCOMB CORE SANDWICH PANEL WITH FRP FACINGS	58
4.1	Introduction	58
4.2	Validation of Modal Damping Ratio	60
4.3	The effect of Stiffness	61
4.3.1	The Influence of Fibre Orientation	62
4.3.2	The Influence of Boundary condition	64
4.4	The effect of Inherent Material Damping	72
4.5	Closure	76
5	STUDIES ON TRUSS CORE SANDWICH PANEL	78
5.1	Introduction	78
5.1.1	Equivalent Elastic Properties for Triangular, Trapezoid, Cellular and Z Core Sandwich Panel	79
5.1.2	Vibration Response Characteristics	80
5.1.3	Acoustic Response Characteristics	81
5.2	Closure	86
6	STUDIES ON FOAM FILLED TRUSS CORE SANDWICH PANEL	88
6.1	Introduction	88

6.2	Formulation of Stiffness Properties for Foam Filled Truss Core Sandwich Panel	88
6.2.1	Bending Stiffnesses D_x and D_y	93
6.2.2	Evaluation of Transverse Shear Stiffness (D_{Qx} and D_{Qy})	96
6.3	Validation for 2D Equivalent Model of Foam Filled Truss Core Sandwich Panel	98
6.4	The effect of Filling Foam on Free Vibration Behavior of Truss Core Sandwich Panel	101
6.5	The effect of Filling Foam on Vibro-Acoustic Response and Transmission Loss Characteristics	103
6.6	Closure	112
7	SUMMARY AND CONCLUSIONS	114
7.1	Summary	114
7.2	Conclusions	115
7.2.1	The Effect of Geometrical Parameters of Honeycomb Core Sandwich Panel	115
7.2.2	The Effect of Inherent Material Damping of Honeycomb Core Sandwich Panel with Composite Facings	115
7.2.3	The Effect of Core Topology of Truss Core Sandwich Panel	116
7.2.4	The Effect of Filling Polyurethane Foam in Truss Core Sandwich Panel	116
7.3	Scope for Future Research	117

LIST OF TABLES

2.1	Comparison of experimental results with numerical results for free vibration frequencies	28
2.2	Comparison of non-dimensional natural frequencies $\bar{\omega}_n$ with zigzag theory and 3D exact solution	30
2.3	Validation of free vibration results with Lok and Cheng (2000a)	34
2.4	Mode shape validation of equivalent 2D FEM model with 3D FEM model	35
3.1	The effect of face sheet thickness on natural frequency (Hz) for honeycomb core sandwich panel	41
3.2	The effect of core height on natural frequency (Hz) for honeycomb sandwich panel	46
3.3	The effect of cell size on natural frequency (Hz) for honeycomb core sandwich panel	52
4.1	Damping ratio (ζ) validation with Sudhagar et al. (Sudhagar <i>et al.</i> , 2015) work	61
4.2	Material properties	62
4.3	The influence of fibre orientation of FRP honeycomb core sandwich panel on natural frequency (Hz)	63
4.4	The influence of boundary condition on natural frequency (Hz)	68
4.5	Natural frequency (Hz) and Damping ratio (ζ) of Epoxy/Graphite FRP [(0/90/c/90/0)]	72
4.6	The effect of inherent material damping on over all sound power level	73
5.1	Dimension of zed core, cellular core, trapezoidal core and triangular core in mm	80
5.2	Equivalent properties of zed core, cellular core, trapezoidal core, triangular core	80

5.3	Natural frequency (Hz) comparison of zed core, cellular core, trapezoidal core, triangular core	81
5.4	The influence of nature of core on free vibration mode shapes of the sandwich panel	82
6.1	Comparison of natural frequencies of foam filled truss core sandwich panel predicted by 3D and its equivalent 2D model.	99
6.2	Comparison of free vibration modes predicted by 3D and 2D equivalent finite element models	101
6.3	Dimension of cellular core, trapezoidal core and triangular core in mm	102
6.4	Influence of foam filling on free vibration behavior of truss core sandwich panel	103
6.5	The effect of filling foam on over all sound power level	105

LIST OF FIGURES

1.1	Different types of sandwich panels generally used in aircraft	2
1.2	Application - Aircraft fuselage Sui <i>et al.</i> (2015)	2
2.1	Methodology followed in the present work	24
2.2	(a) Honeycomb core sandwich panel (b) Unit cell (Paik <i>et al.</i> , 1999)	25
2.3	Schematic diagram of experimental set up to obtain natural frequencies and forced vibration response	28
2.4	Experimental set up used for natural frequency evaluation and forced vibration response	29
2.5	Comparison of experimental and numerical forced vibration responses at resonance frequencies (Hz)	29
2.6	Dimension of truss core sandwich panel unit cell (Lok and Cheng, 2000 <i>a</i>)	31
2.7	(a) 3D Finite element model, (b) Equivalent 2D finite element model	32
2.8	Validation of present approach for sound transmission loss results with experimental and numerical result reported by Lee and Kondo (1999) and Assaf and Guerich (2008)	36
2.9	Validation of present work with Li and Li (2008) for sound power calculation	37
3.1	The effect of face sheet thickness on vibration response	41
3.2	The effect of face sheet thickness on sound power level	42
3.3	The effect of face sheet thickness on sound power level in octave band	42
3.4	The effect of face sheet thickness on over all sound power level . . .	43
3.5	The effect of face sheet thickness on over all sound power level at 100 Hz	43
3.6	The effect of face sheet thickness on over all sound power level at 1000 Hz	44

3.7	The effect of face sheet thickness on transmitted sound power level	44
3.8	The effect of face sheet thickness on sound transmission loss of honeycomb core sandwich panel	45
3.9	The effect of core height on vibration response of honeycomb core sandwich panel	47
3.10	The effect of core height on sound power level of honeycomb core sandwich panel	47
3.11	The effect of core height on sound power level in octave band of honeycomb core sandwich panel	48
3.12	The effect of core height on over all sound power level of honeycomb core sandwich panel	48
3.13	The effect of core height on sound pressure level at 100 Hz of honeycomb core sandwich panel	49
3.14	The effect of core height on sound pressure level at 1000 Hz of honeycomb core sandwich panel	49
3.15	The effect of core height on transmitted sound power level of honeycomb core sandwich panel	50
3.16	The effect of core height on sound transmission loss of honeycomb core sandwich panel	50
3.17	The effect of cell size on vibration response of honeycomb core sandwich panel	52
3.18	The effect of cell size on sound power level of honeycomb core sandwich panel	53
3.19	The effect of cell size on sound power level in octave band of honeycomb core sandwich panel	53
3.20	The effect of cell size on over all sound power level of honeycomb core sandwich panel	54
3.21	The effect of cell size on sound pressure level at 100 Hz of honeycomb core sandwich panel	54
3.22	The effect of cell size on sound pressure level at 1000 Hz of honeycomb core sandwich panel	55
3.23	The effect of cell size on transmitted sound power level of honeycomb core sandwich panel	55

3.24	The effect of cell size on sound transmission loss of honeycomb core sandwich panel	56
4.1	The effect of fibre orientation of FRP on average rms velocity	65
4.2	The effect of fibre orientation of FRP on Sound power level	65
4.3	The effect of fibre orientation of FRP on octave band frequency range	66
4.4	The effect of fibre orientation of FRP on sound transmission loss . .	66
4.5	The effect of fibre orientation of FRP on sound pressure level at 100 Hz	67
4.6	The effect of fibre orientation of FRP on sound pressure level at 1000 Hz	67
4.7	The effect of boundary condition on average rms velocity	69
4.8	The effect of boundary condition on sound power level	69
4.9	The effect of boundary condition on octave band frequency range . .	70
4.10	The effect of boundary condition on sound transmission loss	70
4.11	The effect of boundary condition on sound pressure level at 100 Hz	71
4.12	The effect of boundary condition on sound pressure level at 1000 Hz	71
4.13	The effect of inherent material damping on average rms velocity . .	74
4.14	The effect of inherent material damping on Sound power level	74
4.15	The effect of inherent material damping on octave band frequency range	75
4.16	The effect of inherent material damping on sound transmission loss .	75
5.1	(a) Trapezoidal (b) Triangular (c) Cellular (d) Zed core sandwich panel	79
5.2	The effect of core topology of truss and zed core sandwich panel on Sound power level	83
5.3	The effect of core topology of truss and zed core sandwich panel on octave band frequency range	84
5.4	The effect of core topology of truss and zed core sandwich panel on sound pressure level at 100 Hz	84
5.5	The effect of core topology of truss and zed core sandwich panel on sound pressure level at 600 Hz	85
5.6	The effect of core topology of truss and zed core sandwich panel on sound transmission loss	85

6.1	(a) Schematic diagram of foam filled truss core sandwich panel, (b) Dimensions of unit foam filled truss core sandwich panel	91
6.2	Forces and moments acting on an equivalent element of a panel . . .	92
6.3	Forces and moments acting on foam filled truss core unit cell.	94
6.4	(a) Foam filled truss core sandwich panel subjected to transverse shear and (b) Deformation due to transverse shear	97
6.5	(a) 3D Finite element model, (b) Equivalent 2D finite element model	100
6.6	The effect of core topology of truss core sandwich panel with out foam on average rms velocity	105
6.7	The effect of core topology of truss core sandwich panel filled with foam on average rms velocity	106
6.8	The effect of core topology on sound power radiated	106
6.9	The effect of foam filling on sound power radiated of cellular core sandwich panel	107
6.10	The effect of foam filling on sound power radiated of trapezoidal core sandwich panel	107
6.11	The effect of foam filling on sound power radiated of triangular core sandwich panel	108
6.12	The effect of foam filling on sound power radiated in octave frequency bands	108
6.13	(a) Sound Pressure Level at 100 Hz, (b) Sound Pressure Level at 600 Hz	109
6.14	The effect of core topology on STL of truss core sandwich panel . .	110
6.15	The effect of foam filling on STL of cellular core sandwich panel . .	110
6.16	The effect of foam filling on STL of trapezoidal core sandwich panel	111
6.17	The effect of foam filling on STL of triangular core sandwich panel	111

CHAPTER 1

INTRODUCTION

1.1 Introduction

A number of structural components used in the aircraft industries are made up of sandwich panels due to their high strength to weight ratio. Sandwich construction satisfies the essential requirement of an aircraft structural component which is, reduced structural weight without any compromise in the strength of the structure. Sandwich panels consist of stiff top and bottom face sheets separated by a relatively soft core. Sandwich panels made up of aluminium are preferred for aerospace application because of their lower weight. Similarly a light weight, stiff and strong sandwich panel can be obtained by using fibre reinforced plastic (FRP) laminates as stiff face sheet layers. Also the usage of composites could be very much useful in future aircraft structures to build the smart materials (Noor *et al.*, 2000).

Many types of cores have been developed for use in aerospace application. Generally cores are (a) truss or corrugated core, (b) foam or solid core, and (c) honeycomb core as shown in Figure 2.3. Many researchers analysed the effect of nature of core type on mechanical behavior of sandwich panel. It is reported that each core type has its unique benefit. For example, under bending load, honeycomb core sandwich panel deform mainly by shear while truss core sandwich panel deform due to axial and bending deformation of the members.

Figure 1.2 shows some part of an aircraft which use sandwich constructions. Sandwich panels used in aircraft are subjected to harmonic excitations due to inherent unbalance forces which cause noises. Mellert *et al.* (2008) studied the impact of vibration and noise level on health indices of flight attendants. Their study shows that the effect

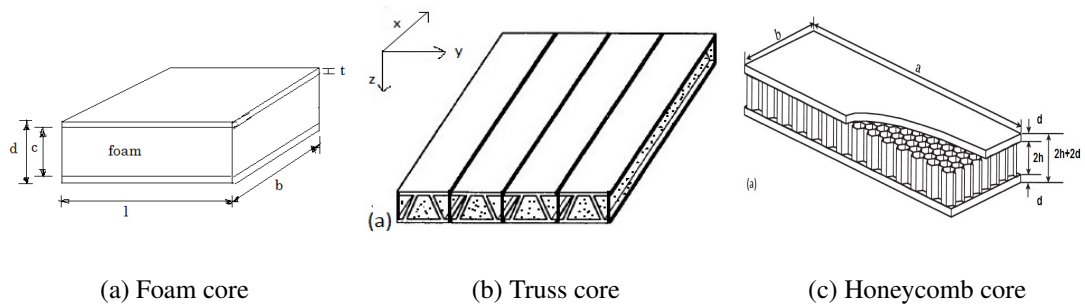


Figure 1.1: Different types of sandwich panels generally used in aircraft

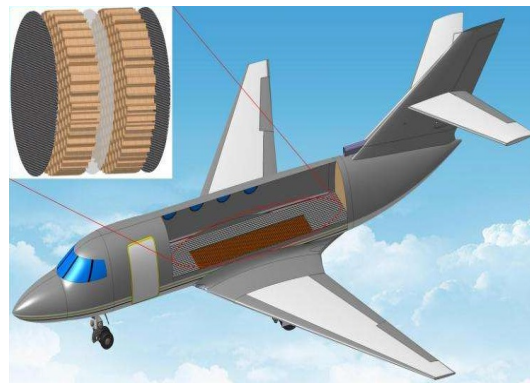


Figure 1.2: Application - Aircraft fuselage Sui *et al.* (2015)

of noise and vibration on the health indices of flight attendants is significant. From Mellert *et al.* (2008) it is clear that, the aircraft structure should not radiate/transmit too much noise. Hence, when a new advanced material is proposed, it is very important to analyse its vibration and acoustic response characteristics. Resonant amplitude of vibration and sound radiation response of a structure can be significantly controlled by damping. Structures made up of FRP composites have better inherent material damping due to the fiber-matrix interaction compared to conventional metallic structures.

The mechanism of sound transmission through the sandwich panel due to the incident pressure wave on the panel is achieved by the normal deflection of the bottom skin. The core transmits this motion to top skin to cause the similar deformation. This deformation of top skin resembles the action of pumping, there by causing sound waves in the fluid medium above the panel (Thamburaj and Sun, 1999). In order to study the

vibration and acoustic behavior of sandwich structure, analytical, numerical and experimental approaches can be used. Experimental study cannot be carried out to investigate the effect of different geometrical parameter variation of the sandwich structure. It would be an expensive and time consuming process. Also, it is quite difficult to obtain the acoustic behavior analytically from the geometrically complex sandwich panels (Cheng *et al.*, 2006). The numerical simulation is thus the only alternative analytical methods. However, simulations from three dimensional (3D) finite element model is a time consuming process and requires high computation effort (Aydincak, 2007). In order to simplify the problem, the actual 3D sandwich structure can be converted to equivalent two dimensional (2D) model by finding its equivalent orthotropic property by comparing it with the orthotropic plate.

1.2 Literature Review

Literature review on homogenisation techniques to obtain the equivalent elastic properties, vibration, sound radiation and sound transmission characteristics of sandwich panels are dealt in detail in the following sections.

1.2.1 Equivalent Stiffness Properties of Sandwich Panels

In general, homogenization theory is used in theoretical and numerical analysis to calculate the elastic properties of corrugated, truss, honeycomb, zed, and foam core sandwich panels equivalent to an orthotropic plate. Then the geometrically complex sandwich panel is converted in to a simple 2D plate with the equivalent elastic properties for the analytical and numerical investigation.

Several studies published on calculating the effective elastic stiffness properties for different types of sandwich panels are grouped in this section.

Libove and Hubka (1951) derived the equivalent properties of corrugated core sandwich panel using force distortion relationship. The derived equivalent properties are applicable for several types of corrugated core, where the unit cell of the sandwich panel

is symmetrical about the vertical plane.

Nordstrand *et al.* (1994) studied the effect of various core shapes of corrugated core on transverse shear property. For this purpose, upper limit of transverse shear across the core is calculated by assuming the facings to be rigid. They validated the accuracy of transverse shear property with 3D finite element model.

Fung *et al.* (1994) presented elastic properties of z-core sandwich panel by comparing the behaviour of a unit z-core sandwich panel with that of a thick plate. They validated their result with the deflection data of 3D finite element model. Similarly, equivalent transverse shear stiffness properties of a honeycomb core sandwich panel is presented by Shi and Tong (1995).

Fung *et al.* (1996) extended their previous work on Z-core sandwich panel to C-core sandwich panel to find the shear stiffness property. The derived equivalent properties of C-core sandwich panel is validated with the deflection result of 3D finite element model.

Samanta and Mukhopadhyay (1999) derived the equivalent properties of folded plates by comparing the folded plate behavior with orthotropic plate. It is extended to find the natural frequency of the folded plate. The accuracy of the result is verified with the 3D finite element results of free vibration.

Lok and Cheng (2000*b*) extended the work of Fung *et al.* (1996) to derive the elastic constants of the truss core sandwich panel. They used the force-distortion relationship to calculate the equivalent elastic properties. The derived elastic properties are validated with the free deflection data of 3D finite element model.

Carlsson *et al.* (2001) derived equivalent elastic properties of corrugated core sandwich panel based on first order shear deformation theory and compared the values with measured data. They showed that in plane extensional stiffness and bending stiffness are dominated by face sheet.

Buannic *et al.* (2003) derived the equivalent properties of corrugated core sandwich

plate based on asymptotic expansion method. Their study is mainly focused on including the effect of transverse shear stiffness in the derivation. The accuracy of the derived properties are verified with the deflection results obtained through the 3D finite element model.

Liew *et al.* (2006) derived the equivalent properties of a corrugated core sandwich plate based on the first order shear deformation theory. The accuracy of the result is verified with the finite element buckling results already reported in the literature.

Ichchou *et al.* (2008) derived the equivalent elastic properties of honeycomb core sandwich panel based on wave number space analysis. The derived properties are validated with the existing analytical and experimental deflection data of sandwich panel with honeycomb core.

Burlayenko and Sadowski (2010) derived the equivalent properties of foam filled honeycomb core sandwich panel. The equivalent properties are obtained using force distortion relationship obtained from the finite element model using commercial finite element solver ABAQUS. The derived equivalent elastic properties are validated with the stress data of 3D finite element model.

Hao *et al.* (2011) studied suitable methods to derive the equivalent properties of honeycomb core sandwich panel. They demonstrated that sandwich plate theory, equivalent plate theory and honeycomb plate theory can be used to derive the equivalent elastic properties of the honeycomb core sandwich panel. Their free vibration result shows that honeycomb plate theory is the most suitable method to derive the equivalent properties of honeycomb core sandwich structure.

Chen and Yang (2011) derived the equivalent properties of a honeycomb core sandwich panel with asymmetrical hexagonal cells based on theoretical and finite element approach. They included the transverse shear to get the accurate stiffness properties.

Xia *et al.* (2012) derived the equivalent properties of corrugated core sandwich panel that can be used for all types of corrugation. They derived the equivalent stiffness

properties from the equivalent energy method by comparing it with the rectangular flat plate.

De Gaetano *et al.* (2013) derived the equivalent properties of honeycomb core sandwich panel from the analytical model considering the governing equation for flexural vibration and torsional vibration. The accuracy of the derived properties are verified with the experimental data of free vibration results existing in the literature.

Bartolozzi *et al.* (2013) derived the equivalent stiffness properties for sinusoidal corrugated structure based on force distortion relationship. The derived properties of corrugated structure are validated with the deflection data of finite element model.

Bartolozzi *et al.* (2014) derived the equivalent properties of corrugated core sandwich structure by considering the corrugation profile in the form of fourier series. The derived stiffness properties based on the equivalent force method is validated with the deflection results of the finite element model.

Ye *et al.* (2014) derived the equivalent properties of corrugated structure based on variational asymptotic method. The derived stiffness properties are valid for both shallow and deep corrugations. The accuracy of the derived stiffness properties are validated with the bending results of the finite element model.

Jiang *et al.* (2014) derived the equivalent properties of honeycomb core sandwich plate based on the experimental modal analysis. They compared their results with the free vibration results obtained based on the numerical models. They showed that the properties derived based on experimental modal data is more accurate.

Malek and Gibson (2015) derived the equivalent elastic properties of periodic hexagonal honeycombs based on both analytical and numerical method. They obtained more accurate results by modifying Ashby and Gibson method.

Sorohan *et al.* (2016) presented the equivalent in-plane properties of honeycombs based on force distortion relationship calculated from the finite element model. The derived properties are compared with the properties derived based on analytical model.

Mukhopadhyay and Adhikari (2016a) derived the effective in plane properties of auxetic honeycombs with spatial irregularity based on bottom line multi scale approach. They compared their results with the existing derived properties based on finite element model.

Qiu *et al.* (2016) reviewed the equivalent elastic properties of flexible honeycomb core by considering the geometric non linearity. The equivalence expressions are improved by including the stretching deformations of the honeycomb structure on an infinitesimal section of a unit cell. They showed that improved analytical expressions gives the closer results in predicting the static and dynamic behavior of flexible honeycomb core.

Mukhopadhyay and Adhikari (2016b) derived the equivalent in-plane elastic stiffness properties of irregular honeycomb core panel with spatially random variations in cell angles. The equivalent modulus obtained for different degree of randomness by proposed analytical method are in very good agreement with the finite element results.

Qiu *et al.* (2017) derived the equivalent elastic properties based on strain energy method. The inaccuracy of the volume-average method in terms of the strain energy is shown by numerical benchmarks.

From the above literature review, it is clear that 2D model with equivalent elastic properties can be successfully used for the numerical investigation to analyse the static and dynamic behavior of the geometrically complex sandwich panel.

1.2.2 Vibration Response of Sandwich Panel

Several research works which are published on free vibration behaviour of different types of sandwich structures are grouped in this section.

Laura and Duran (1975) studied the polynomial approximation and Galerkin approach to predict the vibration characteristics of a thin rectangular plate. Their study shows that a one-term polynomial solution gives accurate results in calculating the vi-

bration responses of a simply supported rectangular plate.

Kanematsu *et al.* (1988) analysed the vibration behaviour of sandwich plates with carbon fibre reinforced polymer based face sheet and an orthotropic core using minimum potential energy and a double fourier series method. Their results associated with the free vibration behavior matches well with the experimental results.

Lee and Fan (1996) analysed a sandwich structure in which the face sheets are modelled with mindlin's plate theory and the displacement fields of the core is linearly interpolated in terms of displacement of the face sheets. Their study shows that natural frequencies decrease when the core is considered as flexible. However, there is no significant change in free vibration mode shapes.

Zhang and Sainsbury (2000) used the Galerkin element method to predict the free vibration response of sandwich plate structures. Their study shows that the use of Galerkin element method to calculate free vibration response over a wide range of frequencies is computationally very efficient.

Lok and Cheng (2000*a*) used the equivalent elastic constants derived in Lok and Cheng (2000*b*) to predict the natural frequencies of truss core sandwich panel. Their results matches well with free vibration data of 3D finite element model.

Lok and Cheng (2001) further used the equivalent elastic properties of truss core sandwich panel derived in Lok and Cheng (2000*b*) to find the natural frequencies for the simply supported boundary condition. Their results match well with the free vibration results of 3D finite element model.

Liu and Zhao (2001) analysed the free vibration behaviour of sandwich panel using thick plate theory by considering the transverse deformation and rotational effect. They compared their results with thin plate theory and showed that thick plate theory is more accurate.

Kant and Swaminathan (2001) used higher order theory to find the natural frequencies of laminated composite sandwich panels. Their study shows very good accuracy

of derived properties by validating with the exact solution.

Nayak *et al.* (2002) used the finite element model based on Reddy's higher order theory to predict the free vibration response of layered composite sandwich panels. Their results match well with the exact solution.

Liu and Zhao (2007) analysed the free vibration behaviour of sandwich panel using low order and high order shear deformation theories. Navier form solution is obtained for a sandwich panel with simply supported boundary condition. A comparison of result showed that higher order theories gives closer results to the 3D finite element results.

Kulkarni and Kapuria (2008) studied the free vibration behavior of sandwich panels with different type of face sheet and soft core using Zigzag theory. Their study shows that natural frequencies predicted using Zigzag theory is in very good agreement with exact solutions.

Wang *et al.* (2008) used the higher order theory to predict the free vibration response of foam core sandwich panel. They found that results for both thin and thick sandwich panel are accurate.

Ghugal and Sayyad (2011) studied the free vibration behaviour of orthotropic thick plate based on trigonometric shear deformation theory. Results obtained for natural frequency is compared and verified with exact solution based on the theory of relativity.

Bilasse *et al.* (2011) studied the nonlinear vibration behaviour of visco elastic sandwich plates based on finite element solution coupled with complex mode Galerkin's approach. They showed that the developed solution can be used for predicting large amplitudes vibrations of visco elastic sandwich plates.

Wennberg *et al.* (2011) studied the free vibration behavior of corrugated core sandwich panel. The equivalent orthotropic plate derived for corrugated core using first order shear deformation theory is used for modal analysis. Their results are in very good agreement with the finite element results.

Boudjemai *et al.* (2012) carried out free vibration study on honeycomb sandwich beam using commercial finite element solver ABACUS. They studied the effect of face sheet and core dimension on natural frequencies and found that natural frequencies increases with the thickness of face sheet and core height.

Li *et al.* (2013) studied the vibration behaviour of composite sandwich plates based on layerwise solid element method. The free vibration results obtained from layer wise theory is in good agreement with 3D finite element model.

Bilasse and Oguamanam (2013) studied the forced vibration behaviour of sandwich structure with visco elastic core based on reduced order model. The response of the reduced model resulting in faster computation and the approach performs well only for low damping scenarios. The higher damping scenarios gives the erroneous results.

Natarajan *et al.* (2014) studied the free vibration characteristic of sandwich plate with carbon nano-tube reinforced face sheets based on higher order structural theory. They developed QUAD-8 shear flexible element based on the higher order theory. Their results are compared and verified with the results reported in literature.

Petrone *et al.* (2014*b*) conducted the experimental modal analysis natural fibre composite core sandwich panels. They found that numerical results are in very good agreement with the experimental data.

Li *et al.* (2016) studied the free vibration behaviour of laminated composite face sheet with two layer honeycomb core using layerwise theory. Their results are in very good agreement with the results of 3D elastic models developed in MSC.Patran/Nastran code.

From the above literature review, it is clear that 2D model with equivalent elastic properties can be successfully used for the numerical investigation to analyse the vibration behavior of the geometrically complex sandwich panel.

1.2.3 Acoustic Response of Sandwich Panels

Several studies published on sound radiation and transmission loss characteristics of different types of structures are grouped in this section.

Kirkup (1994) demonstrated that Rayleigh integral method is the most suitable method to calculate the sound radiation characteristics of flat structural panel like members. He also proved that the Rayleigh integral method is superior to the simple source method as its accuracy is virtually unaffected by the nature of the integrand.

Wen-chao and Chung-fai (1998) investigated the effect of stiffness and damping on noise transmission loss of honey comb core sandwich panels. They have investigated a panel with aluminium face sheet and another panel with fibre reinforced concrete face sheet. Their analytical results shows that the technique of using added-on honeycomb stiffened structure is effective in the noise transmission loss.

Tang *et al.* (1998) investigated the effect of lining the cavity between two panels of a finite double panel structure with porous material on the noise reduction at low frequencies. In their result, it is found that the sound insulation of sandwich panels with air cavities and porous material is more effective than that of the single-layered panel at low frequencies.

Wennhage (2003) optimised the sandwich structure considering mechanical and acoustic constraints. He demonstrated that the design considering the acoustic comfort is heavier than the design considering the mechanical strength.

Ruzzene (2004) analysed the vibration and the sound radiation characteristics of truss core sandwich beams using finite element model. His results indicated that the re-entrant configurations are generally more effective for vibration and sound transmission reduction applications.

Franco *et al.* (2007) studied about the reduction of noise in sandwich structure with honeycomb and truss core by choosing the suitable geometrical parameter.

Van Tooren and Krakkers (2007) analysed the fuselage section of an aircraft which consists of 'Z' and 'C' stiffened sandwich panels. They optimised the stiffened structures for minimum weight subjected to mechanical, acoustical and thermal constraints.

Mellert *et al.* (2008) studied experimentally the impact of sound and vibration on health, travel comfort and performance of flight attendants and pilots. Their results, revealed that noise level has significant effect on various symptoms and health indices, especially when the level increases with time of work.

Daneshjou *et al.* (2008) analysed acoustic behaviour of laminated composite shell based on first order shear deformation theory. They observed that the sound transmission loss calculated from numerical results are in very good agreement with the existing results.

Ng and Hui (2008) presented a new honeycomb core design to improve the noise transmission loss at frequencies between 100 Hz to 200 Hz. A test specimen with fibre reinforced plastic cores and face sheets has been used to investigate the effect of stiffness and damping on noise transmission loss. The measurements of noise transmission loss have been compared with data for common structural panels. Their study shows that the new core fabrication technique uses moulding to improve the noise transmission loss.

Daneshjou *et al.* (2009) studied analytically the transmission loss characteristics of cylindrical shell by applying the damping layer on the surface. They derived the solution by solving the Markus equation and wave equation. Their results are in very good agreement with the results based on modal-impedance method.

Wang *et al.* (2009) performed an optimization study to design a sandwich panel with a balance of acoustical and mechanical properties at minimal weight. In their result, the mass per unit of area of the sandwich panel was minimized by varying the material properties and thickness's of the face sheets and core materials, while meeting the acoustical and mechanical constraints for the sandwich panel.

Wang *et al.* (2010) predicted the sound transmission loss characteristics of sandwich panel using statistical energy method. They observed that their results matches well with the experimental results.

Zhou and Crocker (2010) investigated the sound transmission loss of two different sandwich panels with plane weave fabric reinforced graphite composite face sheets and polyurethane foam filled honey comb core. They have compared the experimental and predicted sound transmission loss values obtained from statistical energy analysis and found that the predicted and experimental transmission loss values of the sandwich panels are in better agreement.

Molla *et al.* (2010) studied the sound transmission loss behaviour of sandwich shells lined with porous materials using statistical energy method. Their results matches well with the results of analytical model only in the higher frequencies because modal density of the sandwich shell is low in lower frequencies.

Jeyaraj *et al.* (2011) studied the acoustic behavior of visco elastic sandwich plate under thermal environment. They showed that sound power level increases with core thickness and number of core and stiff layers.

Daneshjou *et al.* (2011) investigated the STL behavior in a curved cylindrical sandwich panel with porous material as core. In this, the porous layer is modelled as a fluid with equivalent properties. They reported that the results are in very good agreement with the existing results.

Sargianis and Suhr (2012*b*) investigated the effect of a core thickness change on the vibrational properties of Rohacell foam/carbon fibre face sheet sandwich composite beams. They have performed wave number analysis and compared coincidence frequency to investigate acoustic performance. They found that increase in core thickness increases the coincidence frequency.

Sargianis and Suhr (2012*a*) performed wave number analysis and compared the coincidence frequency to investigate acoustic performance. Bamboo with Balsa, cotton

with Rohacell, Carbon fibre with Rohacell, Cotton with pine were used for the analysis. They demonstrated that, by using natural fibre based composite materials, it is possible to create a sandwich beam with superior acoustic performance with minimal sacrifice to stiffness to weight ratio.

Petrone *et al.* (2013) obtained an improvement in damping value by filling the wool fibre in core, there by achieving better acoustic performance in eco-friendly honeycomb core sandwich panels.

D'Alessandro *et al.* (2013) reviewed the acoustics characteristics of sandwich panels. Excessive sound transmitted by these sandwich panels, due to the mechanical excitation is considered as disturbance in the view of acoustic comfort. Since, the sound transmission loss depends on stiffness, damping and mass, a sandwich panel with unique core can not solve all the acoustic problems.

Shojaeefard *et al.* (2014b) studied the transmission loss characteristics of sandwich panel with porous material as core. They have used the biot's theory to extract the wave propagation equation. Their results matches well with the experimental results of sandwich panel.

Chandra *et al.* (2014) studied the vibro acoustic behavior and sound transmission loss of functionally graded plate. They observed, high fluctuation in sound transmission loss in high frequency range for the functionally graded plate.

Shojaeefard *et al.* (2014a) studied the transmission loss behaviour of orthotropic cylindrical shell using third order shear deformation theory. They compared their results obtained using first order shear deformation theory and classical shell theory. They have shown that transmission loss characteristic obtained based on third order shear deformation theory has more accuracy.

Boorle (2014) analyzed the bending, vibration and vibro-acoustic behavior of composite sandwich plates with corrugated core.

Petrone *et al.* (2014a) investigated acoustics power radiated by Aluminium foam sandwich panel. They have investigated influence of nature of Aluminium foam and thickness of core on sound power radiated. They have also validated their numerical results experimentally.

Griese *et al.* (2015) studied the effect of core geometry on sound transmission loss of a honeycomb core sandwich panel. They demonstrated that the shift in natural frequency and associated resonance can be achieved by changing the stiffness in the core without compromising the mass.

Talebitooti *et al.* (2015) studied the sound transmission behavior of orthotropic cylindrical shells. They have used state space method to predict the sound transmission in arbitrarily varying thickness shell. Their results are in very good agreement with the existing for thick shells.

Talebitooti *et al.* (2016a) studied the sound transmission in porous cylindrical shell and double walled cylindrical shells based on biot theory. Their results are matched well with the isotropic shell with good agreement. They also analysed that as shell radius increases, the acoustic behavior is similar to the flat plate.

Talebitooti *et al.* (2016b) studied the sound transmission loss characteristics of composite shell when subjected to an oblique wave. The structural behavior is analysed using third order shear deformation theory. Their results are matches well with the existing experimental results. They also studied the various structural and geometrical properties on sound transmission loss characteristics.

Daneshjou *et al.* (2016) predicted the transmission loss of thick walled shell using 3D elastic theory. The results obtained from 3D elastic theory is compared with classical shell and first order shear deformation theory. From their results they showed that 3D elastic theory is more accurate than other theories compared.

Daneshjou *et al.* (2017) studied the transmission loss characteristics of multi-layered cylindrical shell with outer layer as FGM and inner layer with porous core. The poro

elastic core is described by Biots theory. The shell is modelled with first order shear deformation theory. Their study shows that the present model is more accurate than the existing models.

From the above literature review, it is clear that the investigation on sound transmission loss of the sandwich panel is influenced by various geometric and material parameters very important to investigate in detail.

1.3 Closure

From the literature review it is clear that sandwich panels are used in aerospace structural applications due to its high strength to weight ratio. The noise and vibration from the aircraft structure significantly affects the flight attendants and passengers. So, it is necessary to study the vibro-acoustic behavior of the sandwich structures in order to keep sound radiation and transmission noise as less as possible. The prediction of acoustic characteristics using either analytical or 3D finite element model requires high computational effort and time consuming process. Literature survey revealed that vibration response of geometrically complex sandwich panels can be predicted using equivalent 2D finite element model which requires less time and computational effort. From the literature survey, it is also clear that modification in face sheet and core results in significant changes in vibration and acoustic behavior because it affects the mass, stiffness and damping property of the sandwich panel. It is found that laminated fibre reinforced polymer and foam has high damping property which indirectly affects the vibration and acoustic response level. From the literature survey, it is clear that the detailed investigation on acoustic characteristics of different kinds of sandwich panels is needed.

1.4 Research objectives

Sandwich panels are used as structural members in aerospace industries due to their better vibration and acoustic performance. The main objectives of the proposed work are

- to investigate the influence of nature of core on vibration and acoustic response characteristics of sandwich panels.
- to investigate the sound radiation and transmission loss characteristics of honeycomb core sandwich panel with laminated composite facings.
- to analyse the influence of foam filling on vibration and acoustic characteristics of sandwich panel.
- to validate the numerical studies with experimental results for vibration characteristics of a sandwich panel with honeycomb core.

In the present work, structures used in aerospace applications are specifically considered. The types of sandwich panel considered in the present are (a) honeycomb core sandwich panel (b) honeycomb core sandwich panel with FRP facings (c) truss core sandwich panel and (d) foam filled truss core sandwich panel. In the second chapter, the methodology followed to perform the numerical simulation is discussed in detail. In this work, the vibration and acoustic response of the sandwich panels are calculated from the equivalent 2D finite element model, so in the introduction part of each chapter, corresponding equivalent properties of sandwich panels are explained and followed by results and discussions. Finally, conclusions are presented about the important outcomes of the research work. Different analysis of the current research work is explained in the following sections.

In Chapter 2, methodology and validation studies used to predict the vibration and acoustic response of sandwich panel from equivalent 2D finite element model are presented.

In Chapter 3, the effect of face sheet thickness, core height and cell size of honeycomb core sandwich panel with on vibro-acoustic and transmission loss characteristics

is studied.

In Chapter 4, the effect of laminated composite facing with aluminium honeycomb core in a sandwich panel on vibro-acoustic and transmission loss characteristic is studied.

In Chapter 5, the effect of core topology of truss core sandwich panel on vibro-acoustic and transmission loss is analysed. For this purpose, various core truss topology such as, cellular, trapezoid, triangular are studied and compared with Z-core sandwich panel.

In Chapter 6, the effect of poly urethane foam filling in empty space of truss core sandwich panel on vibro-acoustic and transmission loss characteristic is studied.

In Chapter 7, important findings and conclusions are summarized.

CHAPTER 2

METHODOLOGY AND VALIDATION STUDIES

2.1 Introduction

In this chapter, methodology followed to predict the vibration and acoustic response of sandwich panels using numerical approach is discussed. This is followed by a brief of the validation studies carried out to ensure the accuracy of the results obtained from the present approach. An experiment is conducted to find the vibration response of honeycomb core sandwich panel and the results are compared with the numerical results obtained from equivalent 2D finite element model (FEM). Similarly, the prediction of acoustic response from the present method is compared with the published experimental data for sandwich panel.

2.2 Methodology for Numerical Studies

Equivalent 2D FEM model is used to obtain the free and forced vibration responses of the sandwich panel and the calculated forced vibration response is given as an input to Rayleigh integral in order to obtain the sound radiation and transmission loss characteristics.

The general steps followed in the present numerical approach to analyse the vibro-acoustic response of sandwich panels based on equivalent 2D FEM and Rayleigh integral is briefly presented here. However, more detailed explanation about calculation of equivalent elastic properties used for the analysis is presented in the each chapter related to a respective type of sandwich panel analysed.

Initially, the stiffness properties ($D_x, D_y, D_{xy}, D_{Qx}, D_{Qy}$) of sandwich panel are compared with stiffness properties of an orthotropic rectangular plate to get the 2D equivalent elastic properties ($E_x, E_y, G_{xy}, G_{xz}, G_{yz}$) of the sandwich panel. Equation 2.1 is used to equate the stiffness properties of sandwich panel to the stiffness properties of an orthotropic rectangular plate with thickness h .

$$D_x = \frac{E_x h^3}{12}; D_y = \frac{E_y h^3}{12}; D_{xy} = \frac{G_{xy} h^3}{6}; D_{Qx} = k^2 G_{xz} h; D_{Qy} = k^2 G_{yz} h \quad (2.1)$$

where, D_x and D_y are bending stiffness, D_{xy} is twisting stiffness, and D_{Qx} and D_{Qy} are the transverse shear stiffness, E_x and E_y are the Young's modulus and G_{xy}, G_{xz}, G_{yz} , are the shear modulus, k^2 is the transverse shear correction factor. Using the relation in Equation 2.1, E_x, E_y, G_{xy}, G_{xz} , and G_{yz} are calculated for the sandwich panel analysed.

Followed by this, the orthotropic plate with equivalent elastic properties is discretized by meshing with four node quadrilateral layered structural shell element (SHELL 181). The calculated equivalent modulus and thickness of the plate have been assigned accordingly with options available in commercial finite element solver ANSYS. The free vibration response is obtained by solving the equation

$$(\mathbf{K} - \omega_k^2 \mathbf{M}) \phi_k = \mathbf{0} \quad (2.2)$$

where, \mathbf{K} is the structural stiffness matrix, \mathbf{M} is the structural mass matrix, while ω_k is the circular natural frequency of the sandwich panel and ϕ_k is the corresponding mode shape.

\mathbf{M} and \mathbf{K} are assembled in the usual manner from the element mass matrices [m^e] and element stiffness matrices [k^e]. In general \mathbf{K} and \mathbf{M} are given as

$$\mathbf{K} = \sum_{e=1}^E \int_{V_e} \mathbf{B}^T \mathbf{D} \mathbf{B} dv \quad (2.3)$$

where \mathbf{B} and \mathbf{D} are strain-displacement and material property matrix respectively.

$$\mathbf{M} = \sum_{e=1}^E \int_{V_e} \rho_e \mathbf{N}^T \mathbf{N} dV \quad (2.4)$$

where \mathbf{N} is the shape function vector.

Further, the vibration response under harmonic excitation is obtained from the general equation of motion

$$\mathbf{M}\ddot{\mathbf{U}} + \mathbf{C}\dot{\mathbf{U}} + \mathbf{K}\mathbf{U} = \mathbf{F}(t) \quad (2.5)$$

$$-\omega^2 \mathbf{M}\mathbf{U} + \omega \mathbf{C}\mathbf{U} + \mathbf{K}\mathbf{U} = \mathbf{F}_n \quad (2.6)$$

where,

$$\mathbf{C} = \frac{2\zeta}{\omega} \mathbf{K} \quad (2.7)$$

\mathbf{C} is the damping matrix and it is calculated using Equation 2.7, ζ refers to structural damping ratio, ω refers to excitation frequency. Constant structural damping ratio is assumed for panels with aluminium facings while modal damping ratio calculated based on modal strain energy is used for panels with fibre reinforced composite laminates. Here $\mathbf{F}(t)$ is the applied load vector (assumed time-harmonic), \mathbf{F}_n is the forcing function in frequency domain. $\ddot{\mathbf{U}}$, $\dot{\mathbf{U}}$ and \mathbf{U} are the acceleration, velocity and displacement vector of the panel. To calculate the free and forced vibration response of sandwich panel commercial finite element software ANSYS is used.

Harmonic force of magnitude 1 N is applied at a chosen excitation point. The excitation point has been chosen based on a condition that it should not be a vibration nodal point for any modes in the chosen excitation frequency range. The excitation frequency range is chosen based on the acoustic coincidence frequency of the panel analysed. Based on the convergence study the panel mesh size is decided. It is also ensured that the chosen mesh size satisfies the six elements per wave length requirement

for the numerical vibro-acoustics analysis. For each excitation frequency computed normal velocities have been given as an input to the Rayleigh integral code to calculate sound pressure and power.

$$p(r) = \frac{j\omega\rho_0}{2\pi} \int w(r_s) \frac{e^{-jk|r-r_s|}}{|r-r_s|} ds \quad (2.8)$$

where, $p(r)$ is the complex pressure amplitude, ρ_0 is the density of the medium in which the panel is vibrating, $w(r_s)$ is the normal particle velocity at the surface point, k is the acoustic wave number, $|r-r_s|$ is the distance between the surface and the field point (Kirkup (1994)).

Further, sound power radiated from the vibrating panel can be calculated using the relation given by

$$\bar{W} = \frac{1}{2} Re \left(\oint p(r) \dot{w}^*(r) ds \right) \quad (2.9)$$

where \bar{W} refers sound power, $\dot{w}^*(r)$ refers complex conjugate of the acoustic particle velocity. Sound power level (SWL) can be calculated using the equation as follows

$$SWL = 10 \log \frac{\bar{W}}{W_{ref}} \quad (2.10)$$

where, W_{ref} is equal to 10^{-12} Watts.

Sound transmission loss (STL) in terms of decibels can be calculated as given below:

$$TL = 10 \log_{10} \left(\frac{1}{\tau} \right) \quad (2.11)$$

$$\tau = \frac{\text{Transmitted power}}{\text{Incident power}} \quad (2.12)$$

Transmitted sound power can be calculated using Equation 2.9 and incident sound

power is calculated from the incident sound intensity as follows

$$W_i = \frac{p_i^2 \cos \theta ab}{2\rho c} \quad (2.13)$$

where p_i is the incident pressure assumed to be a real constant 1 N/m^2 , θ is the incidence angle (rad), a and b are the length and breadth of the panel respectively, ρ is the density of air (kg/m^3) and c is the speed of sound (m/s) respectively.

A plane acoustic pressure is investigated for normal (with incident angle 90°) and oblique (with incident angle 45°) incident cases and corresponding transmission loss behavior has been investigated.

The mechanism of sound transmission through the sandwich panel is by the deformation of bottom skin which undergoes normal deflection due to the incident sound. The core transmits this motion to top skin to cause similar deformation. This deformation of top skin resemble to pumping action which causes sound waves in air above (Thamburaj and Sun, 1999). Assumption in the study is constrained only to the incident pressure wave. The deformation of the skin is maximum, due to the normal incidence of sound as the pressure is normal to the bottom skin and there is no shear. When the panel is subjected to oblique incidence, a part of the deflection is reduced due to the shear deformation, there by causing reduction in transmitted sound pressure. In this study, for oblique incidence of pressure there will be slightly increased transmission loss and reduced sound power level is anticipated.

The MATLAB code built-in house to solve the Rayleigh integral has been used to obtain sound transmission loss features of the sandwich panel.

The schematic representation of the methodology followed in the present work is shown in the Figure 2.1. Firstly, equivalent elastic properties of sandwich panel are obtained based on homogenisation technique. Then the sandwich panel is modelled as a plate and meshed with SHELL 181 element. Followed by this, modal analysis is performed to obtain the free vibration characteristics such as natural frequencies, mode

shapes and modal damping. Modal damping is calculated based on modal strain energy only for the panels with laminated composite facings. Then harmonic response analysis is carried out to obtain the forced vibration response in terms of average rms value of the panel at a particular frequency. The normal surface velocity obtained as a function of each excitation frequency is given as an input to Rayleigh integral to obtain the acoustic response characteristics such as sound power, sound pressure and transmission loss.

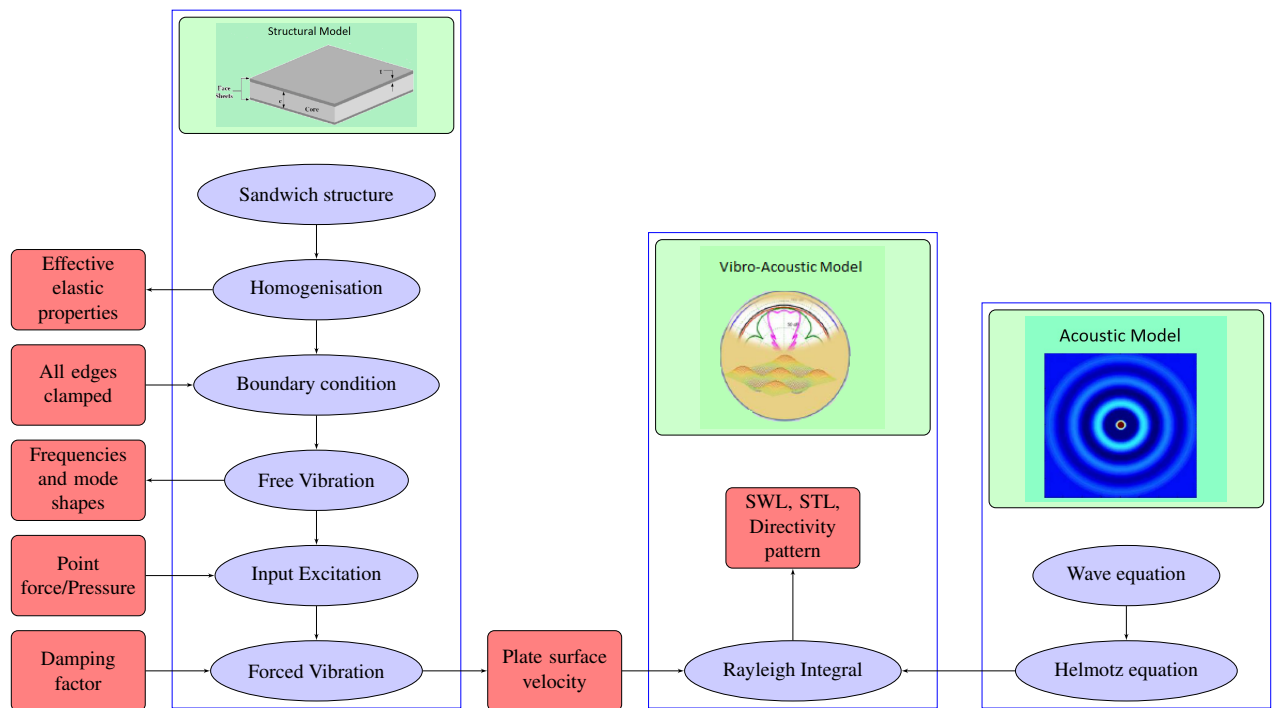


Figure 2.1: Methodology followed in the present work

2.3 Validation Studies

The methodology adopted for the prediction of free vibration response and acoustic response characteristics is validated by comparing the results obtained using the present approach with the published results available in literature. Additionally, natural frequencies and forced vibration response of a honeycomb core sandwich panel obtained experimentally are also compared with the results based on equivalent 2D FEM approach.

2.3.1 Experimental Validation

Experiments are conducted to obtain the natural frequencies and forced vibration responses of honeycomb core sandwich panel. The obtained vibration response is compared with the numerical results obtained based on the equivalent 2D elastic properties given in Equation 2.14, which are derived based on honeycomb plate theory (Hao *et al.*, 2011). The honeycomb core sandwich panel and dimension of unit cell is shown in Figure 2.2(a) and Figure 2.2(b) respectively.

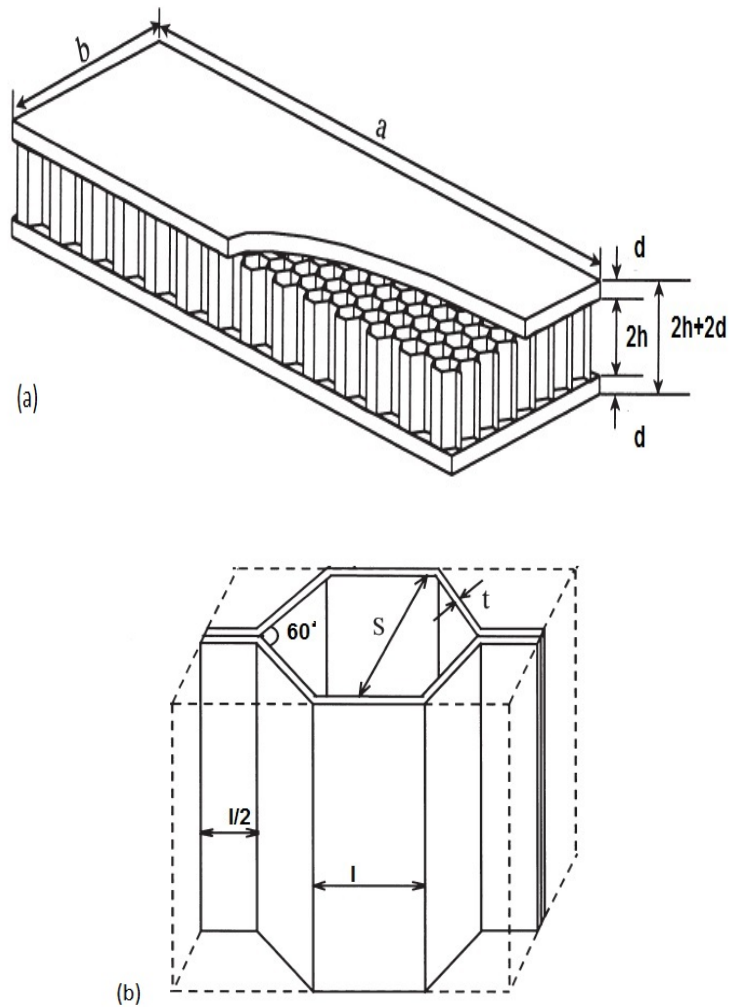


Figure 2.2: (a) Honeycomb core sandwich panel (b) Unit cell (Paik *et al.*, 1999)

$$\begin{aligned}
E_x = E_y &= \frac{4}{\sqrt{3}} \left(\frac{t}{l} \right)^3 E; \quad G_{xy} = \frac{\sqrt{3}}{2} \gamma \left(\frac{t}{l} \right)^3 E \\
G_{xz} &= \frac{\gamma}{\sqrt{3}} \frac{t}{l} G; \quad \gamma_{xy} = \frac{1}{3} \\
\bar{E}_x &= \frac{e_{11}e_{22} - e_{12}^2}{e_{22}}; \quad \bar{E}_y = \frac{e_{11}e_{22} - e_{12}^2}{e_{11}}; \quad \bar{G}_{xz} = e_{44} \\
\bar{G}_{yz} &= e_{55}; \quad \bar{G}_{xy} = e_{66}; \quad \bar{\gamma}_{xy} = \frac{e_{12}}{e_{22}} \\
e_{11} &= \frac{[(h+d)^3 - h^3]e_{f11} + h^3e_{c11}}{(h+d)^3}; \quad e_{22} = \frac{[(h+d)^3 - h^3]e_{f22} + h^3e_{c22}}{(h+d)^3} \\
e_{12} &= \frac{[(h+d)^3 - h^3]e_{f12} + h^3e_{c12}}{(h+d)^3}; \quad e_{44} = \frac{d}{h+d}e_{f44} + \frac{h}{h+d}e_{c44} \\
e_{55} &= \frac{d}{h+d}e_{f55} + \frac{h}{h+d}e_{c55} \\
e_{66} &= \frac{[(h+d)^3 - h^3]e_{f66} + h^3e_{c66}}{(h+d)^3}; \quad e_{c11} = e_{c22} = \frac{1}{1 - \gamma_{xy}^2} E_x \\
e_{c44} &= G_{xz}, \quad e_{c55} = G_{yz}, \quad e_{c66} = G_{xy}; \quad e_{f11} = e_{f22} \frac{1}{1 - \gamma^2} E \\
e_{f44} &= e_{f55} = kG, \quad e_{f66} = G; \quad \rho_{eq} = \frac{d\rho_f + h\rho_c}{h+d}
\end{aligned} \tag{2.14}$$

Where e_{fij} , e_{cij} are the stiffness parameters corresponding to face sheet and the core respectively. E_x and E_y , G_{xy} and G_{yz} are the equivalent Young's modulus and shear modulus of core respectively. Whereas \bar{E}_x and \bar{E}_y , \bar{G}_{xy} and \bar{G}_{yz} refers to the over all equivalent properties of sandwich panel. μ is the poisson's ratio of the face sheet, h is half of the core height, t is the cell wall thickness, l is the side wall length, d is the thickness of the face sheet, ρ_f and ρ_c are the density of face and core respectively. k is the effective coefficient in the range 0.0 and 1.0.

Natural Frequency Evaluation and Forced Vibration Response

Experimental modal analysis is performed to obtain the natural frequencies and forced vibration response of the sandwich panel with honeycomb core. Figure 2.3 shows the schematic diagram of the experimental set up used for measuring natural frequencies and forced vibration response. The signal generator is connected to an amplifier and in turn amplifier is connected to an electro dynamic shaker. The honeycomb structure is fixed at bottom in the centre by a clamping fixture. An IEPE type accelerometer is mounted on the honeycomb structure. The honeycomb structure is excited by means of a shaker and the subsequent signal generated is acquired using the sensors through the NI 9234 signal processing Data Acquisition device (DAQ). The force transducer is attached to the stringer which excites the honeycomb structure. The forced vibration analysis is carried out in order to acquire the wide range of natural frequencies by giving sinusoidal sweep input. The panel is excited at a location (0.3, 0.3) m and the acceleration data is obtained at (0.1, 0.765) m from the lower left corner of the panel. The obtained time domain signal is transformed to frequency domain by the in built fast fourier transform (FFT) analyser in LABVIEW. The honeycomb core sandwich panel is clamped in the portion of 0.25 m in the mid-bottom of panel for a height of 0.04 m. Figure 2.4 shows the picture of the experimental set up used for measuring natural frequencies and forced vibration response. For this experiment, the sandwich panel with honeycomb core made up of Al 3003 and face sheet made up of Al 6061 purchased from Honeycomb India Pvt. Ltd., is used. Young's modulus of Al 3003 and Al 6061 alloy is given as 70 and 68.9 GPa respectively. Density of Al 3003 and Al 6061 Alloy are 2730 and 2700 kg/m³ respectively. Different dimensions of honeycomb core sandwich panel as mentioned in Figure 2.2 are a and $b = 1$ m, $h = 6.8$ mm, $d = 0.5$ mm, $s = 6.2$ mm, $t = 0.001$ mm.

Experimental modal analysis is performed and the predicted natural frequencies are compared with the numerical results as shown in Table 2.1. From Table 2.1, it is clear that the experimental result matches well with the numerical result. Similarly forced

vibration response is calculated in the same location by exciting with the magnitude of 1 N harmonic signal at the individual natural frequencies. The magnitude of force is controlled through LABVIEW. Experimentally calculated forced vibration response excited under harmonic forcing condition is also compared with the ANSYS results as shown in Figure 2.5. From Figure 2.5, it is clear that forced vibration response of experimental data matches well with the numerical value which is calculated based on the equivalent 2D model.

Table 2.1: Comparison of experimental results with numerical results for free vibration frequencies

Mode	Natural frequency (Hz)	
	Experimental	Numerical
1	7	8
2	14	15
3	36	40
4	47	51
5	64	66

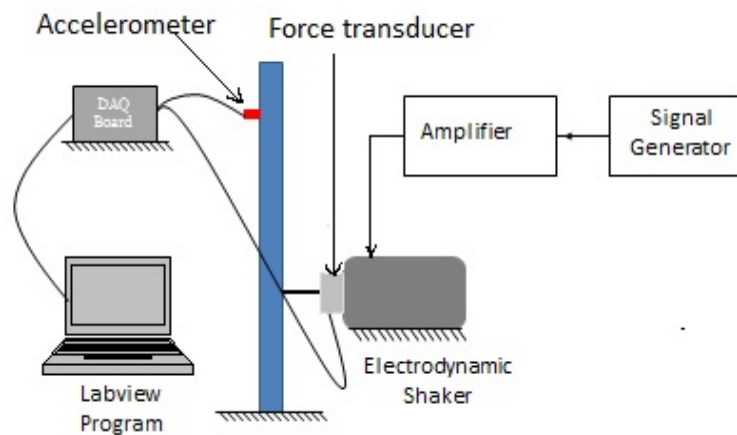


Figure 2.3: Schematic diagram of experimental set up to obtain natural frequencies and forced vibration response

2.3.2 Validation for Element Type SHELL 181

In order to validate the accuracy of using SHELL 181 element for the analysis of sandwich panel, work carried out by Kulkarni and Kapuria (2008) based on layer wise theory is considered. This validation study is carried out, to ensure the capability of capturing

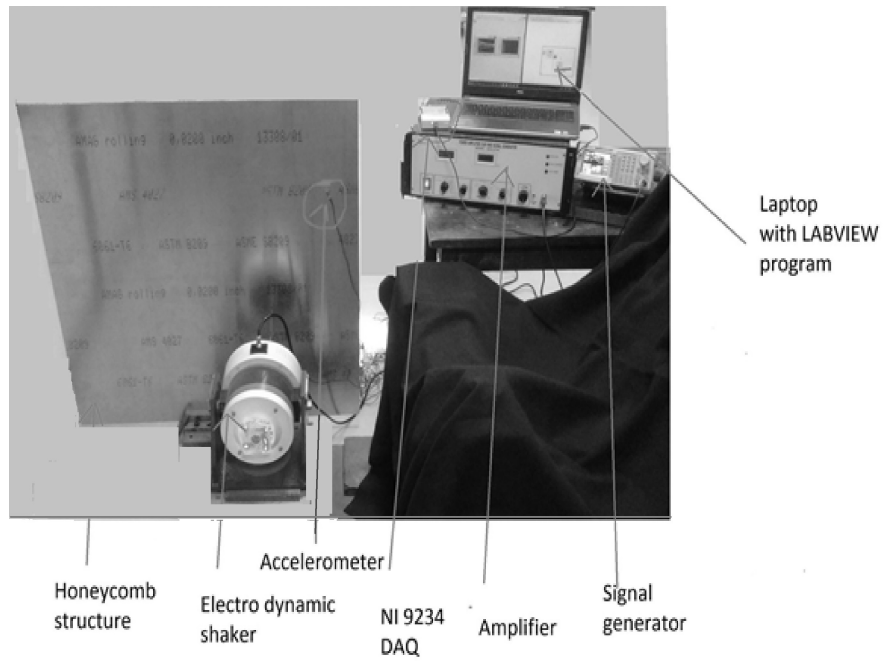


Figure 2.4: Experimental set up used for natural frequency evaluation and forced vibration response

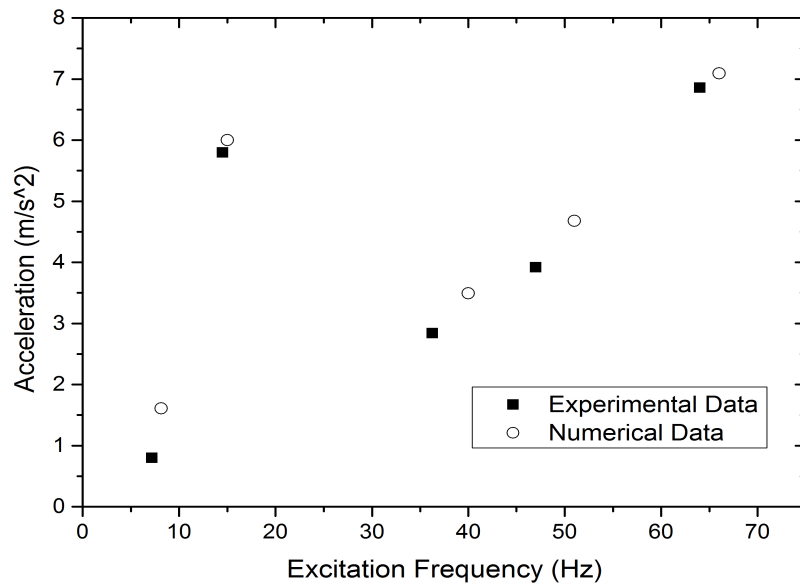


Figure 2.5: Comparison of experimental and numerical forced vibration responses at resonance frequencies (Hz)

the shear effect through thickness by SHELL 181 element while calculating the vibration response. Here, a sandwich panel with composite laminate facing having a length to thickness ratio of 20 is considered. The sandwich panel ($0^\circ/90^\circ/\text{core}/90^\circ/0^\circ$) with core height of $0.8h$, and top and bottom face sheet of thickness $0.05h$ is considered. Where h is the total height of the sandwich panel. The properties of face sheet material as given by Kulkarni and Kapuria (2008) $E_x = 276$ GPa, $E_y = E_z = 6.9$ GPa, $G_{xy} = G_{xz} = G_{yz} = 6.9$ GPa; $\nu_{xy} = \nu_{xz} = 0.25$, $\nu_{yz} = 0.3$. The properties of core material are given as $E_x = E_y = E_z = 0.5776$ GPa; $G_{xy} = 0.1079$ GPa, $G_{xz} = 0.1079$ GPa, $G_{yz} = 0.22215$ GPa, $\nu_{xy} = \nu_{xz} = \nu_{yz} = 0.0025$. Kulkarni and Kapuria (2008) predicted the free vibration frequencies using finite element model based on zig-zag theory and compared their results with 3D exact solution. They represented the natural frequencies in the non dimensional form as given by

$$\bar{\omega}_n = 100\omega_n a \sqrt{\frac{\rho_{core}}{E_{xy}}} \quad (2.15)$$

where a is the side of the plate, E_{xy} is Young's modulus of the face sheet material. SHELL 181 has been used in the present work to model the sandwich panel and the results obtained match well with the results reported by Kulkarni and Kapuria (2008) as seen in Table 2.2.

Table 2.2: Comparison of non-dimensional natural frequencies $\bar{\omega}_n$ with zigzag theory and 3D exact solution

Mode	3D exact solution (Kulkarni and Kapuria, 2008)	Zigzag theory (Kulkarni and Kapuria, 2008)	Present FE model	%error for Zigzag theory
1	7.6882	7.684	7.626	0.75
2	13.8455	13.834	13.763	0.51
3	15.9204	15.910	15.847	0.39
4	19.6563	19.613	19.505	0.55
5	20.6760	20.662	20.488	0.84
6	24.9485	24.877	24.721	0.62

2.3.3 Validation of Free Vibration of Truss Core Sandwich Panel

Numerical Results

A separate validation study is carried out to ensure the accuracy of the free vibration results obtained based on 2D equivalent model by comparing the results with results available in literature for a truss core sandwich panel. A sandwich panel of length 2 m and width 1.2 m with eight identical truss core sandwich units analysed by Lok and Cheng (2000a) is considered. Dimensions and properties of the unit cell shown in Figure 2.6 are: $p = 75$ mm, $f_0 = 25$ mm, $d = 46.75$ mm, $t_f = t_c = 3.25$ mm, $E = 80$ GPa, the Poisson ratio (ν) = 0.3, and material density (ρ) = 2700 kg/m³. Lok and Cheng (2000a) used an analytical method as well as FEM to obtain the natural frequencies of 3D model and its equivalent 2D model while the present method is based on FEM.

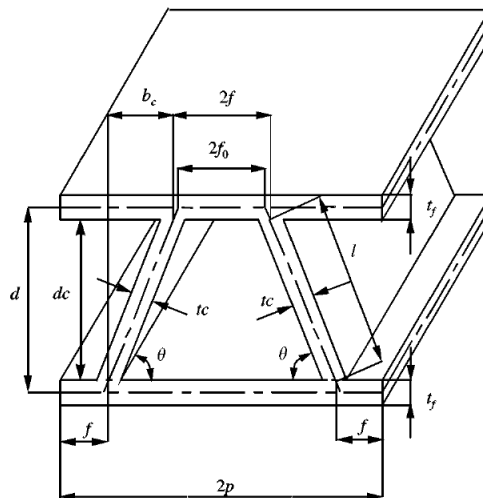
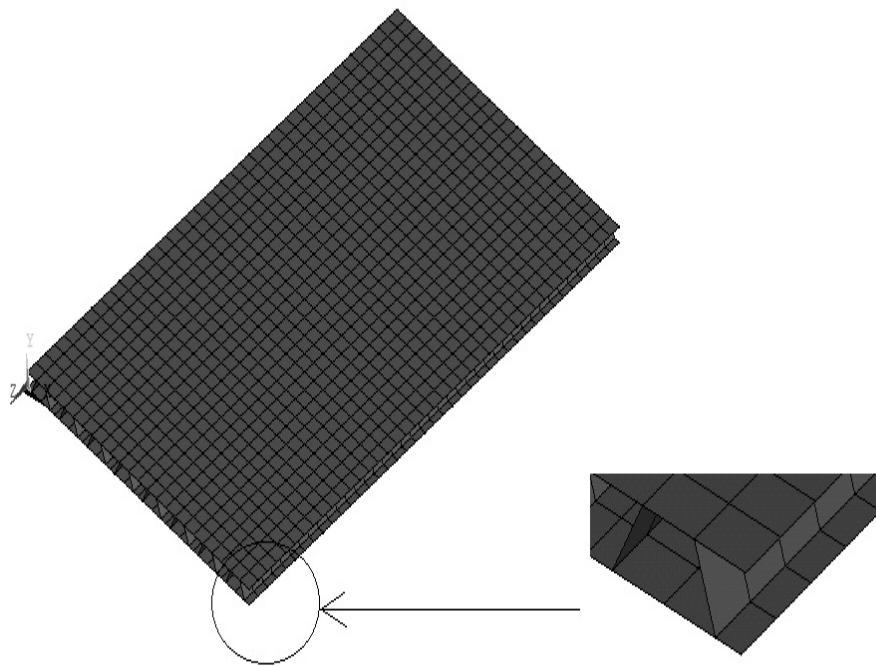
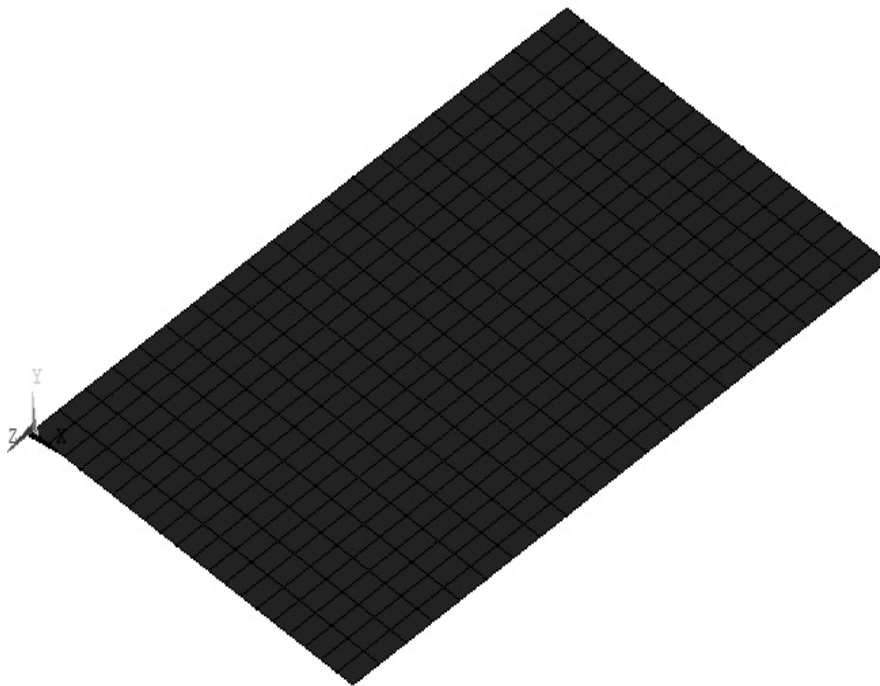


Figure 2.6: Dimension of truss core sandwich panel unit cell (Lok and Cheng, 2000a)

In the present work, both the 3D model and its equivalent 2D model analyses are carried out using SHELL 181 element in ANSYS. In order to model the 3D sandwich panel, initially the unit cell is modelled and meshed, then array of the unit cell is created to develop the entire panel. Mid-surface associated with the facings and core of the sandwich panel are meshed using SHELL 181 element. However, after meshing it is



(a)



(b)
32

Figure 2.7: (a) 3D Finite element model, (b) Equivalent 2D finite element model

ensured that the finite element model does not having any undesirable mesh connectivity problem. Equivalent 2D model is basically a plate with same breadth and width of the sandwich panel in which a rectangular area with dimension 2 m and 1.2 m is created as a geometric model. The assumptions adopted for deriving the elastic properties are

- The deformation of the panel is small.
- The facing plates are thin in comparison to the core thickness.
- During distortion of the panel, straight lines normal to the middle panel do not remain straight.

Equivalent stiffness properties for a truss core sandwich panel given by Lok and Cheng (2000b) are given below

$$\begin{aligned}
 D_x &= E(I_c + I_f); \quad D_y = \frac{EI_f}{1 - \frac{\gamma^2 I_c}{I_c + I_f}}; \quad \gamma_x = \gamma, \gamma_y = \gamma \frac{D_y}{D_x} \\
 D_{xy} &= 2GI_f; \quad D_{Qx} = Gt_c \frac{\frac{d^2 t}{pst_c} + \frac{1}{6} \left(\frac{d_c}{p}\right)^2}{\frac{t}{t_c} + \frac{sd_c}{3pd}}; \quad I_c = \frac{st_c d_c^2}{12p}; \quad I_f = \frac{td^2}{2} \\
 D_{Qy} &= \frac{1}{\frac{1}{d}(\delta_y^c + \delta_y^f) + \frac{1}{p}\delta_{zc}}
 \end{aligned} \tag{2.16}$$

where E and E_c are the elastic modulus of facing material of the plate and core material respectively. δ_y^c , δ_y^f and δ_{zc} are deflection parameters described in reference (Lok and Cheng, 2000b). I_f and I_c are the moment of inertia of face sheet and core respectively. γ_x and γ_y is Poisson's ratio along X and Y axis respectively.

Figure 2.7 shows the 3D and its equivalent 2D FE model of truss core sandwich panel. The free vibration frequencies obtained from ANSYS for both 3D and 2D model match well with the frequencies reported by Lok and Cheng (2000a) as seen in Table 2.3. The maximum error associated with equivalent 2D model is around 3%. Free vibration mode shapes obtained based on both 3D and equivalent 2D models are ob-

tained and compared as shown in Table 2.4. From Table 2.4, it is clear that there is no significant variation in the mode shapes.

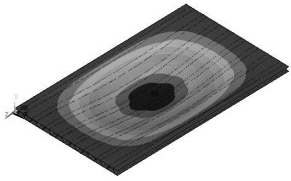
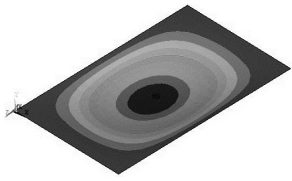
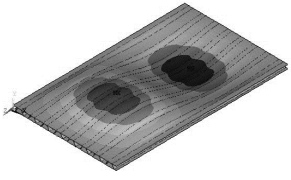
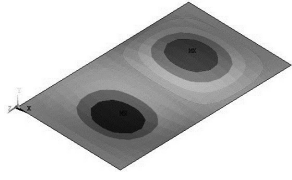
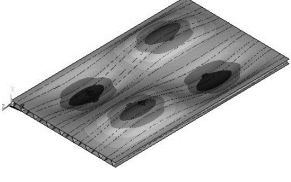
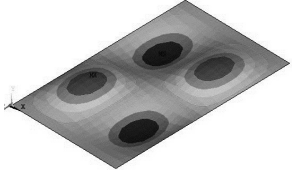
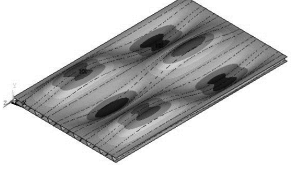
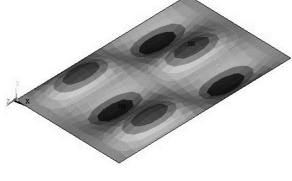
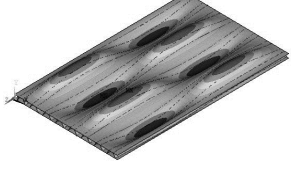
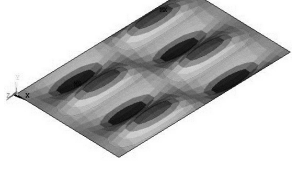
Table 2.3: Validation of free vibration results with Lok and Cheng (2000a)

Mode	Free vibration frequency (Hz)					
	3D Model			Equivalent 2D Model		
	Lok and Cheng [20]	Present	absolute % error	Lok and Cheng [20]	Present	absolute % error
1,1	139.3	136.0	2.3	138.7	138.2	0.2
2,1	213.6	213.6	0.0	211.1	211.5	0.2
1,2	297.4	274.3	7.7	294.2	296.2	0.6
3,1	290.0	297.9	2.7	294.8	296.9	0.7
2,2	348.1	334.4	3.9	352.1	353.5	0.4
4,1	382.0	380.1	0.4	378.9	385.6	1.7
3,2	426.2	411.4	3.6	431.2	434.0	0.6
5,1	466.2	459.8	1.3	463.2	476.1	2.8
4,2	501.6	471.8	5.9	517.7	524.3	1.2
1,3	509.5	491.4	3.5	521.3	532.9	2.2

2.3.4 Validation of Sound Transmission Loss Numerical Results

Validity of the code built, in-house to solve the Rayleigh integral in present work is checked by comparing the results obtained from the present approach with the experimental and numerical sound transmission loss results available in literature. Sound transmission loss behavior of sandwich panel calculated experimentally by Lee and Kondo (1999) and numerical work carried out by Assaf and Guerich (2008) are considered, in order to validate the present approach. The dimensions and properties of a sandwich panel considered in Lee and Kondo (1999) and Assaf and Guerich (2008) are same. A sandwich panel has a dimension of 0.3 m \times 0.2 m with core height 2 mm and face sheet thickness 0.5 mm. Density of face sheet and core material are 2720 kg/m³ and 1.60 kg/m³ respectively. Young's modulus and shear modulus of face sheet and core materials are given as 73.2×10^9 Pa and 4.12×10^9 Pa respectively. Poission's ratio of face sheet and core materials are given as 0.33 and 0.4 respectively. Sound transmission loss calculated based on the present method is in very good agreement

Table 2.4: Mode shape validation of equivalent 2D FEM model with 3D FEM model

Mode	3D FEM model	Equivalent 2D FEM model
(1,1)		
(1,2)		
(2,2)		
(3,2)		
(4,2)		

with experimental and numerical data as seen in Figure 2.8.

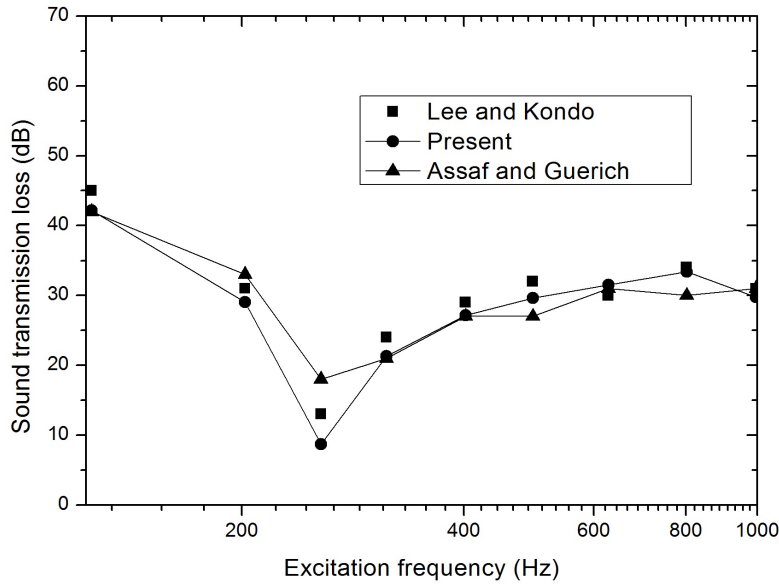


Figure 2.8: Validation of present approach for sound transmission loss results with experimental and numerical result reported by Lee and Kondo (1999) and Assaf and Guerich (2008)

2.3.5 Validation for Sound Power level Evaluation

Similar to the validation of sound transmission loss calculation, validation of sound power radiation calculation is also performed. For this purpose, plate analysed by Li and Li (2008) for sound radiation response is considered. Li and Li (2008) used a mild steel plate with length $l = 0.455$ m, width $w = 0.379$ m, thickness $h = 0.003$ m, Young's modulus $E = 2100$ GPa, the Poisson's ratio $\nu = 0.3$, and density $\rho = 7850$ kg/m³, vibrating in air subjected to a harmonic excitation of 1 N. They assumed a structural damping ratio of 0.01 for all the modes. From Figure 2.9, it is clear that the code used for calculating the sound radiation characteristics in this present work is in excellent agreement with Li and Li (2008) work.

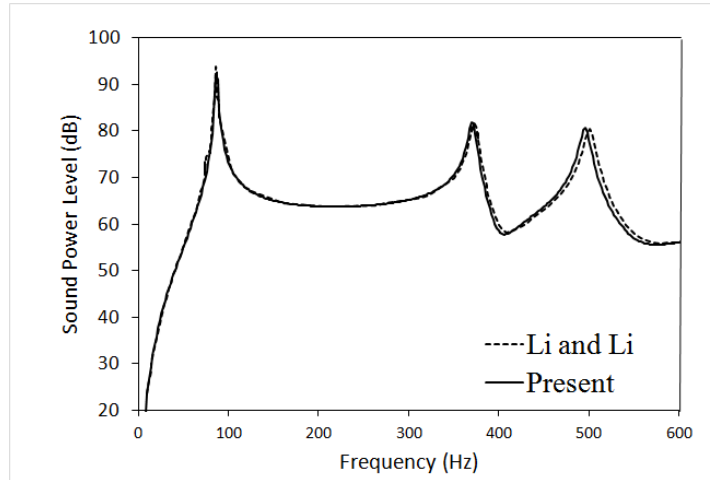


Figure 2.9: Validation of present work with Li and Li (2008) for sound power calculation

2.4 Closure

In this chapter, the methodology adopted to predict vibration and acoustic characteristics is presented. This is followed by validation studies carried out to ensure the accuracy of results based on equivalent 2D finite element model. The natural frequency and forced vibration data from the experiment is compared with the results of equivalent 2D finite element model sandwich panel. It is proved that the experimental results are in good agreement with the numerical results. 3D finite element model and equivalent 2D finite element model of the sandwich panel are compared for their natural frequencies and corresponding mode shapes. Both the results are in very good agreement. Further the acoustic response from present approach is validated with the numerical and experimental results exist in the literature. The results are in very good agreement with the present approach.

CHAPTER 3

STUDIES ON HONEYCOMB CORE SANDWICH PANEL

3.1 Introduction

The literature survey revealed that the impact of sound and vibration on health, travel comfort, performance of pilots and flight attendants is significant. Hence, it is necessary to design the aircraft structural members which takes care of acoustic comfort. But a design which involves the acoustic comfort is always dense and large in size than the design considering only mechanical strength. This drawback can be overcome by exploring the influence of core geometry on vibration and acoustic response of sandwich panel. In this aspect, the present chapter focuses on the study of influence of core geometry on vibration and acoustic response characteristics of honeycomb core sandwich panel. In this chapter, the effect of geometrical parameters of honeycomb core sandwich panel is analysed based on equivalent 2D FEM model. The honeycomb plate theory given in Hao *et al.* (2011) is used to calculate the equivalent properties of the honeycomb core sandwich panel as given in Equation 2.14.

Sandwich panels with honeycomb core is geometrically more complex compared to the panels with other type of core. The dimensions of honeycomb core sandwich panel and its unit cell are shown in Figure 2.2(a) and Figure 2.2(b) respectively. In this investigation, the effect of face sheet thickness, core height and cell size of honeycomb core on vibration and acoustic response and transmission loss characteristics are studied. The panel with length 1.5 m and width 1 m for a CCCC (C - Clamped) boundary condition is chosen. The sandwich panel is excited with a harmonic force of 1 N at

(1.125, 0.75) m from the lower left portion of the panel and its consequent effect on vibro-acoustic response is investigated.

3.1.1 The Effect of Face Sheet Thickness

The core height (15 mm), cell size (2 mm) and cell wall thickness (0.04 mm) are kept constant and face sheet thickness has been varied as 0.5 mm, 1.5 mm and 2 mm in order to analyse the influence of face sheet thickness on vibration and acoustic characteristics of the sandwich panel with honeycomb core. Variation of natural frequencies associated with first few modes of a honeycomb core panel with increase in core thickness is given in Table 3.1. From Table 3.1, it is clear that influence of face sheet thickness on natural frequency is significant as structural stiffness increases with face sheet thickness. In the present work, average root mean square (V_{rms}) velocity of the panel under harmonic excitation calculated as function of excitation frequency in order to analyse the forced vibration response of the sandwich panel. The average root mean square velocities obtained to analyse the influence of face sheet thickness is shown in Figure 3.1. From Figure 3.1, one can observe that forced vibration response of the panel reduces with increase in face sheet thickness as a result of increase in structural stiffness. Variation of sound power radiation of the panel with different face sheet thickness is shown in Figure 3.2. From Figure 3.2, it is observed that the face sheet thickness with 0.5 mm radiates more sound because of its reduced stiffness and equivalent density compared to 2 mm thickness. Similar trends are observed in octave band wise calculations. It is found that sound power level decreases significantly with increasing thickness in all frequency bands as seen in Figure 3.3. From the over all sound power level analysis shown in Figure 3.4, it is clear that sound power level decreases with increase in thickness as anticipated. From the sound radiation directivity pattern analysis carried out at 100 Hz and 1000 Hz, the sound pressure associated with the panel having 0.5 mm face sheet thickness is high as expected because of its higher radiation efficiency. The directivity pattern associated with 1000 Hz is more complex shaped because of higher frequency modes available around 1000 Hz (Refer Figure 3.5 and Figure 3.6). From the results it

is clear that, one cannot select face sheet thickness alone as a parameter to reduce the weight of the structure by considering the sound radiation characteristics. Figure 3.7 shows the effect of face sheet thickness on sound transmission loss characteristics for both normal and oblique incidence. From Figure 3.7, one can observe that, the sound power level has its peak value in the resonance frequencies where as STL curve has sharp dips in the resonance frequencies because of high transmission of sound power at resonance. Figure 3.8 shows the sound transmission loss behavior of panel under the normal and oblique angle of incidence for different face sheet thickness. From Figure 3.8, it is clear that the STL curve has the inverse pattern of SPL as anticipated. From Figure 3.8, STL for various face sheet thickness are clearly distinguished in the stiffness controlled region. The increase in stiffness increases the sound transmission loss in stiffness controlled region which is evident from the high sound transmission loss associated with 2 mm face sheet panel in the stiffness zone till the first resonance frequency. In Figure 3.8, the excitation frequency is shown in logarithmic scale to show the clear dips in damping sensitive regions. The negative transmission loss is seen in first resonance frequency due to the reasons as discussed earlier. Many damping sensitive regions appears in the mass dominant region and hence multiple peaks and valleys are observed in the higher frequency region. The mass dominant zone is also clearly distinguishable because of increase in mass due to increase in face sheet thickness. From the above discussion, it is clear that effect of face sheet thickness on sound transmission loss is significant in all three regions of the STL curve. Same kind of variation has been observed in the STL behavior for the oblique incidence also as seen in Figure 3.8. One can observe from Figure 3.7 and 3.8 that, for oblique incidence sound radiation is lower and sound transmission loss is higher than the normal incident excitation as discussed earlier.

Table 3.1: The effect of face sheet thickness on natural frequency (Hz) for honeycomb core sandwich panel

Mode	Face sheet thickness		
	0.5 mm	1.5 mm	2 mm
1	131.79	167.17	177.02
2	203.14	257.56	272.68
3	322.29	408.13	431.92
4	324.61	411.26	435.28
5	387.10	490.01	518.48

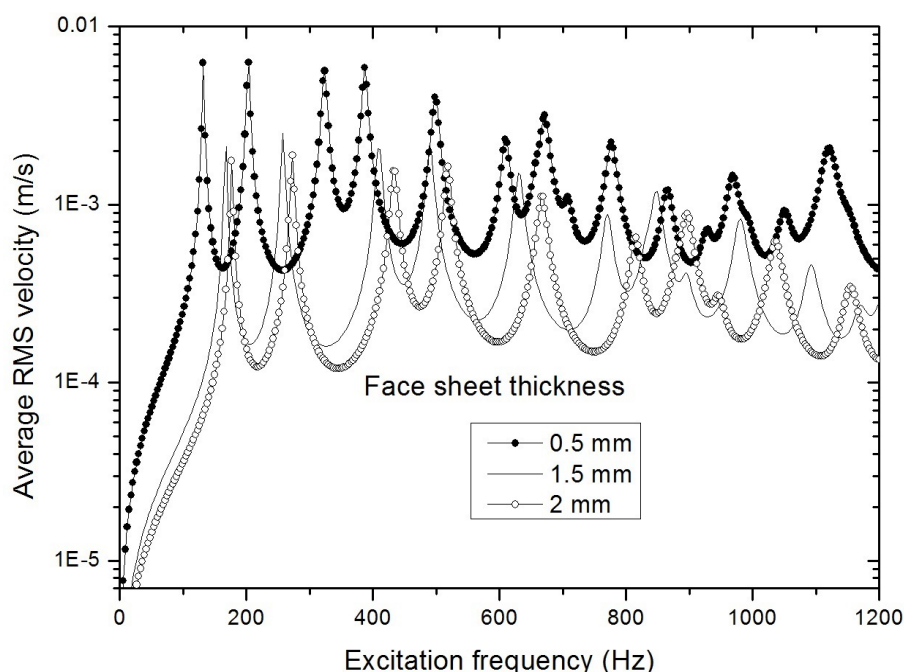


Figure 3.1: The effect of face sheet thickness on vibration response

3.1.2 The Effect of Core Height

In order to study the effects of core height on vibration and acoustic response of the honeycomb core sandwich panel, cell size (2 mm) and cell wall thickness (0.04 mm) are kept constant and the core height has been varied as 10 mm, 15 mm and 20 mm. If the core height is varied as mentioned, then increasing the core height with constant cell size, cell wall and face sheet thickness, increases the stiffness of the sandwich panel there by reducing the sound power level. The present work focuses on reducing the size

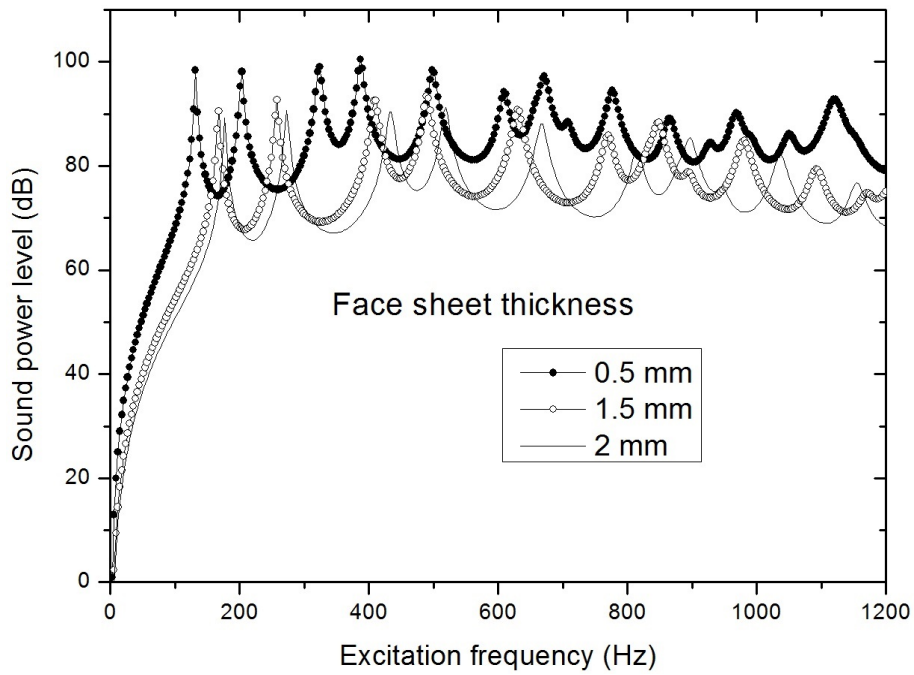


Figure 3.2: The effect of face sheet thickness on sound power level

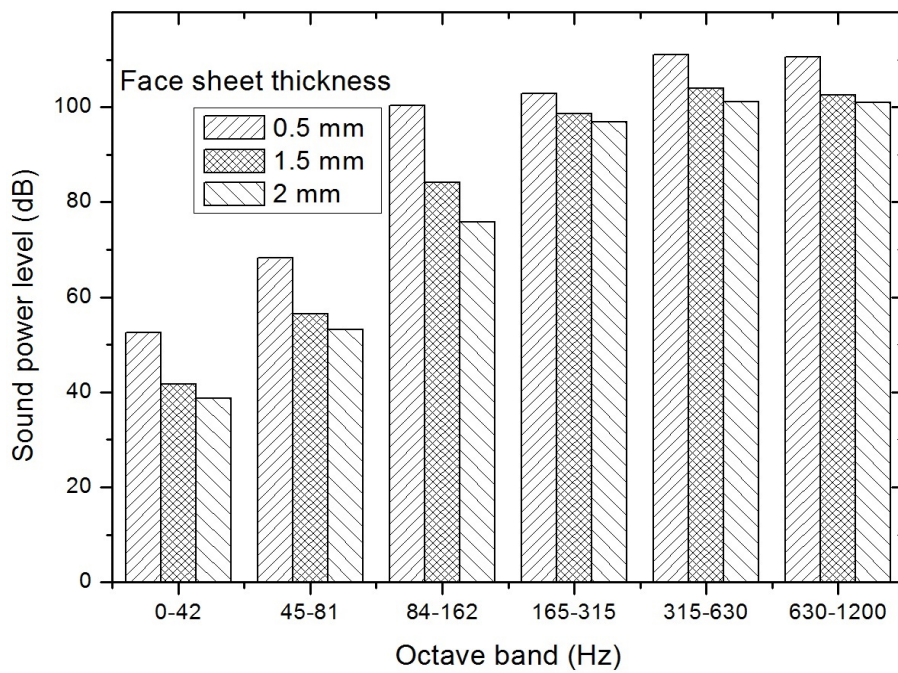


Figure 3.3: The effect of face sheet thickness on sound power level in octave band

of the panel and also to keep the sound power level at desirable level by reducing the core height in due considerations with the space constraints. In order to achieve this, the

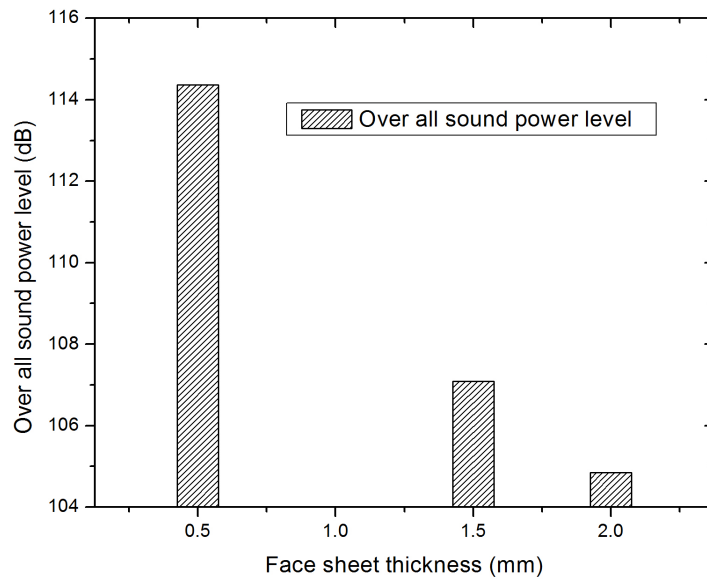


Figure 3.4: The effect of face sheet thickness on over all sound power level

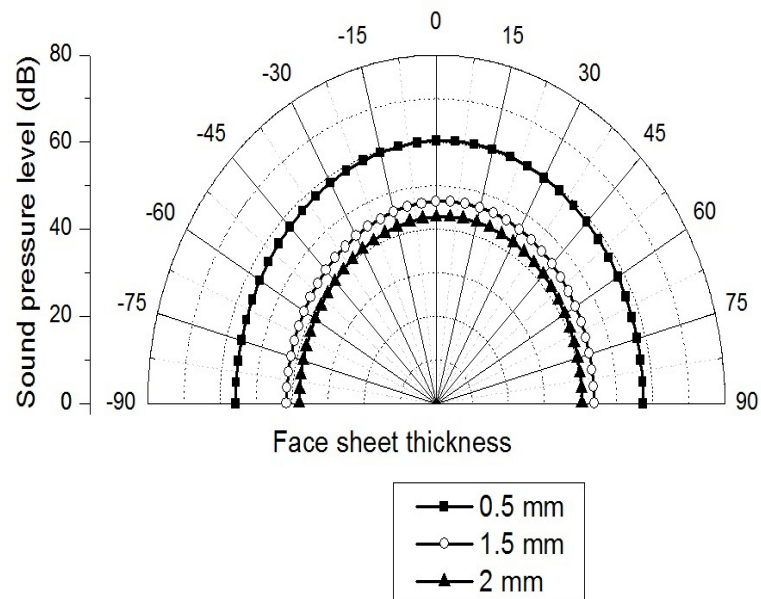


Figure 3.5: The effect of face sheet thickness on over all sound power level at 100 Hz

face sheet thickness of 2 mm, 1.5 mm, 0.5 mm are selected respectively in the increasing order of the core height. By doing so, the equivalent stiffness and its equivalent density can be increased effectively in the lower core height, with an incremental increase in

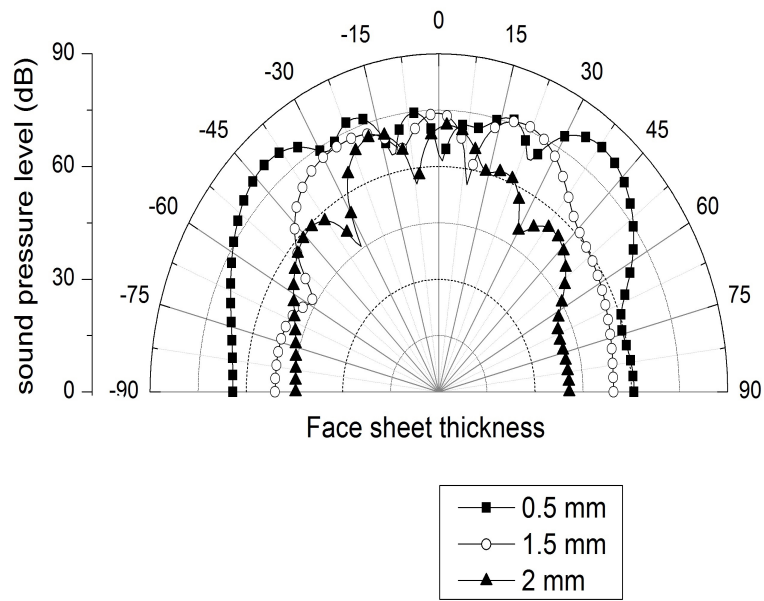


Figure 3.6: The effect of face sheet thickness on over all sound power level at 1000 Hz

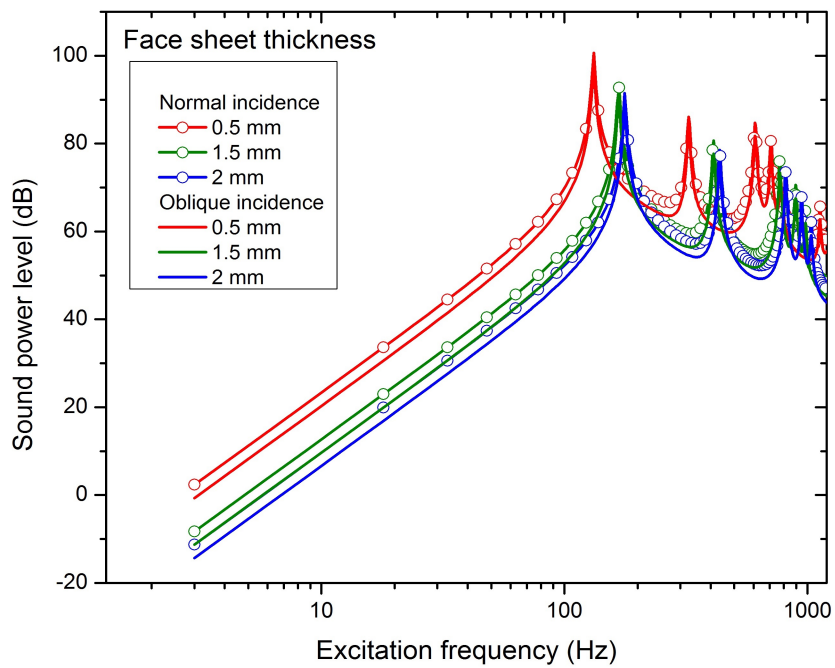


Figure 3.7: The effect of face sheet thickness on transmitted sound power level

weight. From Table 3.2, one can observe that effect of increase in core height on natural frequency is significant as core height increases because face sheet thickness is assigned in a order of 2 mm, 1.5 mm, 0.5 mm for 10 mm, 15 mm and 20 mm core height sandwich

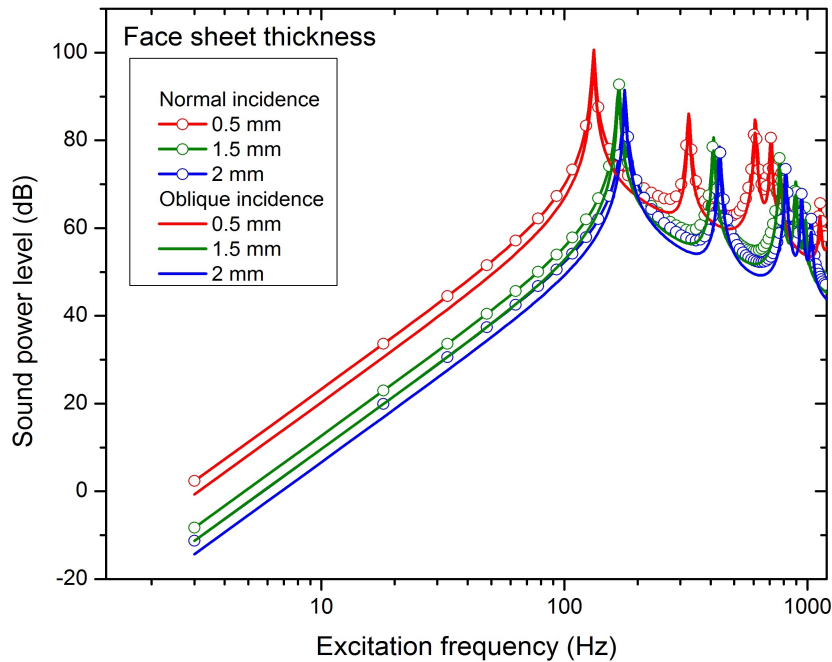


Figure 3.8: The effect of face sheet thickness on sound transmission loss of honeycomb core sandwich panel

panel . Influence of core height on forced vibration response is shown in Figure 3.9. From Figure 3.9, one can observe that forced vibration response of the panel reduces with decrease in core height as a result of increase in structural stiffness. This is made possible only by selecting higher face sheet thickness for lower core height. From Figure 3.10, it is clear that the honeycomb core of height 20 mm radiates more sound compared to the honeycomb core of height 10 mm and 15 mm because of reduction in stiffness and its equivalent density. From the octave band wise calculation it is found that sound power level variation with core height is significant only in the range 84-162 frequency band (Refer Figure 3.11). From the over all sound power level analysis it is clear that sound power level increases with increase in core height because of reduction in stiffness and also by the effect of reduced weight as seen in Figure 3.12(d). From the sound radiation directivity pattern analysis carried out at 100 and 1000 Hz, it is observed that panel with a core height of 20 mm radiates more sound as seen in Figure 3.13, 3.14. From the results, it is clear that the reduced sound power level can be achieved for smaller size (i.e volume) sandwich panels by increasing the face sheet thickness.

Figure 3.15 shows the effect of core height on sound power level for both the normal and oblique incidences. Variation of sound power radiated with respect to core height has been given in Figure 3.15. From Figure 3.15, it is clear that resonant amplitude of sound power is influenced by the core height. Figure 3.16 shows the influence of core height on STL. From Figure 3.16, one can observe the anti-peaks and stiffness sensitive region curves are not clearly distinguished. This indicates that stiffness of the panel is not enhanced by increase in core height, due to the counter balance effect of face sheet thickness and core height. But in the mass controlled region, anti-peaks in the curves are clearly distinguished. This indicates that increase in face sheet thickness increases the mass significantly compared to the stiffness. Due to this approach, the higher sound transmission loss is achieved in mass controlled region with lesser core height. The effect of damping is clearly seen in the resonance frequencies. Due to this multiple peaks and valleys are seen in higher frequency segment. From the result, it is clear that, it is possible to achieve good transmission properties in lower core height sandwich panel with due consideration to space constrain. From the assumption made for oblique incidence, the same trend is observed for sound transmission loss and sound power level analysis.

Table 3.2: The effect of core height on natural frequency (Hz) for honeycomb sandwich panel

Mode	Core height		
	10 mm	15 mm	20 mm
1	129.32	163.25	175.11
2	199.47	251.54	269.51
3	316.68	398.66	426.54
4	319.03	401.69	429.69
5	380.59	478.66	511.64

3.1.3 The Effect of Cell Size

In order to study the effect of cell size of the honeycomb panel on sound radiation characteristics, the cell size is varied as 2 mm, 3 mm and 4 mm with a core height of 15 mm,

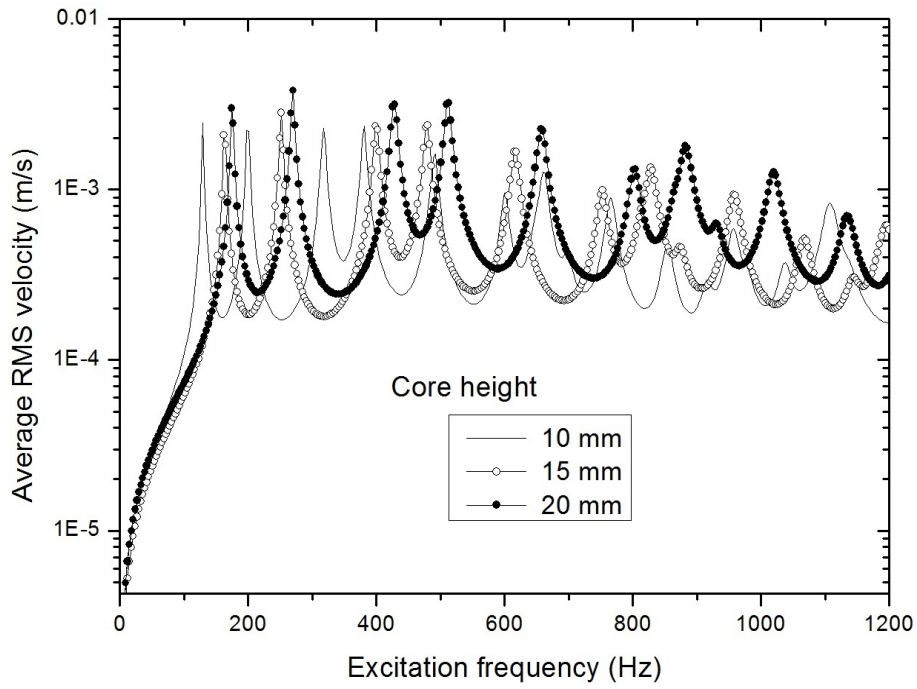


Figure 3.9: The effect of core height on vibration response of honeycomb core sandwich panel

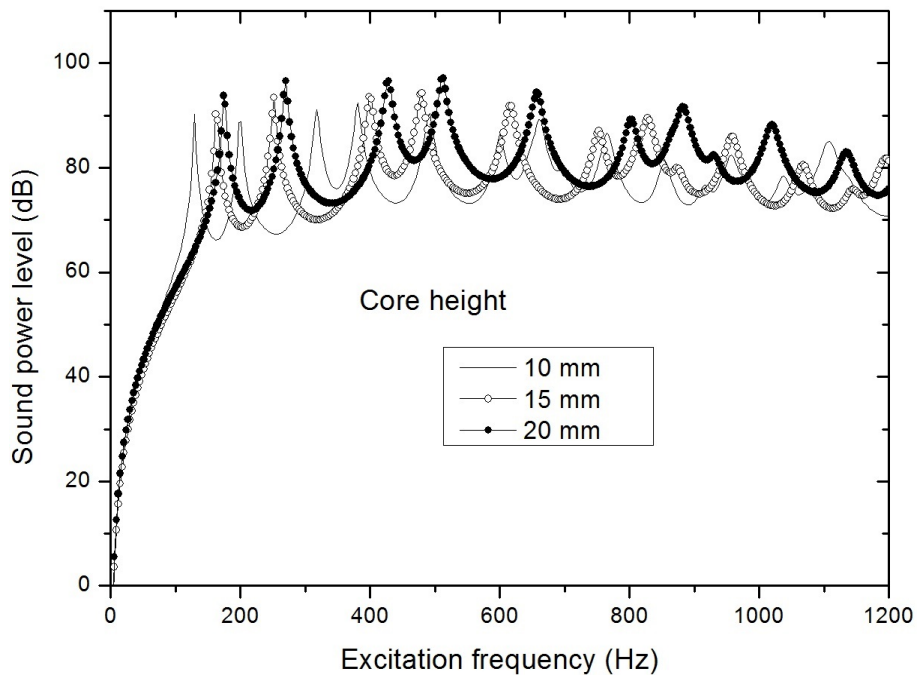


Figure 3.10: The effect of core height on sound power level of honeycomb core sandwich panel

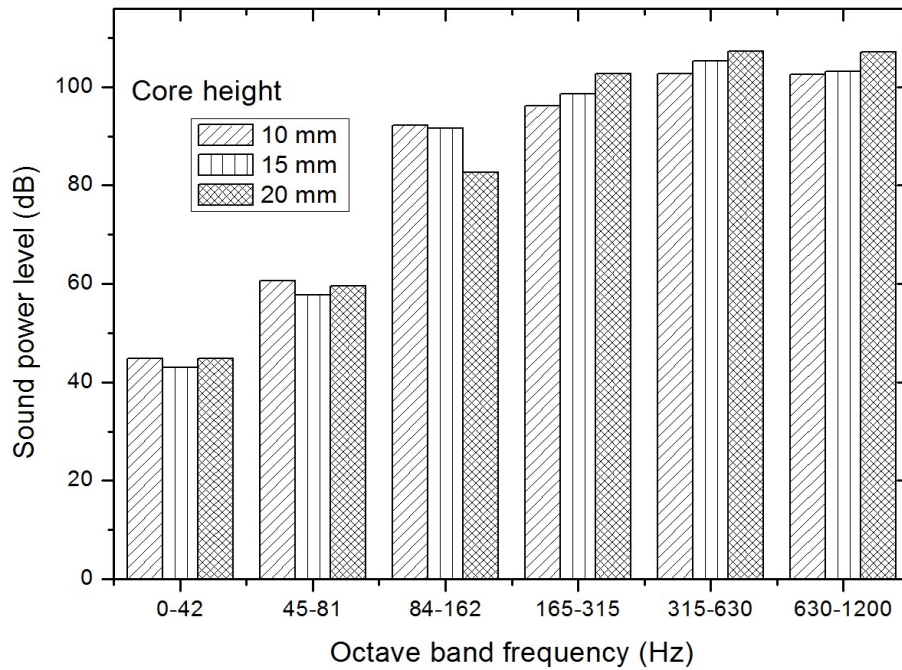


Figure 3.11: The effect of core height on sound power level in octave band of honeycomb core sandwich panel

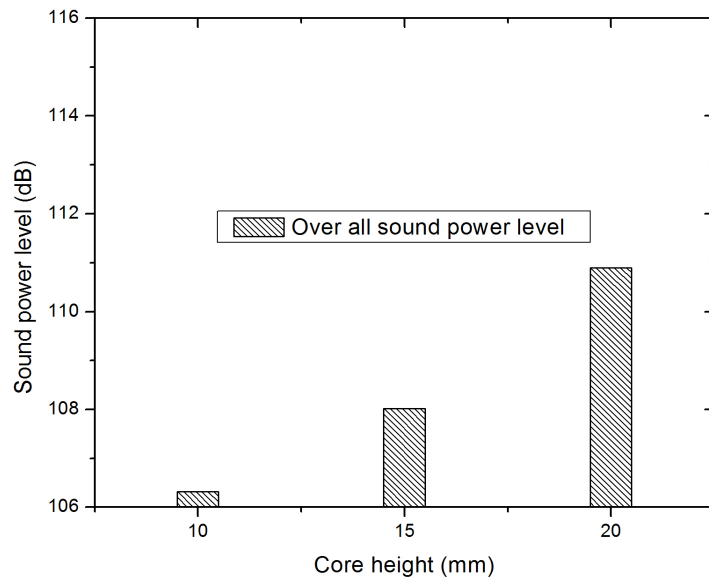


Figure 3.12: The effect of core height on over all sound power level of honeycomb core sandwich panel

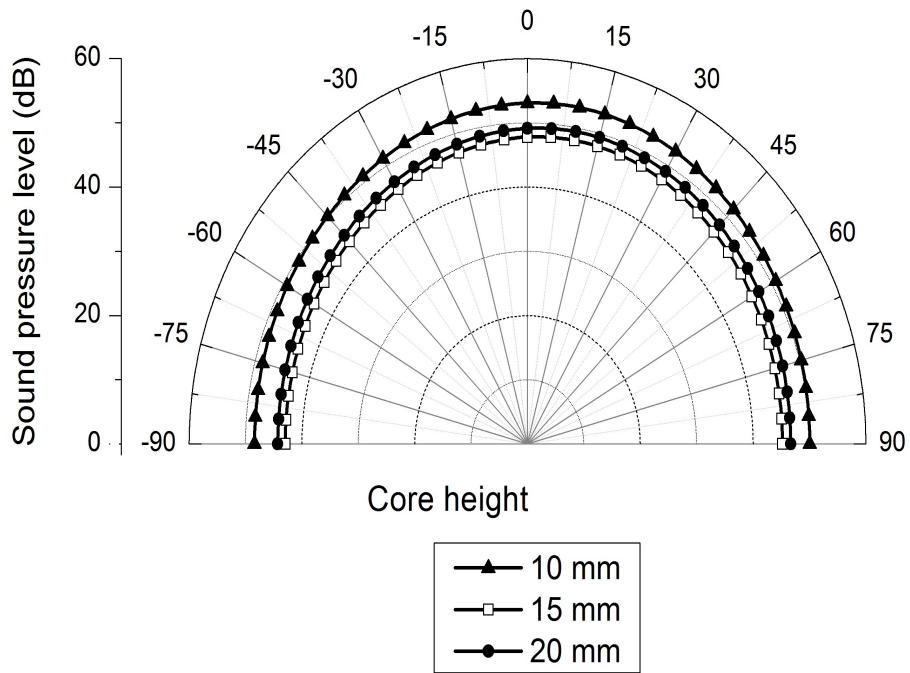


Figure 3.13: The effect of core height on sound pressure level at 100 Hz of honeycomb core sandwich panel

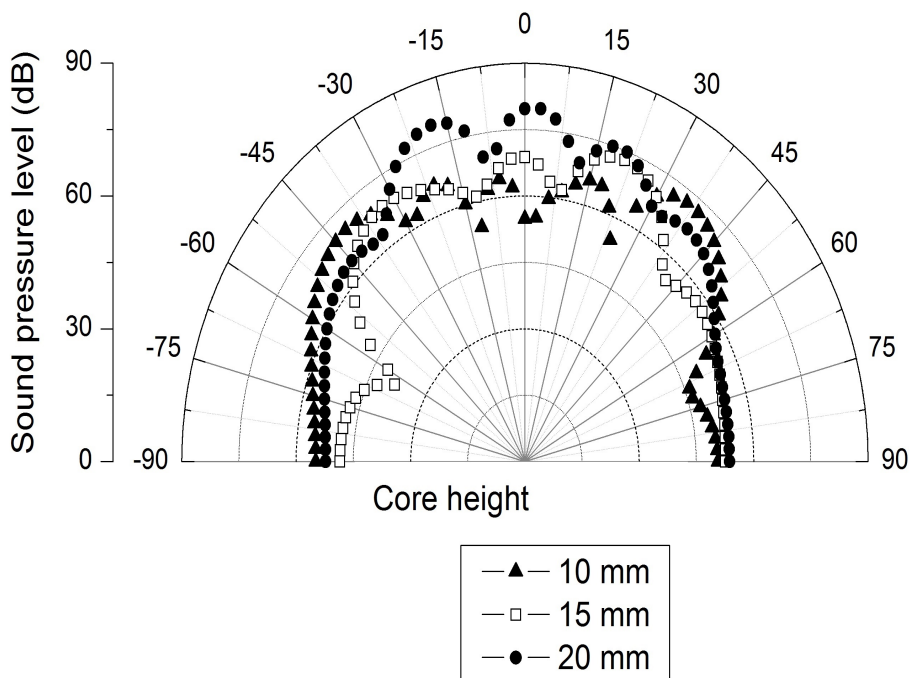


Figure 3.14: The effect of core height on sound pressure level at 1000 Hz of honeycomb core sandwich panel

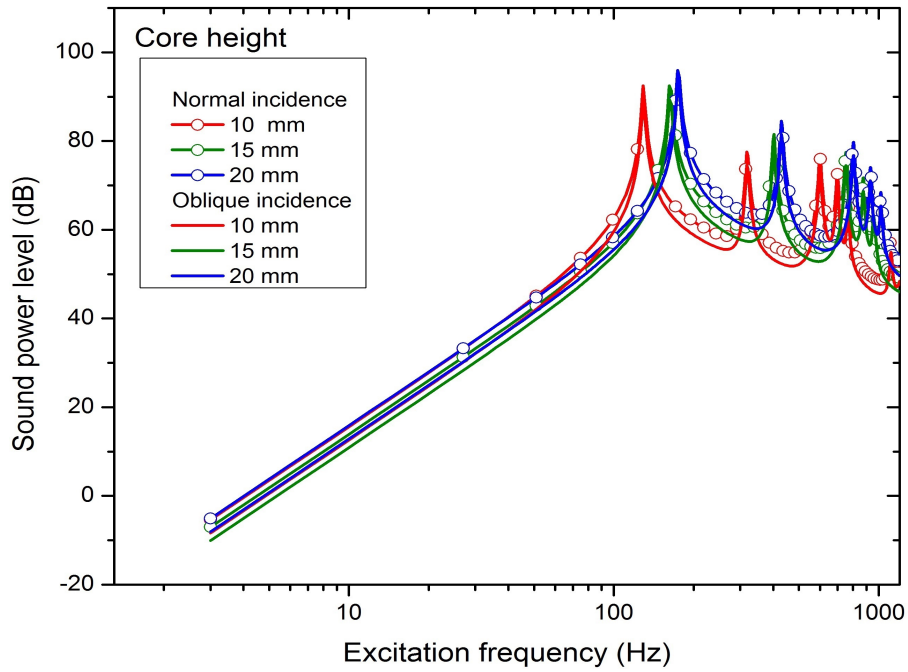


Figure 3.15: The effect of core height on transmitted sound power level of honeycomb core sandwich panel

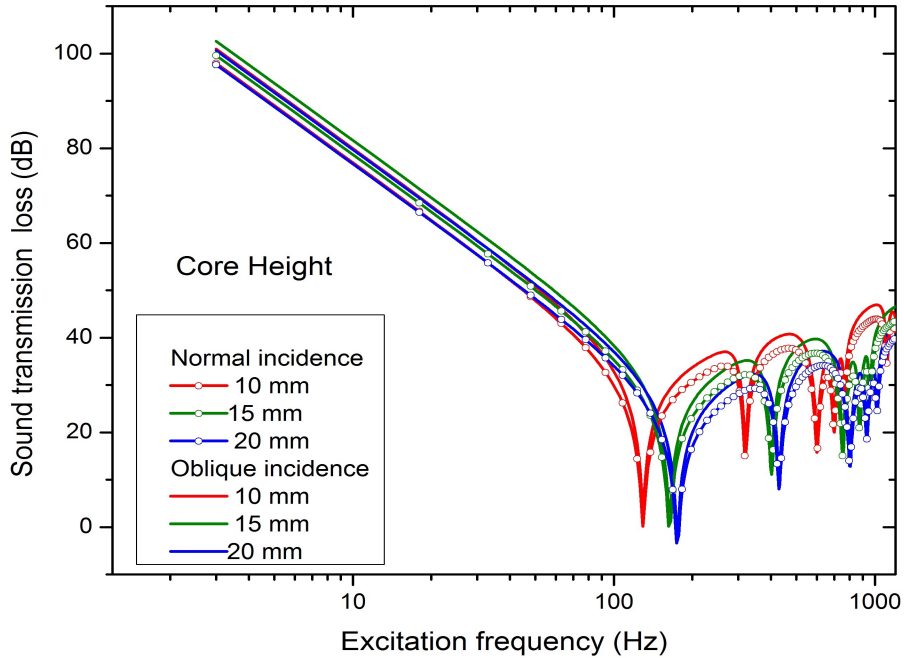


Figure 3.16: The effect of core height on sound transmission loss of honeycomb core sandwich panel

a face thickness of 1 mm and cell wall thickness of 0.04 mm is considered. The effect of cell size on natural frequencies of the honeycomb core sandwich panel is given in Table 3.3. From Table 3.3, it is clear that the change in cell size does not affect the natural frequency of the panel significantly due to the counter balance variation between the stiffness and weight of the panel respectively. The average root mean square velocities obtained to analyse the influence of cell size is shown in Figure 3.17. Same trend is seen in Figure 3.17 for the forced vibration response of the panel also. From Figure 3.18, one can say that effect of cell size on sound radiation characteristics is not significant. Usually increase in cell size reduces stiffness and also reduces density, so there is no significant change in the sound power level. Same trend is seen in octave band, over all and sound radiation pattern at 100 Hz and 1000 HZ as shown in Figure 3.19, 3.20, 3.21 and 3.22 respectively. From the results, one can select cell size as the parameter to reduce weight without affecting the sound radiation properties. However, its mechanical strength is also to be considered for better design. Figure 3.23 shows the effect of cell size on sound power level for both normal incidence and oblique incidences. Influence of cell size on sound power variation and sound transmission loss are shown in Figure 3.23 and Figure 3.24 respectively. Due to the counter-balance variation between the mass and stiffness, both the sound power radiated as well as transmission loss variation is not sensitive to the variation on cell size. From Figure 3.23 and 3.24, it is also observed that, there is no distinguished variation in peaks of curve in both stiffness and mass sensitive region. The effect of damping in all resonance frequency is clear and sound transmission loss in damping controlled region is proportionally same due to the constant damping ratio assumption of 0.01 for all cases.

Table 3.3: The effect of cell size on natural frequency (Hz) for honeycomb core sandwich panel

Mode	Cell size		
	2 mm	3 mm	4 mm
1	154.18	162.06	166.47
2	237.59	249.72	256.52
3	376.67	395.82	406.56
4	379.50	398.84	409.68
5	452.31	475.29	488.17

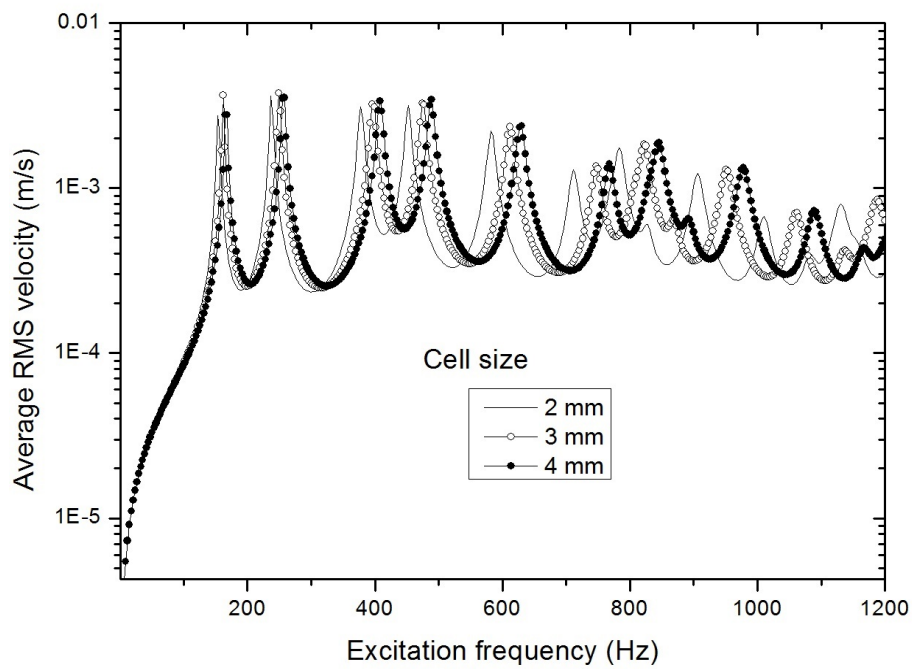


Figure 3.17: The effect of cell size on vibration response of honeycomb core sandwich panel

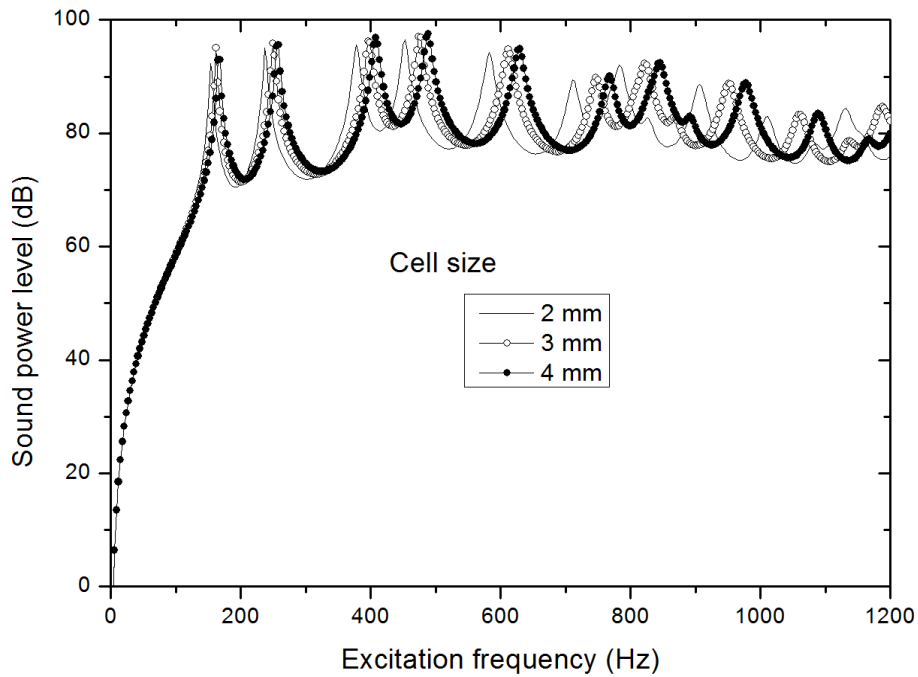


Figure 3.18: The effect of cell size on sound power level of honeycomb core sandwich panel

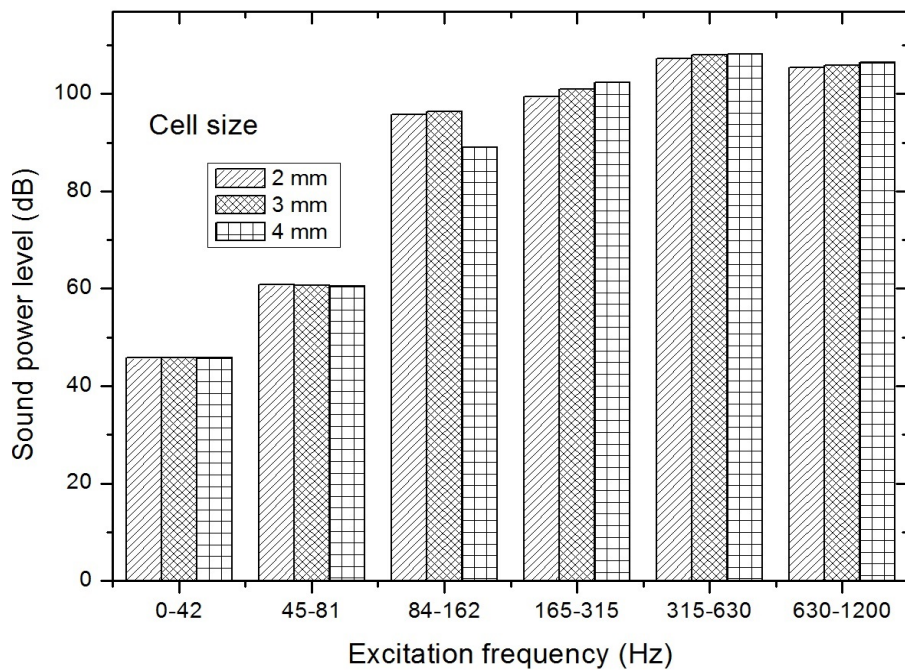


Figure 3.19: The effect of cell size on sound power level in octave band of honeycomb core sandwich panel

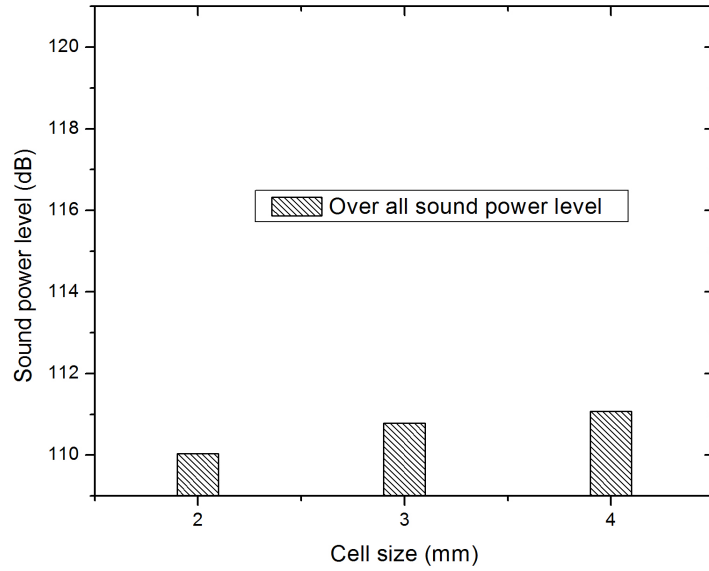


Figure 3.20: The effect of cell size on over all sound power level of honeycomb core sandwich panel

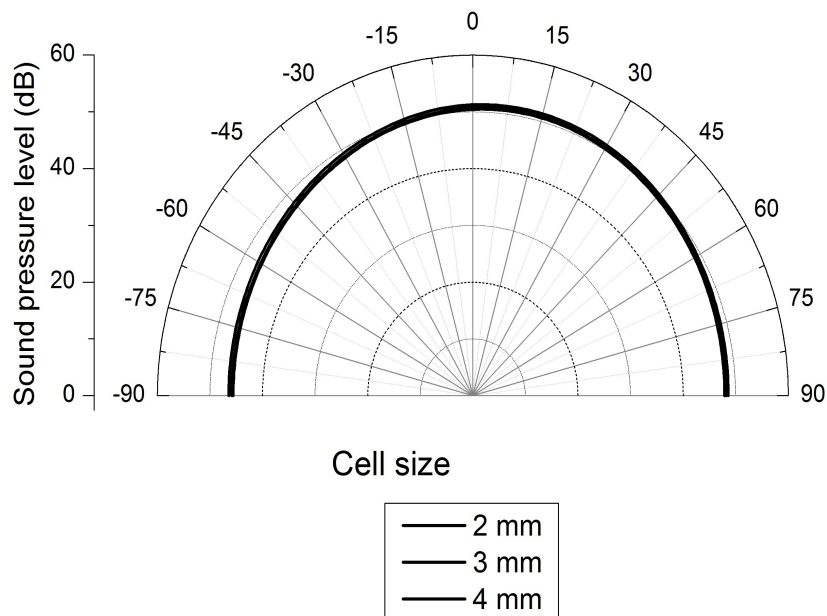


Figure 3.21: The effect of cell size on sound pressure level at 100 Hz of honeycomb core sandwich panel

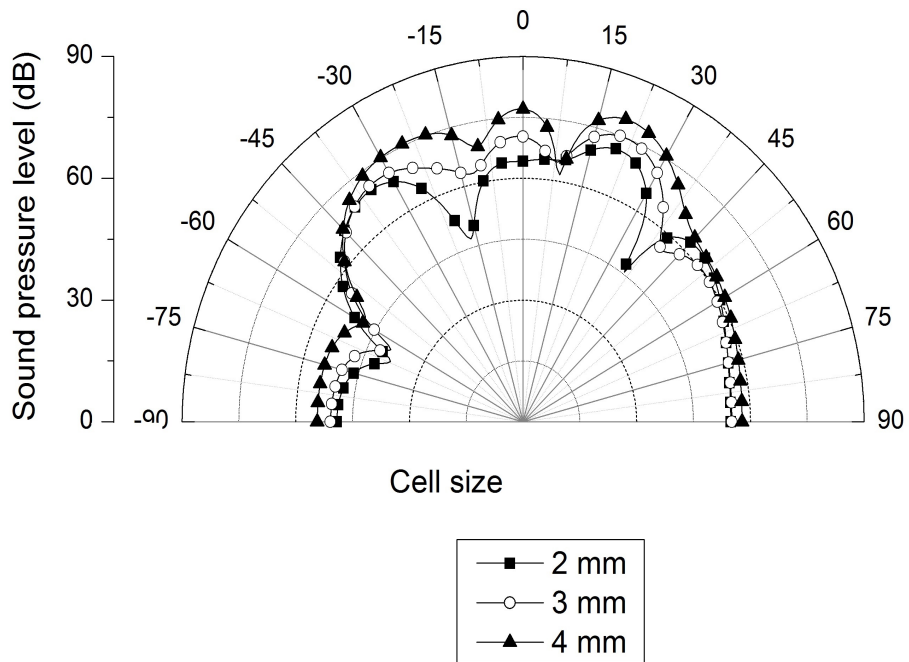


Figure 3.22: The effect of cell size on sound pressure level at 1000 Hz of honeycomb core sandwich panel

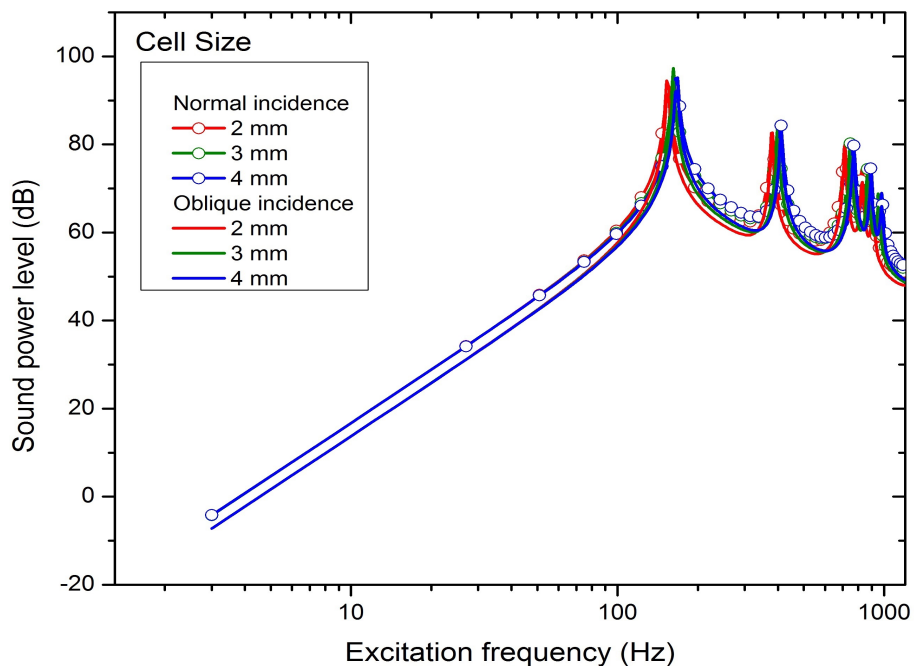


Figure 3.23: The effect of cell size on transmitted sound power level of honeycomb core sandwich panel

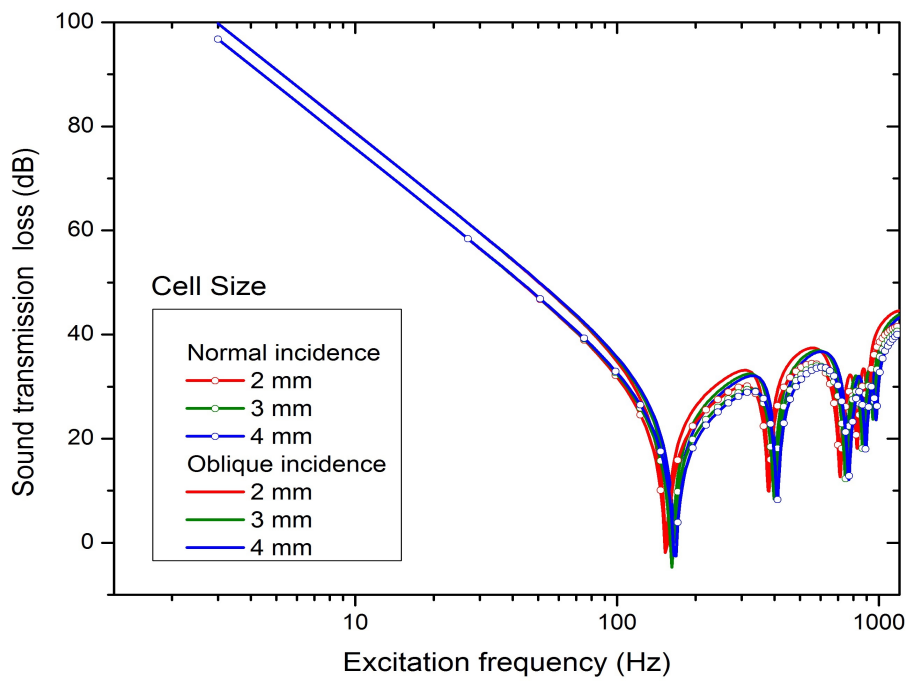


Figure 3.24: The effect of cell size on sound transmission loss of honeycomb core sandwich panel

3.2 Closure

A detailed investigation carried out to study the effect of core geometry on vibro-acoustic and sound transmission loss characteristic of honeycomb core sandwich panel is presented. From the calculated equivalent property of honeycomb core sandwich panel, 2D finite element model is created using the SHELL 181 element available in ANSYS library. Further, Free and forced vibration response of sandwich panel is obtained from the equivalent 2D finite element model. Next, the panel is excited at suitable location to predict the vibro-acoustic behavior. Further, the panel is excited by applying a pressure to predict the transmission loss characteristics. The obtained forced vibration response is given as an input to the in-house developed Rayleigh integral MATLAB code to obtain the vibro-acoustic and transmission loss characteristics. In lower core height honeycomb core sandwich panel better acoustic characteristic is achieved in due consideration to the space constraint.

CHAPTER 4

STUDIES ON HONEYCOMB CORE SANDWICH PANEL WITH FRP FACINGS

4.1 Introduction

Resonant amplitude of vibration and acoustic responses can be effectively controlled by damping. Typical aircraft structural components made of metals have very less structural damping. However, this can be overcome by using fibre reinforced plastic laminates as facing sheets instead of metallic face sheets in the sandwich panels. The fibre-matrix interaction associated with the FRP results in higher structural damping. Materials having low damping value, density and stiffness will radiate more sound compared to a material with high damping value, density and stiffness material. The low density material, graphite fibre reinforced epoxy plastic would radiate more sound compared to high density material. But the stiffness and damping ratio of epoxy-graphite plastic is very high compared to conventional metals used in aerospace structural applications.

The objective of this study is to investigate the vibration and acoustic characteristics of the aluminium honeycomb core sandwich panel when the aluminium facings are replaced by FRP facings. The honeycomb core sandwich panel with FRP facings can reduce approximately half of the weight of honeycomb core sandwich panel with aluminium facings. In this chapter, detailed investigation on sound radiation and transmission characteristics of honeycomb core sandwich panel with laminated FRP facing is carried out. Results of FRP sandwich panel are compared with sandwich panel having aluminium facings.

A constant structural damping ratio is assumed for the previous analysis. Here, modal damping ratio obtained based on modal strain energy is used while calculating

the responses to account for inherent material damping associated with the FRP facing material. The modal loss factor (η_i) of i^{th} mode is obtained based on modal strain energy method. The loss factor (η_i) calculated based on modal strain energy method is discussed further. The equation of motion for a complex stiffness system can be written as

$$\mathbf{M}\ddot{\mathbf{U}}(\mathbf{j}\omega) + (\mathbf{K}_R + \mathbf{K}_I)\mathbf{U}(\mathbf{j}\omega) = \mathbf{0} \quad (4.1)$$

where \mathbf{M} is the mass matrix; \mathbf{K}_R and \mathbf{K}_I are the elastic and loss stiffness matrices of the system, respectively. \mathbf{U} is the displacement vector in the frequency domain. Equation 4.1 can be converted to an eigenvalue problem by assuming a solution as

$$u(t) = \phi^* e^{j\lambda_i^* t} \quad (4.2)$$

where ϕ^* and λ_i^* are the i^{th} complex mode shape and square root of the eigenvalue and respectively. Equation 4.1 can be written as eigen value problem.

$$(\mathbf{K}_R + \mathbf{jK}_I)\phi^* = \lambda_i^{*2}\mathbf{M}\phi^* \quad (4.3)$$

Now λ_i^{*2} is expressed as

$$\lambda_i^{*2} = \lambda^2(1 + j\eta) \quad (4.4)$$

Approximate ϕ^* by its real part ϕ_R and pre multiply ϕ_R^T on both sides of Equation 4.3, we get

$$\lambda^2(1 + j\eta) = \frac{\phi_R^T \mathbf{K}_R \phi_R}{\phi_R^T \mathbf{M} \phi_R} + j \frac{\phi_R^T \mathbf{K}_I \phi_R}{\phi_R^T \mathbf{M} \phi_R} \quad (4.5)$$

Substituting M matrix from Equation 4.3 and equating the real and imaginary part

of Equation 4.5 leads to

$$\lambda^2 = \frac{\phi_R^T \mathbf{K}_R \phi_R}{\phi_R^T \mathbf{M} \phi_R} \quad (4.6)$$

$$\eta_i = \frac{\phi_R^T \mathbf{K}_I \phi_R}{\phi_R^T \mathbf{K}_R \phi_R} \quad (4.7)$$

Honeycomb sandwich panel with FRP facing is modelled using layered structural shell element available in commercial finite element solver ANSYS. The finite element model of honeycomb core sandwich panel consists of three layers such as two FRP stiff layers and one honeycomb core layer. The equivalent elastic properties for honeycomb core is calculated from Equation 2.14 and thickness of each layer have been assigned accordingly with options available in ANSYS. In order to calculate damping ratio, real stiffness matrix $[K_R]$ and imaginary stiffness matrix $[K_I]$ is obtained by performing the modal analysis separately assigning storage modulus and loss modulus values as an input material properties respectively. From ANSYS the real and imaginary stiffness matrix are obtained in the form of Harwell Boeing format. In order to convert the matrix from Harwell Boeing format to full matrix format MATLAB code is used. Further, the modal loss factor for the i^{th} mode is calculated in the frequency range using Equation 4.7. Further, the forced vibration response of the sandwich panel obtained from FEM is given as an input to Rayleigh integral code to calculate the acoustic characteristics.

4.2 Validation of Modal Damping Ratio

In order to validate the procedure followed to obtain the modal damping ratio in the present analysis, Sudhagar *et al.* (2015) work is considered. Composite laminate plate with fibre orientation of $[(90/90/90/90/90/90)]_s$ and having a material property of $E_x = 30.5(1+0.0125j)$ GPa, $E_y = 6.99(1+0.0150j)$ GPa, $G_{xy} = G_{xz} = 2.51(1+0.00715j)$ GPa, $G_{yz} = 2.8$ GPa, $\mu_{xy} = 0.31$, $\rho = 1745 \text{ kg/m}^3$ is considered in Sudhagar *et al.* (2015)

work. Sudhagar *et al.* (2015) calculated modal damping ratio of the i^{th} mode based on modal strain energy. The damping ratio calculated for each mode is shown in Table 4.1. From Table 4.1 it is very clear that the calculated modal damping ratio in the present approach matches well with Sudhagar *et al.* (2015) work.

Table 4.1: Damping ratio (ζ) validation with Sudhagar et al. (Sudhagar *et al.*, 2015) work

Mode	Damping ratio(ζ)	
	(Sudhagar <i>et al.</i> , 2015)	Present work
1	0.016	0.015
2	0.009	0.009
3	0.016	0.015
4	0.011	0.011
5	0.012	0.012

4.3 The effect of Stiffness

A square honeycomb core sandwich panel having a side dimension of 1 m and unit cell dimensions of $h = 4$ mm, $d = 1$ mm, $s = 4$ mm, $t = 0.04$ mm is now considered for detailed investigation to analyse the effect of structural stiffness and inherent material damping. Initially the effect of stiffness on vibro-acoustic response and sound transmission loss behavior is studied by varying the fibre orientation and boundary conditions. Based on these analyses, better acoustic characteristics honeycomb core sandwich panel is selected for the further analysis. The chosen configuration is further analysed by including the modal damping of all the mode available in the chosen excitation frequency range.

The effect of fibre orientation and boundary condition of FRP facing with aluminium honeycomb core sandwich panel on vibro-acoustic response and sound transmission loss characteristics are studied. The material properties of Epoxy/Graphite FRP and aluminium used in this analysis is given in Table 4.2. In acoustic studies, the responses calculated are sound power level, octave band analysis, sound pressure

level at 100 Hz and 630 Hz and sound transmission loss characteristics. The maximum frequency is chosen as 630 Hz based on coincidence frequency of the panel, for the harmonic response and its analysis. Mesh size has been chosen based on the convergence study and it is also ensured that, the chosen mesh size satisfies the six elements per wave length requirement for the numerical vibro-acoustic analysis. Mesh size adopted for all the case is 24 by 24 elements.

Table 4.2: Material properties

Elastic Constants	Material	
	Epoxy-Graphite FRP	Aluminium
E_x (GPa)	181.0	68.0
E_y (GPa)	10.3	68.0
E_z (GPa)	10.3	68.0
G_{xy} (GPa)	7.17	26.15
G_{yz} (GPa)	2.87	26.15
G_{zx} (GPa)	7.17	26.15
ν_{xy}	0.28	0.3
ν_{xz}	0.28	0.3
ν_{yz}	0.33	0.3
Density ρ kg/m ³	1578	2700

4.3.1 The Influence of Fibre Orientation

Free and forced vibration response, sound pressure level and sound transmission loss of facings with fibre orientation of single layered unidirectional (0/c/0) FRP and laminated cross-ply (0/90/c/90/0) FRP with aluminium honeycomb core is compared with the sandwich panel made up of aluminium facings with aluminium honeycomb core (Al/c/Al). The fibre oriented at 90° and 0° are more appropriate to flexural loads. Due to this reason, FRP with these type of configuration is selected in this analysis. Here, for all the cases CCCC boundary condition is considered.

Natural frequencies obtained for the panels with three different lay up configuration for first few modes are given in Table 4.3. From Table 4.3 one can say that, the natural frequency of [(0/90/c/90/0)] sandwich panel is high compared to [(0/c/0)] sandwich

Table 4.3: The influence of fibre orientation of FRP honeycomb core sandwich panel on natural frequency (Hz)

Sl.No	Material		
	0/90/c/90/0	Al/c/Al	0/c/0
1	159.40	122.66	151.95
2	315.64	239.99	188.30
3	317.49	245.06	267.12
4	425.48	346.54	366.05
5	555.60	411.40	390.51
6	560.89	428.78	390.58
7	629.49	504.11	444.94
8	635.14	515.90	539.91
9	792.18	624.12	556.78
10	847.40	656.20	644.14

panel. If the free vibration results of 0/c/0 honeycomb core sandwich panel is compared with the case [(Al/c/Al)], there is no specific trend in terms of natural frequencies obtained, this can be attributed to difference in mode shapes of the panels due to different mass density and stiffness. In order to analyse the forced vibration response, the average root mean square velocity (V_{rms}) of the sandwich panel is calculated by harmonic excitation force of 1 N excited at a point where no nodal line exists. The panel is excited at the location of (0.75 m, 0.75 m) from the lower left corner of the plate. From the average rms velocity shown in Figure 4.1. From Figure 4.1, it is observed that resonant amplitude of V_{rms} of [(0/c/0)] FRP honeycomb core is high compared to other two cases. This can be attributed to less density and stiffness. Sound power level variation shown in Figure 4.2 indicates that the sound power level of [(Al/c/Al)] sandwich panel is slightly less compared to other two cases. However, one can observe that shift between the radiation mode is high for [(0/90/c/90/0)] sandwich panel. If the structure is very stiff, the shift in their natural frequencies will also be high. This effect makes [(0/90/c/90/0)] sandwich panel to have less radiation modes in the interested excitation frequency range. But due to its low density, the sound power level at resonant amplitude is high for [(0/90/c/90/0)] and [(0/c/0)] sandwich panels compared to [(Al/c/Al)] panel. The effect of this radiation modes and shift in natural frequency on

sound power level can be clearly captured in octave band analysis as shown in Figure 4.3. From Figure 4.3, it is observed that, except in the frequency range 315-630, there is no significant change in the sound power level, even though in the V_{rms} and sound power level analysis, the resonance amplitude of aluminium honeycomb core sandwich panel is comparatively less. In octave band analysis there is no significant change in sound power level. This can be attributed to the reduced number of radiation modes for [(0/90/c/90/0)] and [(0/c/0)] sandwich panel in the excitation frequency range. To study the effect of transmission behavior of honeycomb core sandwich panel, a plane acoustic pressure with an amplitude of 1 N/m^2 is applied on the surface of the panel and investigated for normal incidence and results are given in Figure 4.4. From Figure 4.4, one can observe that, effect of mass is clearly seen, high mass associated with [(Al/c/Al)] sandwich panel results in high sound transmission loss at high frequencies and due to low stiffness it has low sound transmission loss in low frequencies compared to other two cases.

Sound pressure directivity pattern obtained at 100 Hz and 600 Hz are shown in Figure 4.5 and Figure 4.6 respectively. Directivity pattern at 100 Hz indicates that [(Al/c/Al)] panel radiates more sound compared to the other two panels. This is due to closeness of fundamental natural frequencies of [(Al/c/Al)] panel to the excitation frequency. However, directivity pattern obtained at 600 Hz indicates that [(0/90/c/90/0)] panel radiates more sound. This can be attributed to more number of sound radiation modes available for the [(0/90/c/90/0)] panel.

4.3.2 The Influence of Boundary condition

In this section, the effect of boundary condition on vibro-acoustic response and sound transmission loss characteristics of Epoxy/Graphite FRP honeycomb core sandwich panel is studied. In this analysis, damping and mass of the panel are kept constant as the purpose of this study is to investigate the effect of stiffness by varying the boundary conditions. For this purpose, layered Epoxy/Graphite [(0/90/c/90/0)] is considered.

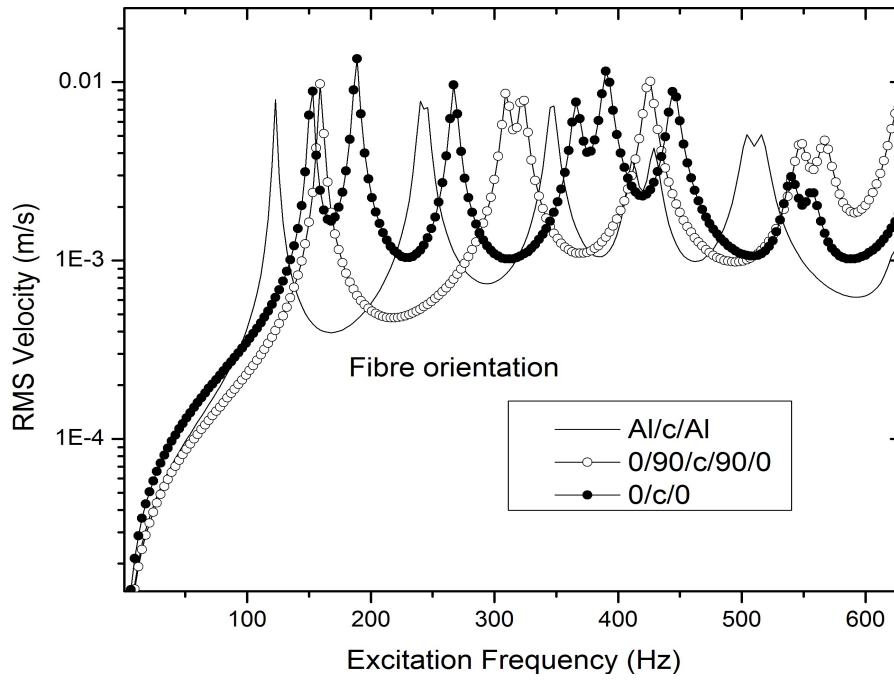


Figure 4.1: The effect of fibre orientation of FRP on average rms velocity

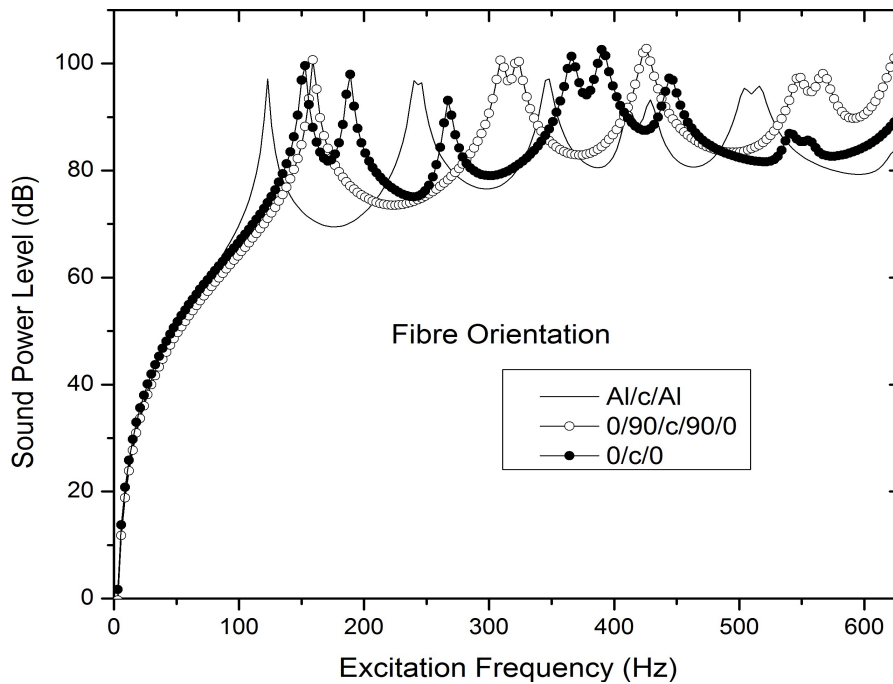


Figure 4.2: The effect of fibre orientation of FRP on Sound power level

The boundary conditions analysed in this section are CCCC,SSSS,CSCS. (Note: C refers clamped, S refers simply supported). Natural frequencies of first 10 modes asso-

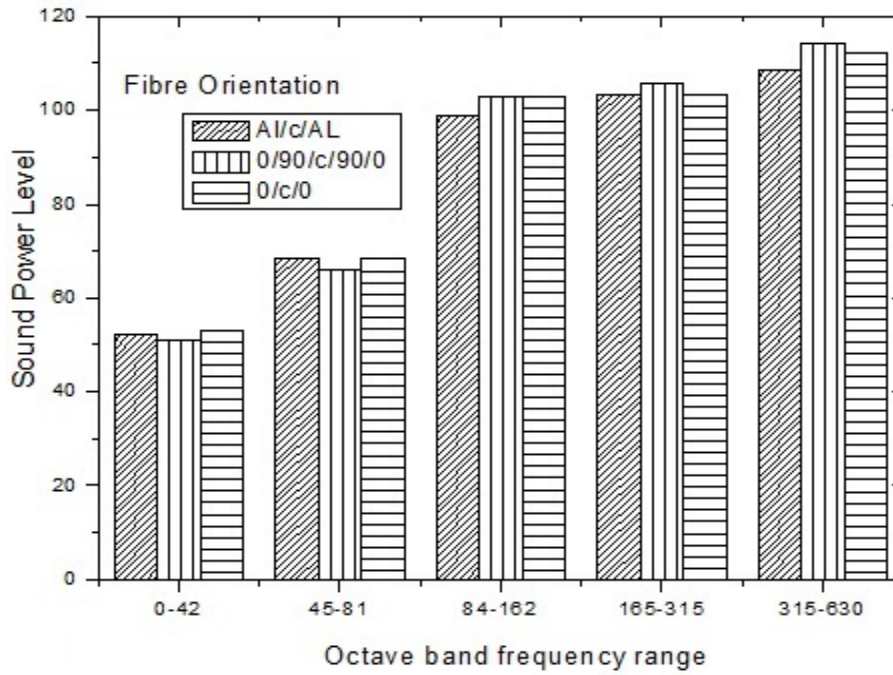


Figure 4.3: The effect of fibre orientation of FRP on octave band frequency range

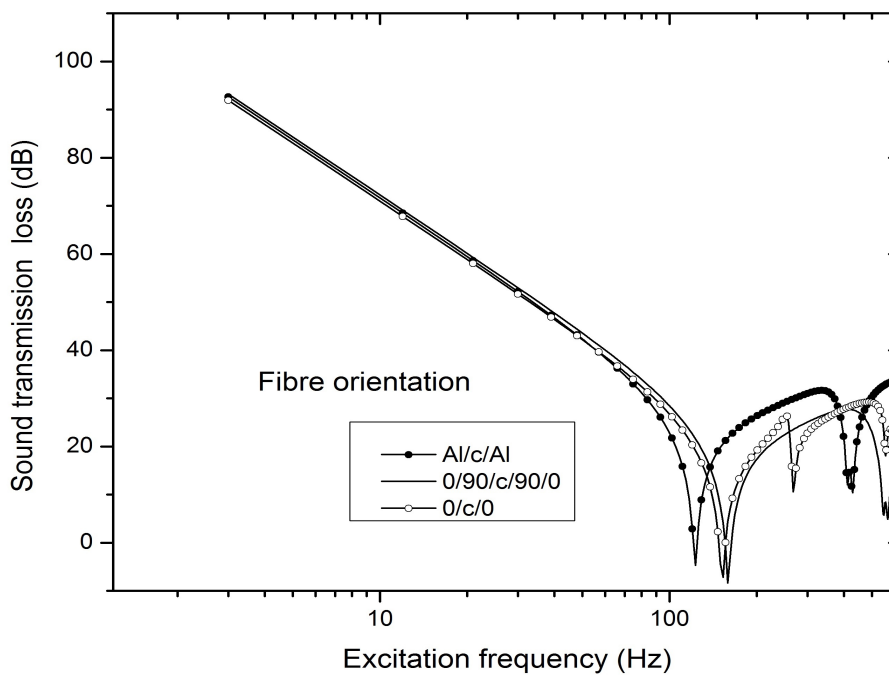


Figure 4.4: The effect of fibre orientation of FRP on sound transmission loss

ciated with the three different boundary conditions are given in Table 4.4. From Table 4.4 it is clear that, natural frequency of CCCC is high compared to SSSS and CSCS

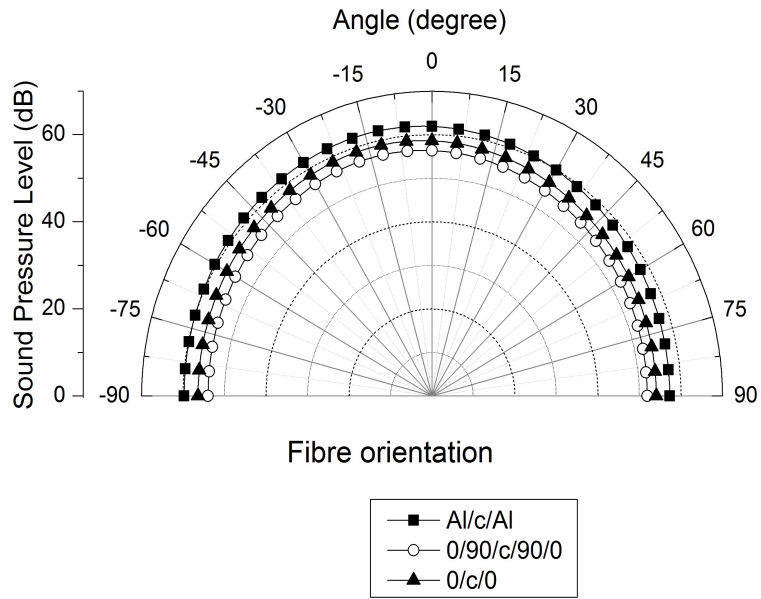


Figure 4.5: The effect of fibre orientation of FRP on sound pressure level at 100 Hz

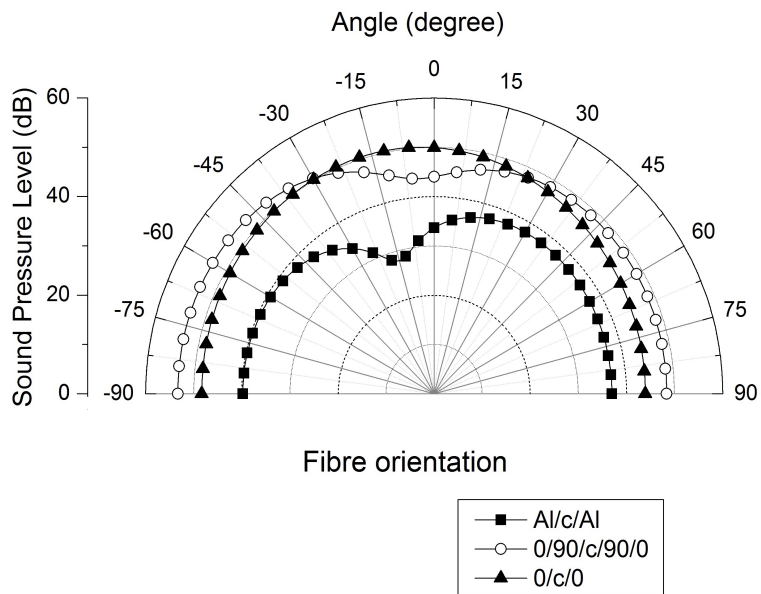


Figure 4.6: The effect of fibre orientation of FRP on sound pressure level at 1000 Hz

due to the fact that increase in stiffness in CCCC for the structure with same geometric conditions. The effect of boundary condition on forced vibration is shown in Figure 4.7. From Figure 4.7 it is clear that the average rms velocity is higher for SSSS case because of its poor stiffness. This can be clearly seen in the lower excitation frequency range.

Table 4.4: The influence of boundary condition on natural frequency (Hz)

Mode	Boundary condition		
	CCCC	SSSS	CSCS
1	151.95	76.161	147.43
2	188.30	111.67	168.67
3	267.12	187.06	225.78
4	366.05	265.13	327.40
5	390.51	288.23	363.72
6	390.58	302.19	380.16
7	444.94	339.95	419.54
8	539.91	430.56	473.19
9	556.78	456.44	494.28
10	644.14	543.12	612.97

The effect of boundary condition on sound power level is shown in Figure 4.8. From Figure 4.8 it is very clear that number of radiation modes for CCCC is very less compared to other two cases due to its higher stiffness. The effect of lesser radiation modes on sound power radiated can be clearly seen in octave band analysis as shown in Figure 4.9. Significant variation in sound power level due to variation in structural boundary condition can be observed in low frequency bands. This clearly indicates the effect of structural boundary condition on sound radiation characteristics. Sound transmission loss behavior is shown in Figure 4.10. The effect of stiffness is clearly seen below first natural frequency and also in mass controlled region. Due to increase in stiffness for CCCC, it does not have many dips in STL, there by maintaining high transmission loss compared to other two cases. Sound pressure directivity pattern obtained at 100 Hz and 600 Hz are shown in Figure 4.11 and Figure 4.12 respectively. Directivity pattern at 100 Hz indicates that SSSS panel radiates more sound compared to the other two panels. This is due to the closeness of fundamental natural frequencies of SSSS panel to the excitation frequency. However, directivity pattern obtained at 600 Hz indicates that CSCS panel radiates more sound. This can be attributed to more number of sound radiation modes available for the CSCS panel.

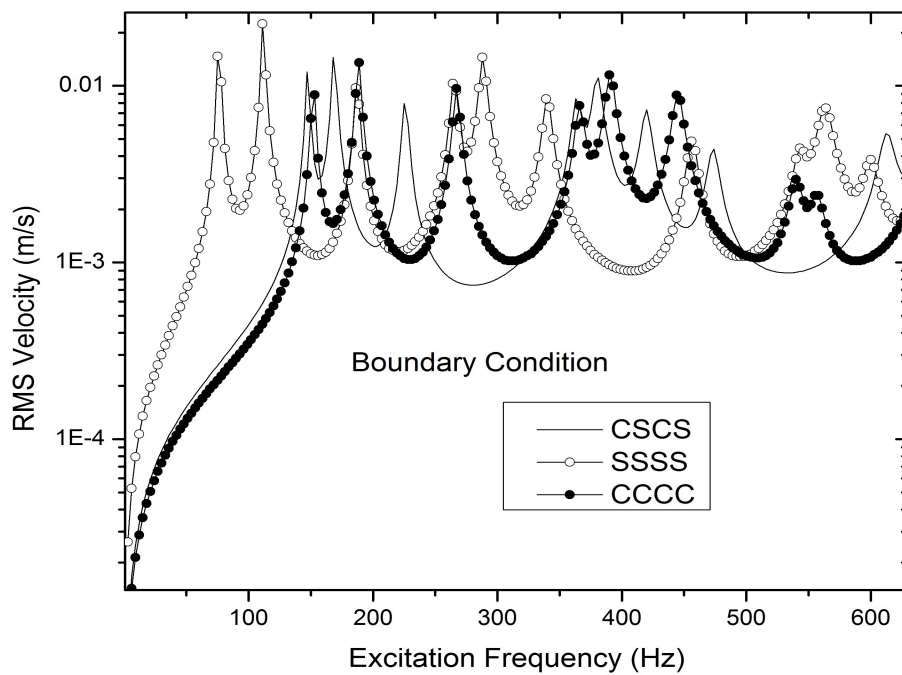


Figure 4.7: The effect of boundary condition on average rms velocity

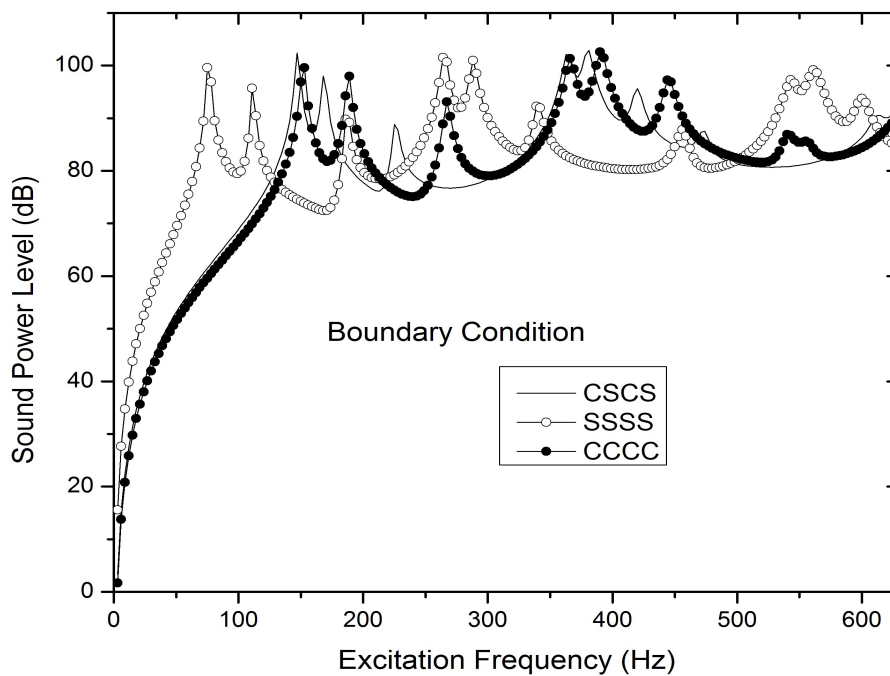


Figure 4.8: The effect of boundary condition on sound power level

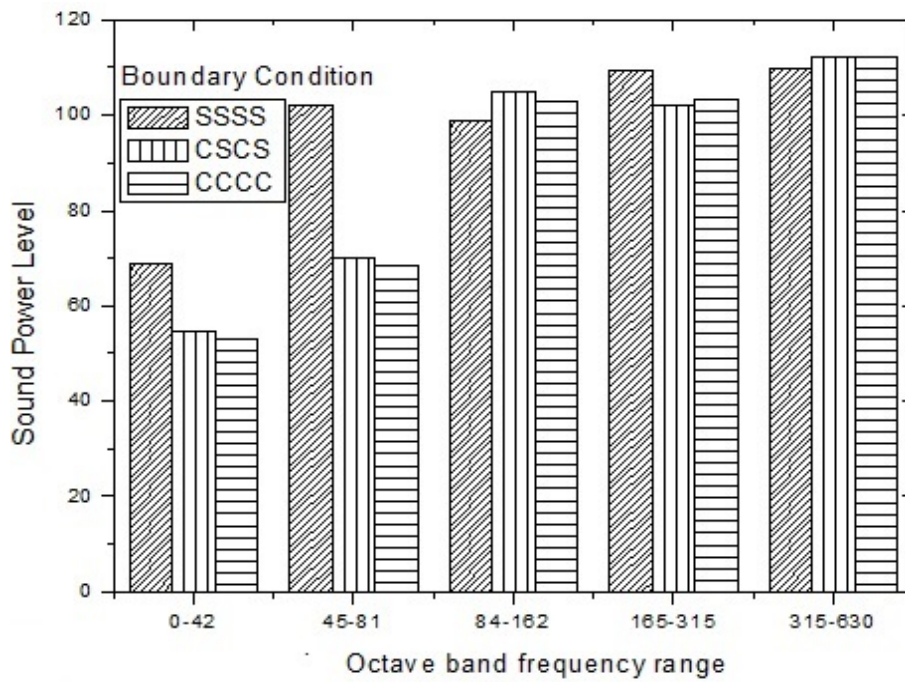


Figure 4.9: The effect of boundary condition on octave band frequency range

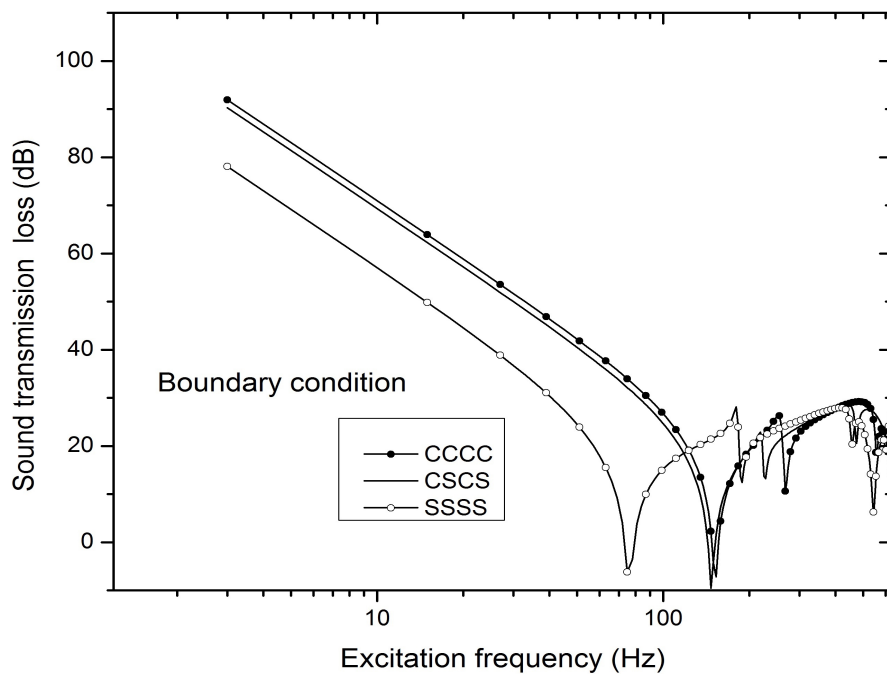


Figure 4.10: The effect of boundary condition on sound transmission loss

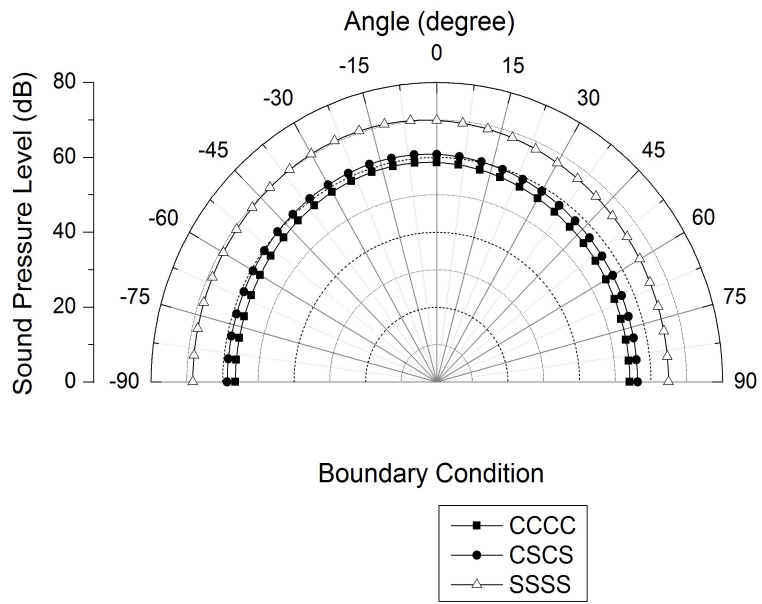


Figure 4.11: The effect of boundary condition on sound pressure level at 100 Hz

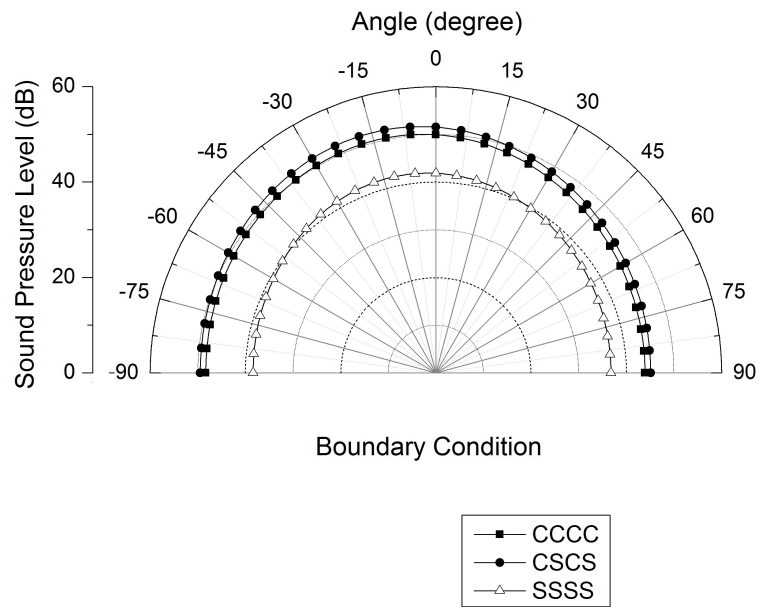


Figure 4.12: The effect of boundary condition on sound pressure level at 1000 Hz

4.4 The effect of Inherent Material Damping

In this section, the effect of material damping of FRP on sound radiation and transmission loss behavior of honeycomb core sandwich panel with FRP facing is presented. In FRP composites fibre provides the stiffness and damping is provided by the fibre matrix interaction during the vibration. It is assumed that FRP facing is made of Graphite/Epoxy material with following elastic properties given by Oh Oh (2008). $E_x = 119(1+i0.00118)$ GPa, $E_y = 8.67 (1+i0.0062)$ GPa, $G_{xy} = G_{xz} = 5.18 (1+i0.00812)$ GPa, $G_{yz} = 3.9 (1+i0.00846)$ GPa, $\mu_{xy} = 0.31$, $\rho = 1570 \text{ kg/m}^3$. Here, the layered Epoxy/Graphite FRP (0/90/c/90/0) with CCCC boundary condition is chosen based on the stiffness analysis carried out in the previous section. Modal damping ratio associated with the free vibration modes available in the chosen excitation frequency range are calculated based on Equation 4.7 and it is shown in Table 4.5. This is carried out to include the inherent material damping effect of FRP laminates in the numerical analysis. These calculated modal damping ratios are used to form the damping matrix given in Equation 2.5 which is later used to calculate the forced vibration response. Sound

Table 4.5: Natural frequency (Hz) and Damping ratio (ζ) of Epoxy/Graphite FRP [(0/90/c/90/0)]

Mode	Epoxy/Graphite FRP (0/90/c/90/0)	
	Natural frequency (Hz)	Damping ratio (ζ)
1,1	129.08	0.0495
1,2	164.67	0.0848
1,3	240.09	0.0953
2,1	317.60	0.1016
2,2	341.57	0.1369
1,4	356.39	0.1507
3,3	394.30	0.1376
2,4	485.49	0.1469
1,5	512.24	0.1587
3,1	572.39	0.1944

radiation and transmission behavior of Epoxy/Graphite FRP [(0/90/c/90/0)] honeycomb core sandwich panel with and without damping is compared with that of aluminium

honeycomb core sandwich panel [(Al/c/Al)]. Forced vibration response shown in Figure 4.13, clearly indicates that the resonance amplitude of average root mean square velocity (V_{rms}) of Epoxy/Graphite FRP [(0/90/c/90/0)] with damping is less compared to other two cases. Sound power level shown in Figure 4.14 indicates that sound power level obtained for Epoxy/Graphite FRP [(0/90/c/90/0)] with damping is less, but still at anti resonant frequencies, sound power level of [(Al/c/Al)] sandwich panel is less. This variation of sound power level can be clearly seen in octave band analysis shown in Figure 4.15. From Figure 4.15, it is very clear that the effect of damping is significant in all the frequency bands. Sound transmission behavior is shown in Figure 4.16. Calculated over all sound power level is shown in Table 4.6. From Table 4.6, it is clear that Epoxy/Graphite FRP [(0/90/c/90/0)] honeycomb core sandwich panel is radiating significantly lesser sound power. From Figure 4.16, the sound transmission loss of (Al/c/Al) is higher but in resonance frequencies, STL drops down. The STL behavior of Epoxy/Graphite FRP [(0/90/c/90/0)] with damping is lesser than that of (Al/c/Al) sandwich panel due to less density. In the damping region the transmission loss of Epoxy/Graphite FRP [(0/90/c/90/0)] with damping is high compared to other cases. The importance of damping on finding sound radiation and transmission characteristics is clearly shown in all analysis carried out in this section.

Table 4.6: The effect of inherent material damping on over all sound power level

Acoustic response	Epoxy/Graphite FRP [(0/90/c/90/0)]	Aluminium
Over all SPL(dB)	103.81734	109.99162

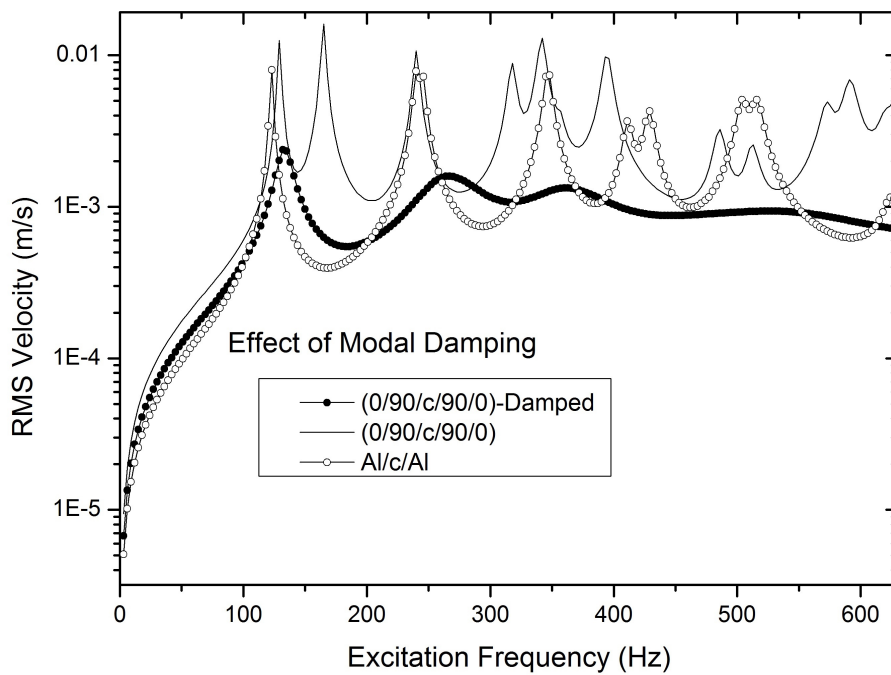


Figure 4.13: The effect of inherent material damping on average rms velocity

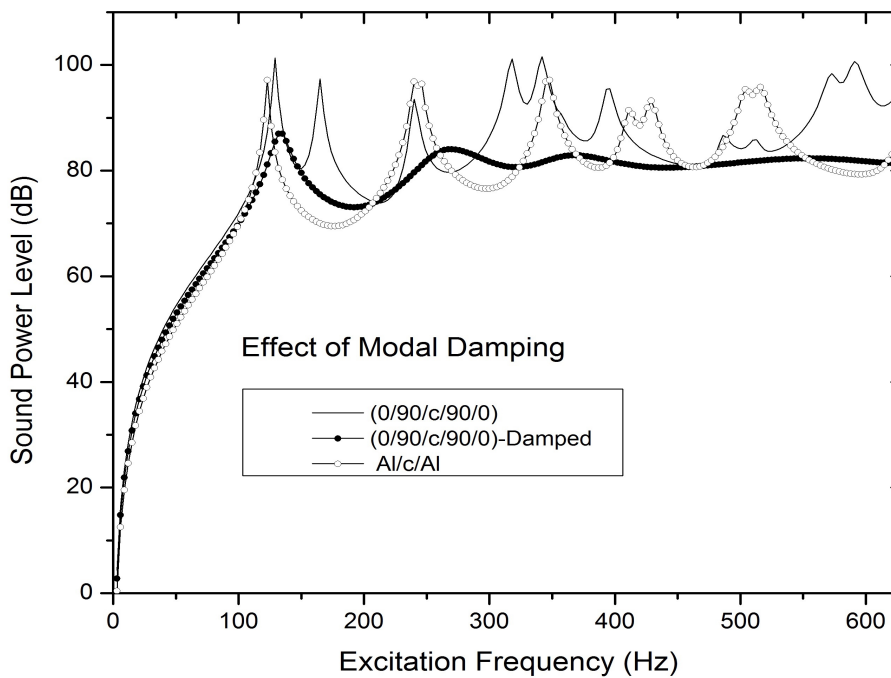


Figure 4.14: The effect of inherent material damping on Sound power level

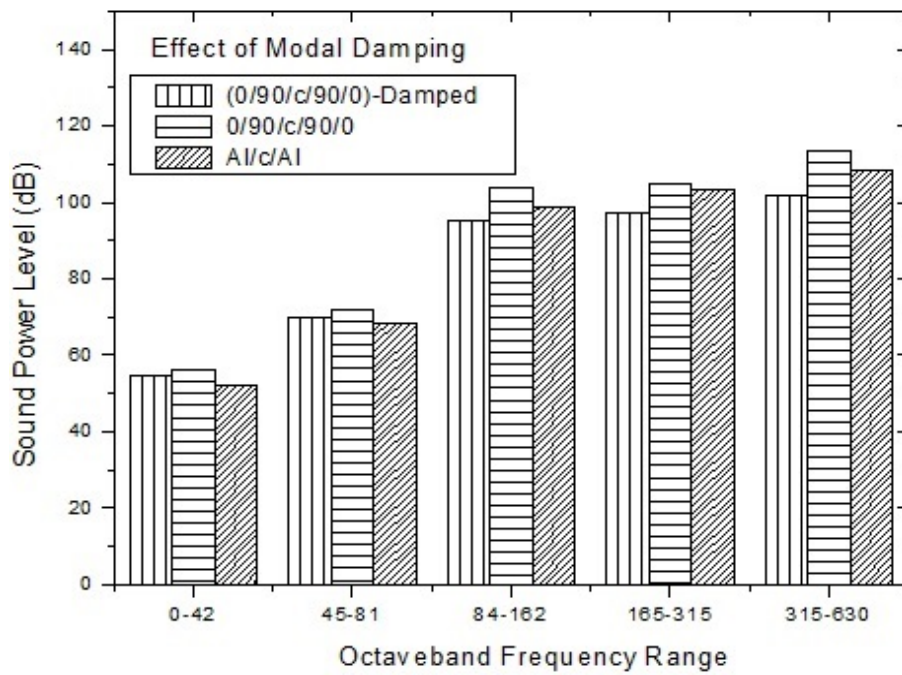


Figure 4.15: The effect of inherent material damping on octave band frequency range

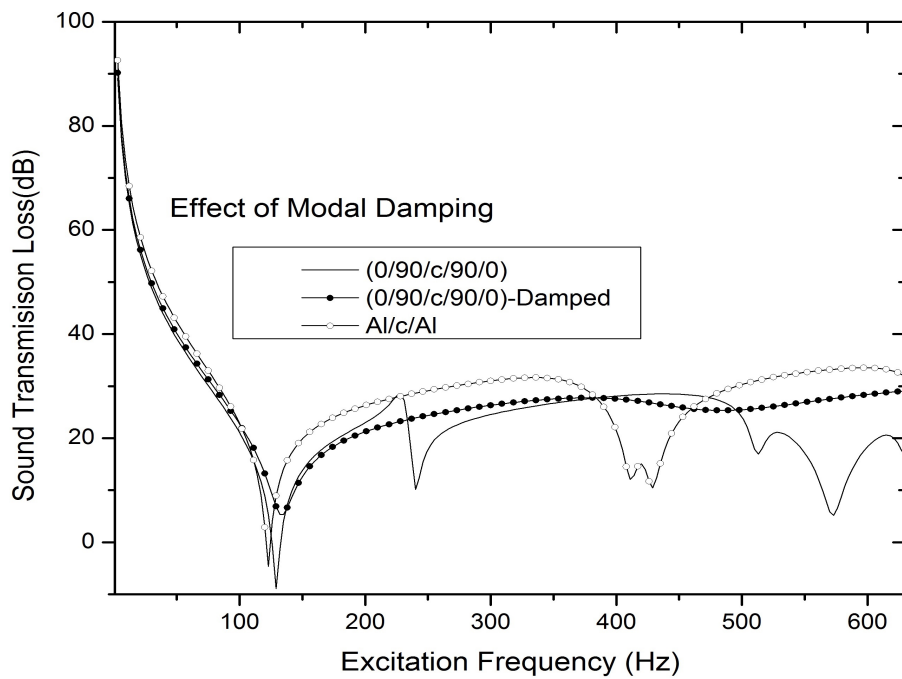


Figure 4.16: The effect of inherent material damping on sound transmission loss

4.5 Closure

A detailed investigation on the effect of inherent material damping on vibro-acoustic and sound transmission loss characteristic of honeycomb core sandwich panel with FRP facings is presented. Initially, from the calculated equivalent property of honeycomb core sandwich panel 2D finite element model is created using a SHELL 181 element available in ANSYS library. Here three layers are modelled as top core and bottom layers. Free and forced vibration response of sandwich panel is obtained from the 2D finite element model. The loss factor is calculated based on the modal strain energy method. The stiffness matrices are extracted from the commercial finite element analysis software ANSYS. Then the panel is excited at suitable location to predict the sound radiation behavior and also the panel is excited by applying a pressure to predict the transmission loss characteristics. The obtained forced vibration response is given as an input to the in-house developed Rayleigh integral MATLAB code to obtain the vibro-acoustic and transmission loss characteristics. It is clear that the aluminium honeycomb core sandwich panel can be replaced in to Epoxy/Graphite FRP [(0/90/c/90/0)] without losing acoustic comfort. If these Epoxy/Graphite FRP [(0/90/c/90/0)] honeycomb core sandwich panel are used it would avoid high transmission noises at resonance and also nearly 40% of the weight can be reduced compared to aluminium honeycomb core sandwich panel.

CHAPTER 5

STUDIES ON TRUSS CORE SANDWICH PANEL

5.1 Introduction

Investigation on influence of core topology on vibro-acoustic characteristics of truss core sandwich panel is carried out. The results are compared with the web core type sandwich panel. Here the web chosen is Z-section. Figure 5.1 shows the various truss core topology like trapezoidal, triangular, cellular and Z type core analysed in present work. Geometrical parameters for z core sandwich panel is shown in Figure 5.1 as t is thickness of face sheet, a_f is length of z, t_w is thickness of web, h is height of the core. The equivalent elastic properties for truss core sandwich panel are given in Equation 2.16. Equivalent stiffness properties for Z core sandwich panel are derived with the same assumptions used for deriving equivalent stiffness properties of truss core sandwich panel given by Fung *et al.* (1994) are summarized in Equation 5.1

$$\begin{aligned} D_x &= \frac{Eh^2t}{2(1-\gamma^2)} + \frac{E_c I_c}{2p}; \quad D_y = \frac{Eh^2t}{2(1-\gamma^2)} \\ D_{xy} &= \frac{1}{2}Gh^2t; \\ D_{Qx} &= G_c \frac{\left(\frac{h^2t}{2} + \frac{E_c I_c}{2pE}\right)ht_w}{s_c g - \frac{E_c}{24E}t_w g^3} \\ \left(\frac{1}{D_{Qy}}\right) &= \left[\frac{1-\gamma^2 p^2}{EI} \frac{1}{6}\right] + \left[\frac{1-\gamma_c^2}{E_c I_c} \left(\frac{pag^2}{h^2} + \frac{pg^3}{6h^2}\right)\right] \end{aligned} \tag{5.1}$$

where E and E_c are the elastic modulus of facing layer material and core material

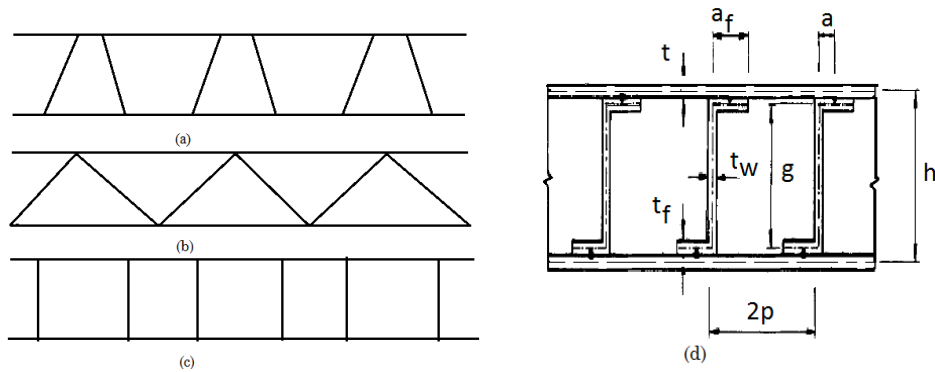


Figure 5.1: (a) Trapezoidal (b) Triangular (c) Cellular (d) Zed core sandwich panel

of the sandwich panel respectively. The geometrical parameters of truss core sandwich panel are shown in Figure 2.6. The geometrical parameters h , p , t and t_w are shown in Figure 5.1(d). I_f and I_c are the area moment of inertia of face sheet and core respectively. γ_x and γ_y are poisson's ratio along x and y axis respectively.

5.1.1 Equivalent Elastic Properties for Triangular, Trapezoid, Cellular and Z Core Sandwich Panel

An Aluminium sandwich panel of length 1.5 m and width 1.5 m with ten identical truss core sandwich units is compared with 20 discrete zed section sandwich unit in order to have the same representative number of core webs. To calculate the equivalent elastic properties for cellular and triangular core, it is assumed that f/p varies from $0 \leq f/p \leq 0.5$ for truss cores. In that, the ratio $f/p = 0$ corresponds to a triangular truss core, and $f/p = 0.5$ represents a cellular truss core. The dimensions of the sandwich panels as shown in Figure 2.6 and the thickness of plate are calculated in such a way that all the sandwich panels has the same cross sectional area in order to maintain the same weight. The dimensions are calculated and tabulated in Table 5.1 for the sandwich plate with the different types of core analysed.

Table 5.1: Dimension of zed core, cellular core, trapezoidal core and triangular core in mm

Different types of sandwich panels	parameter			
	p	d	f	$t = t_c$
Zed core	75	32.4	25	1.2
Cellular core	75	32.4	37.5	1.53
Trapezoidal core	75	32.4	22	1.42
Triangular core	75	32.4	0	1.19

The equivalent stiffness properties for truss and Z core are calculated based on the Equation 2.16 and Equation 5.1 respectively and the calculated values are listed in Table 5.2. From Table 5.2, it can be seen that E_x, E_y, G_{xy}, G_{xz} increases while the f/p ratio increases and the G_{yz} increases while the f/p ratio decreases. For example, $f/p = 0.5$ for cellular core, E_x, E_y, G_{xy}, G_{xz} is high for cellular core compared to other cases but G_{yz} is less for cellular core compared to other cases.

Table 5.2: Equivalent properties of zed core, cellular core, trapezoidal core, triangular core

Elastic constants	Type of core			
	Zed core	Cellular core	Trapezoidal core	Triangular core
E_x (Pa)	2.0287×10^{10}	2.0428×10^{10}	1.9546×10^{10}	1.7676×10^{10}
E_y (Pa)	1.5453×10^{10}	1.9334×10^{10}	1.8064×10^{10}	1.5383×10^{10}
G_{xy} (Pa)	5.8038×10^9	7.3915×10^9	6.8975×10^9	5.8391×10^9
G_{yz} (Pa)	4.1667×10^5	1.6636×10^6	3.1481×10^6	2.2778×10^8
G_{xz} (Pa)	5×10^8	5.2469×10^8	3.3642×10^8	1.5062×10^8
γ_{xy}	0.3	0.3	0.3	0.3
γ_{yz}	0.2285	0.2839	0.2773	0.2611

5.1.2 Vibration Response Characteristics

From the calculated elastic modulus and shear modulus for the panels with different core, an equivalent 2D FEM model is created for each case. Influence of nature of core on free vibration frequencies of the sandwich panel is given in Table 5.3. From Table 5.3, it is clear that, sandwich panel with triangular core has significantly higher natural frequencies compared to the sandwich panel with other type of cores. Natural

frequencies of the triangular core sandwich panel is greatly influenced by the increased transverse shear stiffness (D_{Qy}) as f/p ratio is zero for the triangular core sandwich panel. Influence of nature of core on the free vibration mode shapes of the sandwich panel is shown in Table 5.4 for some of the modes. From Table 5.4, it is clear that the stiffness values significantly influences the mode shape, especially for the triangular core panel, which in turn change the sound radiation characteristics. The frequency range of 0-630 Hz is chosen based on the coincidence frequency of the sandwich panel to compare the sound radiation characteristics. An appropriate location for excitation of the harmonic force is chosen based on the mode shapes of the equivalent orthotropic plate where it should not lie on the nodal lines of modes in the range of 0-630 Hz. The displacement and velocity responses associated with various truss core and zed core are obtained for the equivalent orthotropic plate.

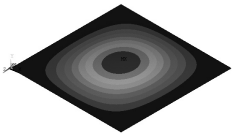
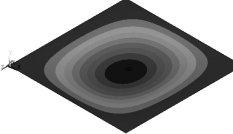
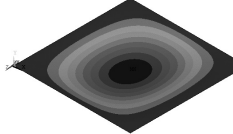
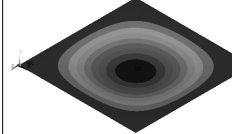
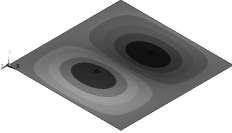
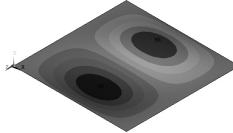
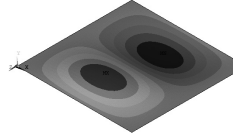
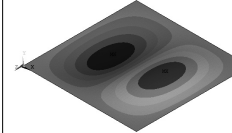
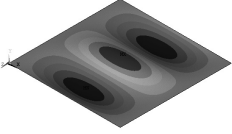
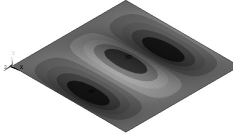
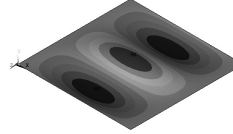
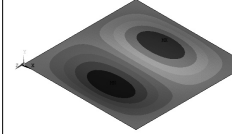
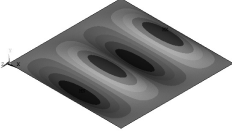
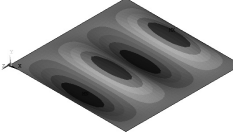
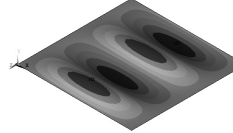
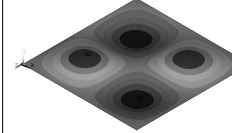
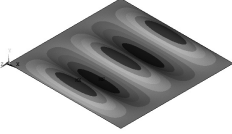
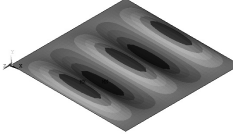
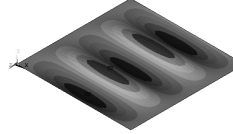
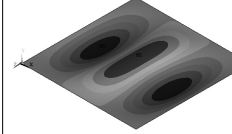
Table 5.3: Natural frequency (Hz) comparison of zed core, cellular core, trapezoidal core, triangular core

Mode	Type of core			
	Z	Cellular	Trapezoidal	Triangular
1	121.15	125.23	121.95	156.791
2	128.62	138.95	140.43	291.55
3	143.40	161.57	167.53	297.31
4	161.63	188.47	198.84	407.63
5	181.54	217.04	231.69	469.99

5.1.3 Acoustic Response Characteristics

Influence of various truss core and zed core on sound power level response and octave band wise sound power level is shown in Figure 5.2 and Figure 5.2 respectively. From Figure 5.2, the zed core sandwich panel has more number of radiation modes in the excitation frequency range 0-600 Hz there by high radiation efficiency and also shift in natural frequency is seen for triangular core because of high transverse shear stiffness. From Figure 5.2, one can observe that less sound power level for triangular core in

Table 5.4: The influence of nature of core on free vibration mode shapes of the sandwich panel

Mode	Type of core			
	Z	Trapezoid	Cellular	Triangle
1				
2				
3				
4				
5				

the lower frequency band because of high transverse shear stiffness. From the results, one can select triangular core for low frequency applications compared to trapezoidal, cellular and Z core (Refer Figure 5.2 and Figure 5.3). From Figure 5.4(c) and Figure 5.5 the sound radiation pattern level of zed core is high at 100 Hz and sound radiation pattern level of cellular core is high at 600 Hz. The result of radiated pattern level can be justified with respect to sound power level calculation shown in Figure 5.2.

Influence of various truss core and Z core on sound transmission loss variation is shown in Figure 5.6. From Figure 5.6 it is clear that, in stiffness controlled region the sound transmission loss of triangular core sandwich panel is high due to its increased transverse shear stiffness compared to other panels as shown in Table 5.2. This reflects

as a distinct variation of STL associated with triangular core in the stiffness region also. In mass controlled region, distinguished curve is not seen. Since STL is proportional to the mass, STL of all the panels is almost equal. This can be attributed to the equal weight associated with different core sandwich panels. In damping sensitive region, there is negative value in the first resonance frequency. The multiple peaks and valleys are seen in higher frequency range due to influence of damping effect at resonance frequencies. It is seen that the peaks and valleys for triangular core sandwich panel is less due to the shift in natural frequency due to higher stiffness. Due to less number of dips in STL, these triangular core sandwich panel has good acoustic performance in the frequency range 0-630 Hz. From the results observed in this analysis, one can select triangular core sandwich panel for low frequency application due to its increased transmission loss in stiffness sensitive region and also less dips in mass controlled region in STL. The STL variation with different core for normal and oblique incidents is observed. However the amplitude of STL is relatively high for the oblique incident due to the reduced applied pressure on plate compared to normal incidence.

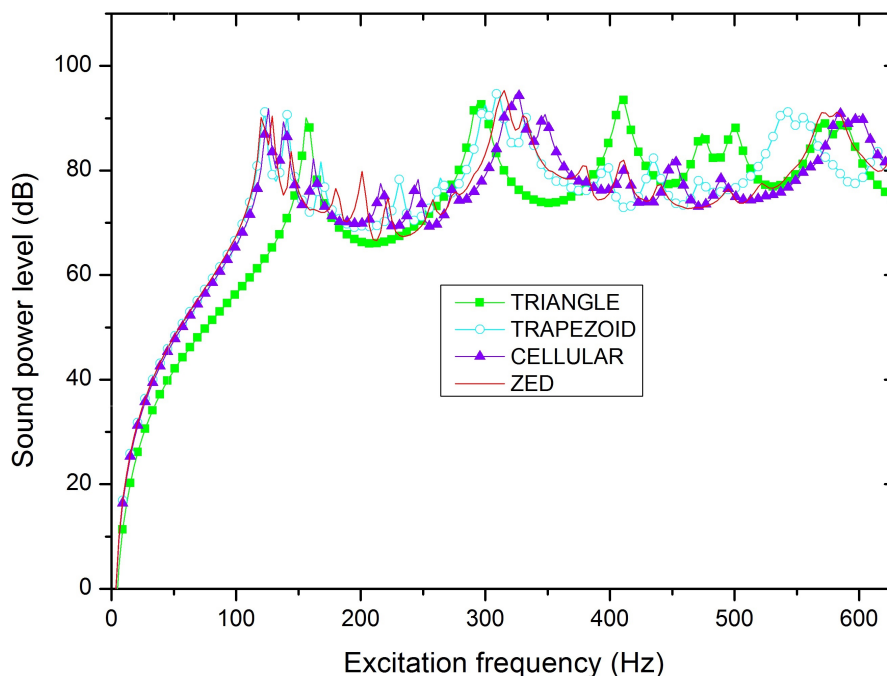


Figure 5.2: The effect of core topology of truss and zed core sandwich panel on Sound power level

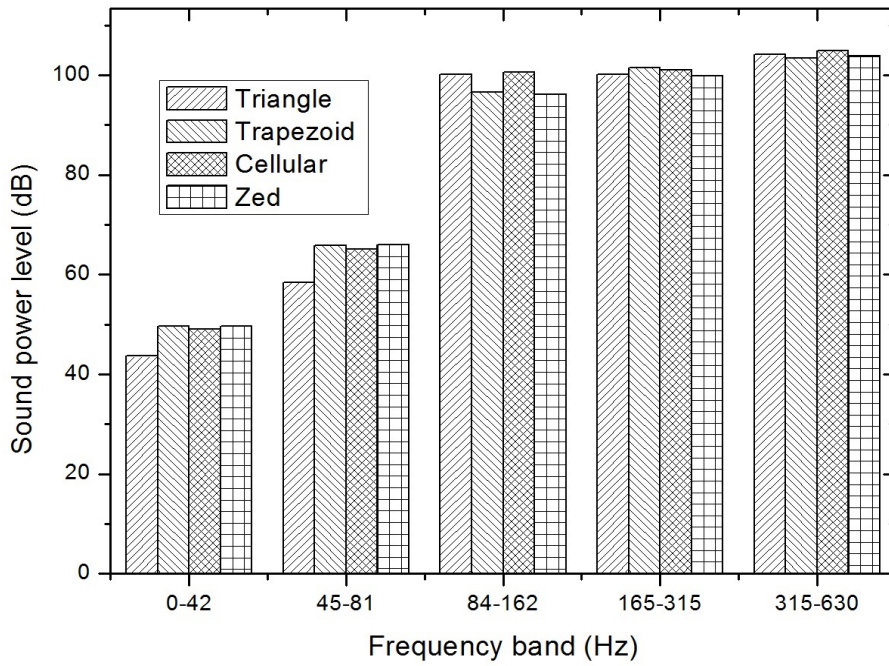
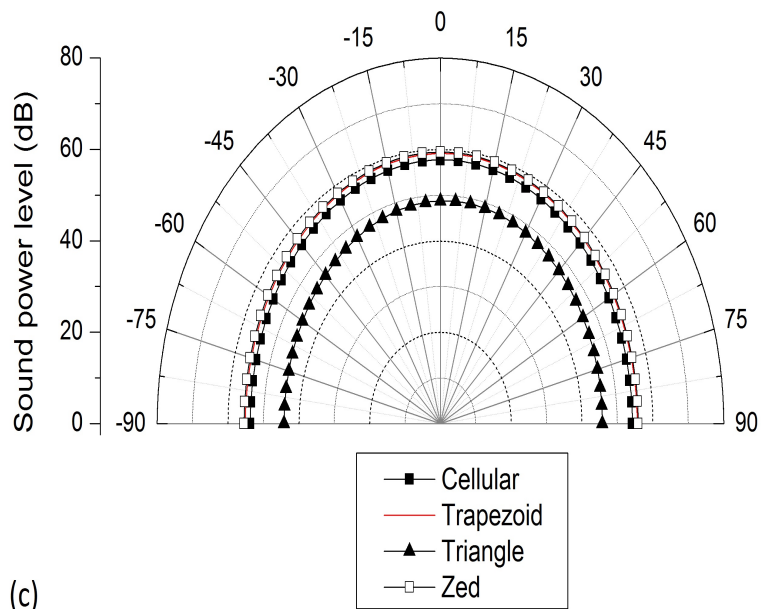
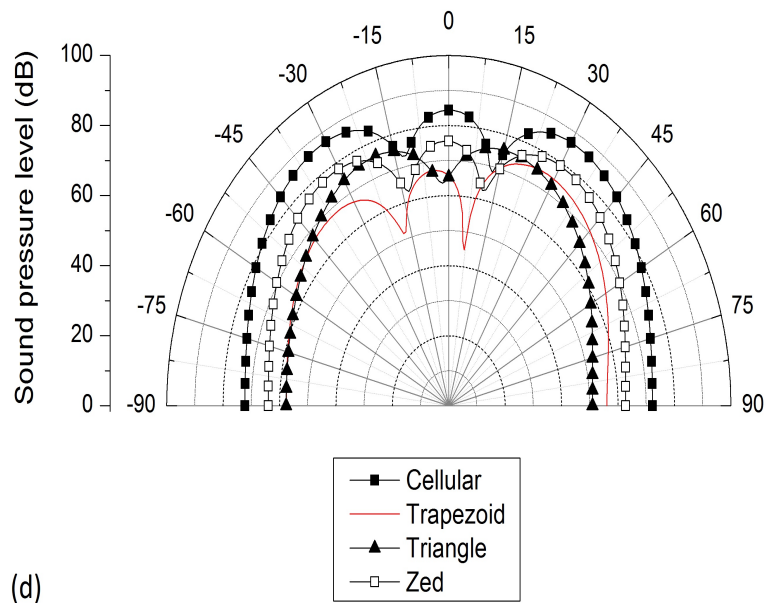


Figure 5.3: The effect of core topology of truss and zed core sandwich panel on octave band frequency range



(c)

Figure 5.4: The effect of core topology of truss and zed core sandwich panel on sound pressure level at 100 Hz



(d)

Figure 5.5: The effect of core topology of truss and zed core sandwich panel on sound pressure level at 600 Hz

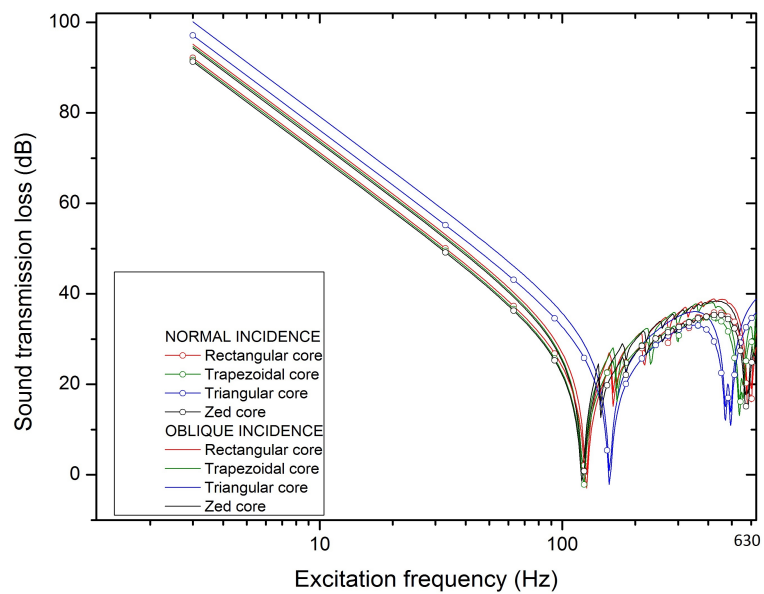


Figure 5.6: The effect of core topology of truss and zed core sandwich panel on sound transmission loss

5.2 Closure

A detailed investigation on the effect of core topology of truss core sandwich panel is presented. Initially, from the calculated equivalent property of truss and zed core sandwich panel 2D finite element model is created using the SHELL 181 element available in ANSYS library. Free and forced vibration response of sandwich panel is obtained from the 2D finite element model. The panel is excited at suitable location to calculate the sound radiation characteristic. Further, the panel is excited by applying a pressure to predict the transmission loss characteristics. From the results, it is clear that the triangular core sandwich panel may be suitable among the different core topologies of truss core sandwich panel for better acoustic comfort due to the increased transverse shear stiffness and reduced radiation modes in the interested frequency zone.

CHAPTER 6

STUDIES ON FOAM FILLED TRUSS CORE SANDWICH PANEL

6.1 Introduction

The effect of inherent material damping on vibro-acoustic and transmission loss behavior is studied in the previous chapter. In order to enhance the damping of sandwich panel further, this chapter focuses on the study of the effect of filling foam in the empty space of truss core sandwich panel. In order to achieve better acoustic comfort, most designers increase the thickness of face sheet or height of the core. In this way it increases the weight and also occupies more space. This drawback can be overcome by filling the foam in empty space of the core. Foams are lesser in weight compared to conventional metals and anticipated to provide better damping without altering the structural stiffness and mass of the panel significantly.

6.2 Formulation of Stiffness Properties for Foam Filled Truss Core Sandwich Panel

Schematic diagram of a truss core sandwich panel and different dimensions associated with unit cell of the foam filled truss core are shown in Figure 6.1(a) and Figure 6.1(b) respectively. The truss core unit can be re-modelled as a thick plate with equivalent elastic constants defined by seven parameters as given by Libove and Batdorf (1948): D_x and D_y are the bending stiffnesses in X and Y direction respectively, D_{xy} twisting

stiffness, D_{Q_x} and D_{Q_y} are the transverse shear stiffnesses, μ_x and μ_y are the bending Poisson's ratio in corresponding directions. The definition of the stiffness constants are obtained by considering the distortion of element under loading condition as shown in Figure 6.2.

By assuming only M_x is acting, the effect of M_x is to produce primary curvature $\frac{\partial^2 w}{\partial x^2}$ and also a secondary curvature $\frac{\partial^2 w}{\partial y^2}$ which is a Poisson effect.

$$D_x = \frac{-M_x}{\frac{\partial^2 w}{\partial x^2}} \quad (6.1)$$

μ_x is defined as the ratio of Poisson curvature to the primary curvature.

By assuming only M_y is acting, the effect of M_y is to produce primary curvature $\frac{\partial^2 w}{\partial y^2}$ and also a secondary curvature $\frac{\partial^2 w}{\partial x^2}$ which is a Poisson effect.

$$D_x = \frac{-M_y}{\frac{\partial^2 w}{\partial y^2}} \quad (6.2)$$

μ_y is defined as the ratio of Poisson curvature to the primary curvature.

Assuming all the forces and moments are zero and only M_{xy} is acting, the distortion produced is a twist $\frac{\partial^2 w}{\partial x \partial y}$, and D_{xy} is defined as the ratio of twisting moment to twist.

$$D_{xy} = \frac{M_{xy}}{\frac{\partial^2 w}{\partial x \partial y}} \quad (6.3)$$

The transverse shear stiffness D_{Q_x} is defined, when the shear (Q_x) acts on opposite faces of the element, the two faces along XZ plane are distorted by an angle γ_x (shear angle). Thus the shear stiffness D_{Q_x} is defined as the ratio of shear to shear angle

$$D_{Q_x} = \frac{Q_x}{\gamma_x} \quad (6.4)$$

The existent of $\frac{\partial Q_x}{\partial x}$ produces a curvature.

$$\frac{\partial Q_x}{\partial x} = D_{Q_x} \frac{\partial^2 w}{\partial x^2} \quad (6.5)$$

when Q_x is acting alone, the slope of the mid plane is given as $\gamma_x = \frac{\partial w}{\partial x}$.

Similarly D_{Q_y} is defined as

$$D_{Q_y} = \frac{Q_y}{\gamma_y} \quad (6.6)$$

when Q_y is acting alone, the slope of the mid plane is given as $\gamma_y = \frac{\partial w}{\partial y}$ Finally from the above equations, equations for the curvature are given in Equation 6.7 from the force distortion relationship of a thick orthotropic plate.

$$\begin{aligned} \frac{\partial^2 w}{\partial x^2} &= -\frac{M_x}{D_x} + \gamma_y \frac{M_y}{D_y} + \frac{1}{D_{Q_x}} \frac{\partial Q_x}{\partial x} \\ \frac{\partial^2 w}{\partial y^2} &= \gamma_x \frac{M_x}{D_x} - \frac{M_y}{D_y} + \frac{1}{D_{Q_y}} \frac{\partial Q_y}{\partial y} \\ \frac{\partial^2 w}{\partial x \partial y} &= \frac{M_{xy}}{D_{xy}} + \frac{1}{2} \frac{1}{D_{Q_x}} \frac{\partial Q_x}{\partial x} + \frac{1}{2} \frac{1}{D_{Q_y}} \frac{\partial Q_y}{\partial y} \\ \gamma_x &= \frac{Q_x}{D_{Q_x}}; \quad \gamma_y = \frac{Q_y}{D_{Q_y}} \end{aligned} \quad (6.7)$$

where Q_x and Q_y are internal shear forces, M_x and M_y are internal bending moments and M_{xy} is the internal twisting moment. where $\frac{\partial^2 w}{\partial x^2}$, $\frac{\partial^2 w}{\partial y^2}$ are curvatures and $\frac{\partial^2 w}{\partial x \partial y}$ is twist about the middle plane. γ_x and γ_y are the transverse shear strains. The governing

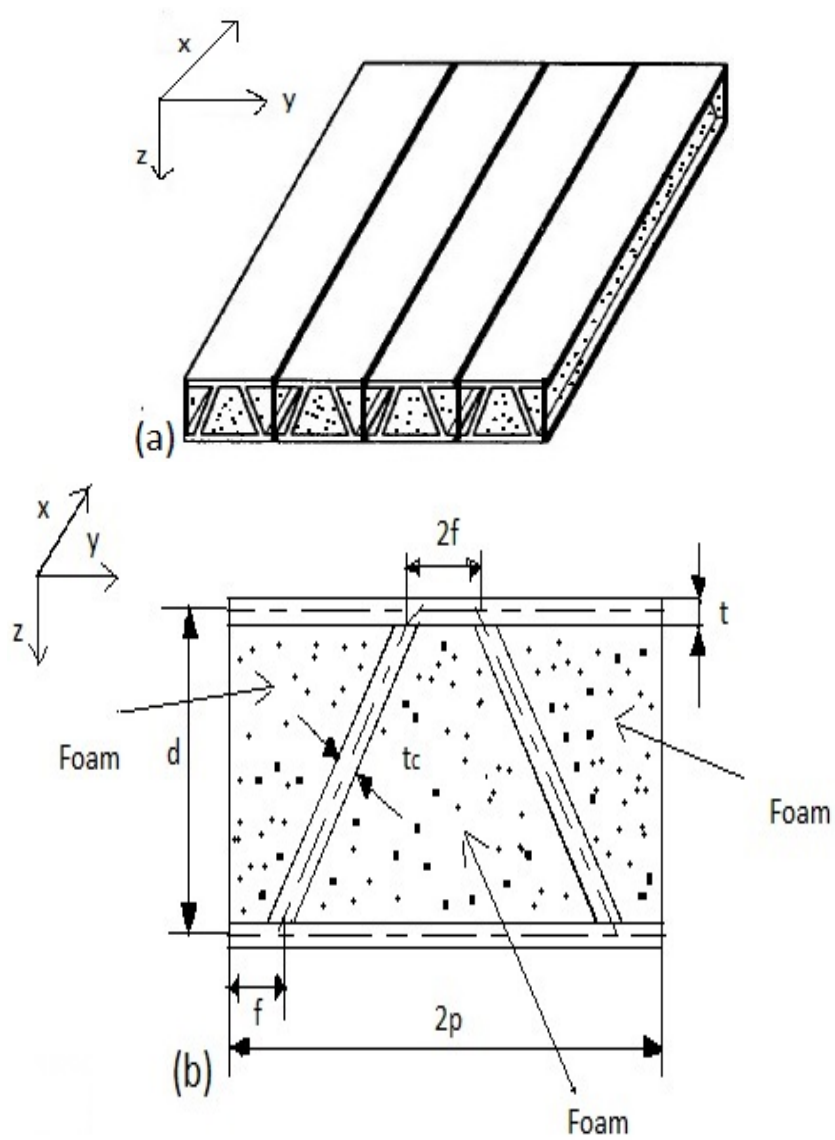


Figure 6.1: (a) Schematic diagram of foam filled truss core sandwich panel, (b) Dimensions of unit foam filled truss core sandwich panel

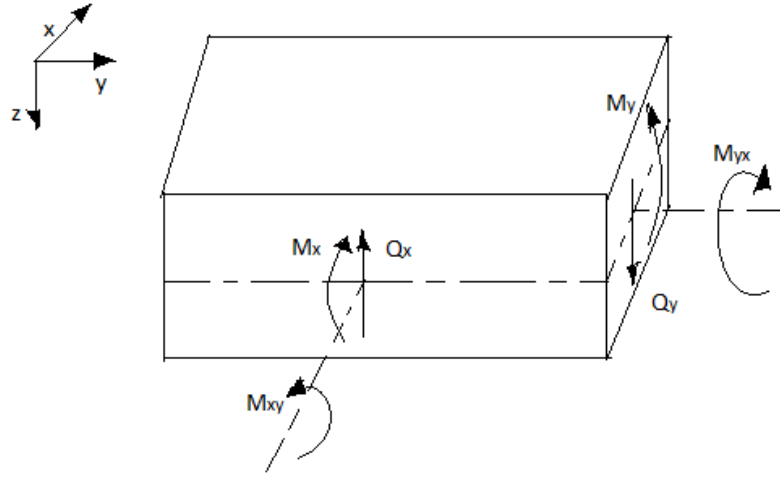


Figure 6.2: Forces and moments acting on an equivalent element of a panel

differential equation for the dynamic analysis of orthotropic plate are given as follows

$$\begin{aligned}
 D_{Qx} \left(\frac{\partial^2 w}{\partial x^2} - \frac{\partial \theta_x}{\partial x} + D_{Qy} \left(\frac{\partial^2 w}{\partial y^2} \right) - \frac{\partial \theta_y}{\partial y} \right) + q &= \rho h \frac{\partial^2 w}{\partial t^2} \\
 D_{Qx} \left(\frac{\partial w}{\partial x} - \theta_x \right) + \frac{D_{xy}}{2} \left(\frac{\partial^2 \theta_x}{\partial y^2} + \frac{\partial^2 \theta_y}{\partial x \partial y} \right) + \frac{D_x}{1 - \mu_x \mu_y} \left(\frac{\partial^2 \theta_x}{\partial x^2} + \mu_y \frac{\partial^2 \theta_y}{\partial x \partial y} \right) &= J_x \frac{\partial^2 \theta_x}{\partial t^2} \\
 D_{Qy} \left(\frac{\partial w}{\partial y} - \theta_y \right) + \frac{D_{xy}}{2} \left(\frac{\partial^2 \theta_y}{\partial x^2} + \frac{\partial^2 \theta_x}{\partial x \partial y} \right) + \frac{D_y}{1 - \mu_x \mu_y} \left(\frac{\partial^2 \theta_y}{\partial y^2} + \mu_x \frac{\partial^2 \theta_x}{\partial x \partial y} \right) &= J_y \frac{\partial^2 \theta_y}{\partial t^2}
 \end{aligned} \tag{6.8}$$

where w is the displacement at a point in the plate along the Z direction; θ_x and θ_y are rotations of the normal of the plate with respect to the Y and X axis respectively; J_x and J_y are moments of inertia per unit area of plate respectively and t denotes time, q is load per unit area. Equation 6.8 is first order shear deformation theory, where transverse shear strain is constant through the thickness. Equation 6.8 is solved to predict the dynamic behavior of the orthotropic plate by incorporating the boundary conditions. The assumptions adopted for deriving the elastic properties are as follows

- Deformation of the panel is small.

- Elastic modulus of the equivalent plate in the Z direction is assumed infinite. Local buckling of the facing plates does not occur and overall thickness of the panel remains constant.
- Truss core contributes to the panel flexural stiffness in the X direction but not in the Y direction.
- The facing plates are thin compared to the core thickness.
- During distortion of the panel, straight lines normal to the middle plane of the plate remain straight but not normally to the middle plane.
- Panel width in the y-direction is many times the unit pitch $2p$.

6.2.1 Bending Stiffnesses D_x and D_y

Forces and moments acting on a foam filled truss core unit cell with stiff isotropic material facing layers are given in Figure 6.3. Elastic modulus, shear modulus and Poisson's ratio of the stiff layer are E , G and μ respectively. It is assumed that under the action of bending moments M_x and M_y , vertical line associated with the cross section in middle surfaces of upper and lower facing plate remains perpendicular. This develops strains in the middle surfaces of the facing sheets in X and Y directions. Then the curvature can be written as

$$\frac{\partial^2 w}{\partial x^2} = \frac{\varepsilon_{x2} - \varepsilon_{x1}}{d}; \quad \frac{\partial^2 w}{\partial y^2} = \frac{\varepsilon_{y2} - \varepsilon_{y1}}{d} \quad (6.9)$$

Where ε_{x1} and ε_{x2} , are the strain in X direction of the lower and upper face sheets respectively. similarly ε_{y1} and ε_{y2} are the strain in Y direction of the lower and upper face sheets respectively.

In the absence of foam, the moment M_y is resisted only by the extensional stiffness of the facing plates. The normal stresses developed in Y direction, as a result of bending by M_y , in the middle surfaces of the upper and lower face sheets can be given as

$$\sigma_{y1} = \frac{M_y}{td}; \quad \sigma_{y2} = -\frac{M_y}{td} \quad (6.10)$$

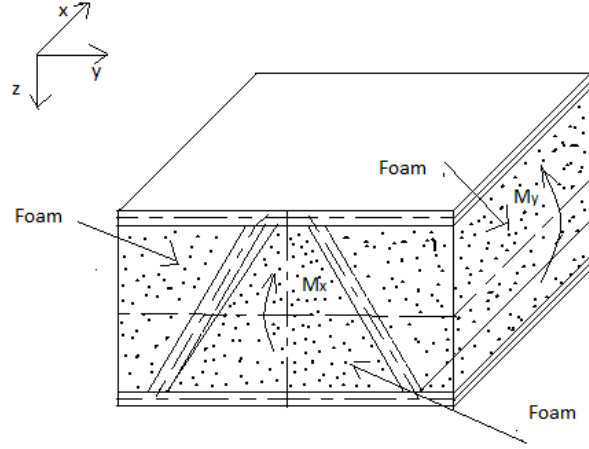


Figure 6.3: Forces and moments acting on foam filled truss core unit cell.

However, the moment M_x is resisted by both the bending stiffness of the core and extensional stiffness of the facing plates. Then the moment M_x for truss core alone can be written as

$$M_x = \sigma_{x1} \frac{td}{2} - \sigma_{x2} \frac{td}{2} - EI_c \frac{\partial^2 w}{\partial x^2} \quad (6.11)$$

Then the moment M_x for foam filled truss core can be written as

$$M_x = \left[\sigma_{x1} \frac{td}{2} \right] - \left[\sigma_{x2} \frac{td}{2} \right] - \left[EI_c + E_{Fo}(I_t - (I_c + \frac{td^2}{2})) \right] \frac{\partial^2 w}{\partial x^2} \quad (6.12)$$

where σ_{x1} and σ_{x2} are the stresses in the X direction in the middle surfaces of the lower and upper face plates respectively. I_c is the moment of inertia of web core and I_t is the moment of inertia per unit width of the cross section in YZ plane about the bending neutral axis.

The strains in the top and bottom face sheets along the X and Y directions are given by

$$\begin{aligned} \varepsilon_{x1} &= \frac{1}{E}(\sigma_{x1} - \gamma\sigma_{y1}); & \varepsilon_{x2} &= \frac{1}{E}(\sigma_{x2} - \gamma\sigma_{y2}); \\ \varepsilon_{y1} &= \frac{1}{E}(\sigma_{y1} - \gamma\sigma_{x1}); & \varepsilon_{y2} &= \frac{1}{E}(\sigma_{y2} - \gamma\sigma_{x2}) \end{aligned} \quad (6.13)$$

From Equation 6.9 to Equation 6.13, the moment-curvature relationship of the unit truss alone cell can be written as

$$\frac{\partial^2 w}{\partial x^2} = -\frac{M_x}{E(I_c + \frac{td^2}{2})} + \frac{\gamma M_y}{E(I_c + \frac{td^2}{2})} \quad (6.14)$$

$$\frac{\partial^2 w}{\partial y^2} = \frac{\gamma M_x}{E(I_c + \frac{td^2}{2})} - \frac{1 - \frac{\gamma^2 I_c}{td^2}}{E \frac{td^2}{2}} \quad (6.15)$$

Also from Equation 6.9 to Equation 6.13, the moment-curvature relationship of the unit cell filled with foam can be written as

$$\frac{\partial^2 w}{\partial x^2} = -\frac{M_x}{E(I_c + \frac{td^2}{2}) + E_{Fo}(I_t - (I_c + \frac{td^2}{2}))} + \frac{\gamma M_y}{E(I_c + \frac{td^2}{2}) + E_{Fo}(I_t - (I_c + \frac{td^2}{2}))} \quad (6.16)$$

Comparing Equation 6.16 with Equation 6.7, the equivalent bending stiffness and Poisson's ratios of the sandwich panel can be obtained as

$$D_x = E(I_c + \frac{td^2}{2}) + E_{Fo}(I_t - (I_c + \frac{td^2}{2})) \quad (6.17)$$

Comparing Equation 6.15 with Equation 6.7, the equivalent bending stiffness D_{xy} of the sandwich panel with out foam based on the assumption that truss contributes to the panel flexural stiffness in the X direction but not in the Y direction can be obtained as

$$D_y = \frac{EI_f}{1 - \frac{\gamma^2 I_c}{I_c + I_f}} \quad (6.18)$$

The bending stiffness of foam in Y direction can be derived as $E_{fo} \frac{d_c^3}{12}$. Where E_{fo} is Youngs modulus of the foam and d_c is the height of the foam. Then ,the bending stiffness D_y of the truss core foam filled sandwich panel can be written as

$$D_y = \frac{EI_f}{1 - \frac{\gamma^2 I_c}{I_c + I_f}} + E_{fo} \frac{d_c^3}{12} \quad (6.19)$$

6.2.2 Evaluation of Transverse Shear Stiffness (D_{Qx} and D_{Qy})

The total shear stiffness in the XZ plane can be given by sum of shear stiffness of truss and foam. The shear stiffness of truss is referred from Lok and Cheng (2000b) and it is summed up with the shear stiffness of foam. The transverse shear stiffness D_{Qx} of the foam is AG_{fo} (A - refers surface area). For unit width it is written as ($G_{fo}d_c$). Further, the transverse shear stiffness D_{Qx} of foam filled truss core can be written as

$$D_{Qx} = Gt_c \frac{\frac{d^2 t}{p s t_c} + \frac{1}{6} \left(\frac{d_c}{p} \right)^2}{\frac{t}{t_c} + \frac{s d_c}{3 p d}} + G_{fo} d_c \quad (6.20)$$

where G_{fo} is the shear modulus of foam.

Unit cell of a foam filled truss core sandwich panel subjected to transverse shear load is given in Figure 6.4(a). The shear displacements δ_y and δ_z of the foam filled truss core panel are shown in Figure 6.4(b). These displacements are proportional to transverse shear force Q_y . The average shear strain γ_y can be written as

$$\gamma_y = \frac{\delta_y}{d} + \frac{\delta_z}{p} \quad (6.21)$$

Thus, according to the definition of Equation 6.7 and utilising Equation 6.21, the equiv-

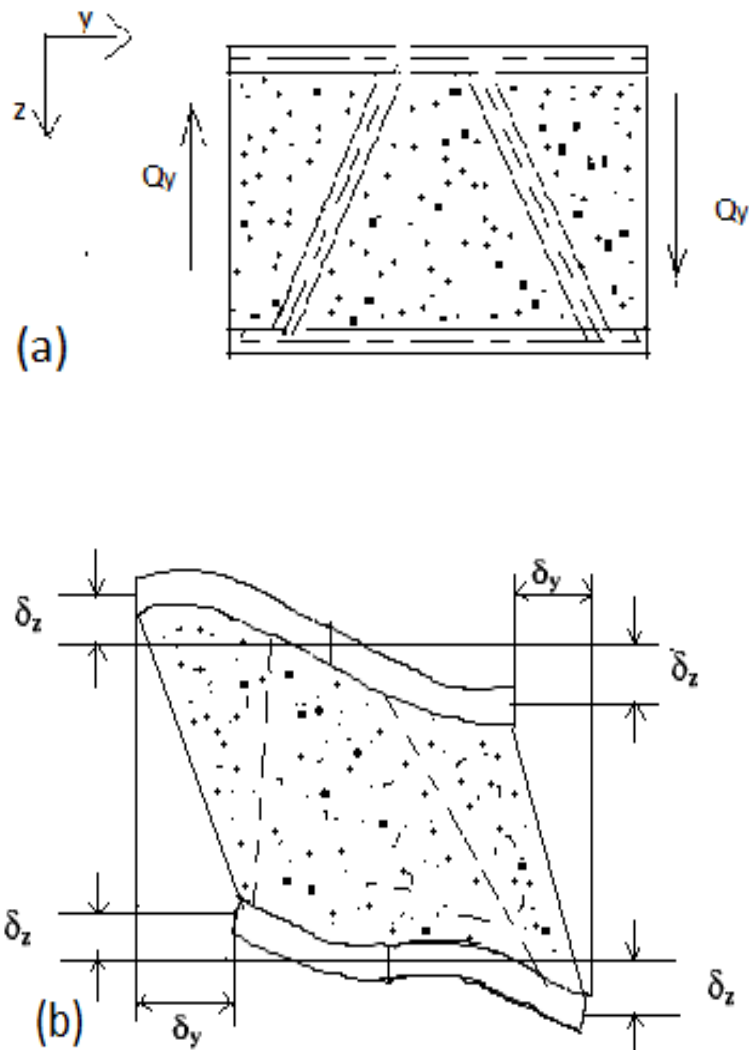


Figure 6.4: (a) Foam filled truss core sandwich panel subjected to transverse shear and
(b) Deformation due to transverse shear

alent transverse shear stiffness D_{Q_y} can be obtained as:

$$D_{Q_y} = \frac{Q_y}{\gamma_y} \quad (6.22)$$

The total transverse shear stiffness D_{Qy} can be given by sum of shear stiffness of truss and foam. Then the expression for shear stiffness can be written as

$$D_{Qy} = \frac{Q_y}{\frac{\delta_y}{d} + \frac{\delta_z}{p}} + G_{fo}d_c \quad (6.23)$$

(Note: $G_{xz} = G_{yz}$ for foam, So it is mentioned as G_{fo} in Equation 6.20 and 6.23).

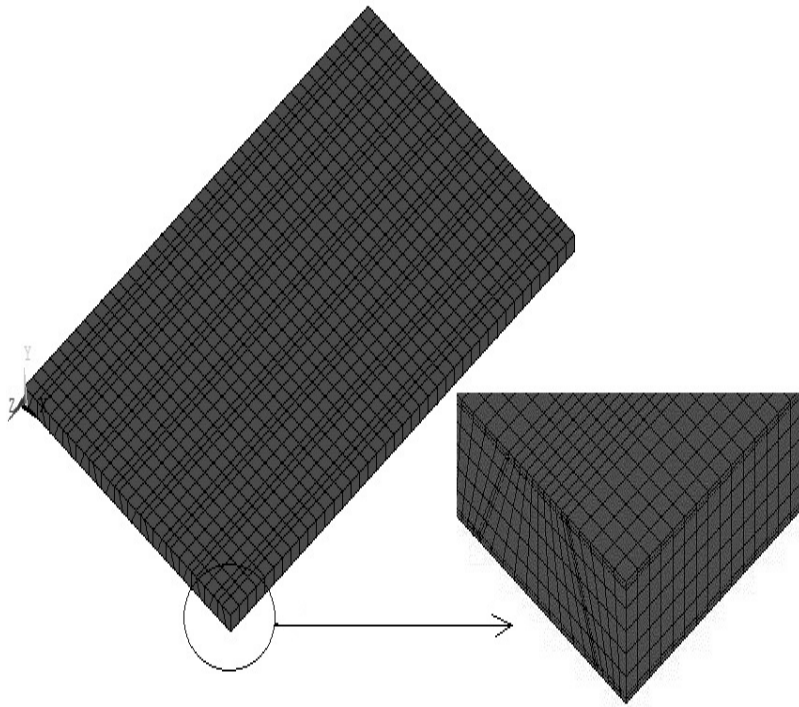
6.3 Validation for 2D Equivalent Model of Foam Filled Truss Core Sandwich Panel

The validity of the proposed 2D equivalent model is checked by comparing its results with the actual 3D model for free vibration characteristics. For this purpose, sandwich panel of length 2 m and width 1.2 m with eight identical truss core sandwich units is considered. Dimensions and properties of the unit cell shown in Figure 2.6 are: $p = 75$ mm, $f_0 = 25$ mm, $d = 46.75$ mm, $t_f = t_c = 3.25$ mm, $E = 80$ GPa, the Poisson ratio $\nu = 0.3$, and density $\rho = 2700$ kg/m³. It is assumed that empty spaces of a truss core panel is filled with Polyurethane foam (PUF). The material properties of PUF are Young's modulus 17×10^5 Pa and density 30 kg/m³ (Harne *et al.*, 2012). Here, the equivalent properties for 2D finite element model are calculated from the derived equivalent stiffness properties of foam filled truss core sandwich panel. In the 3D model mid surfaces associated with the stiff facing layers and webs are modelled using SHELL181 elements while the volume of the foam is modelled using SOLID185 elements. SHELL 181 is a four node layered structural shell element formulated based on first order shear deformation theory while SOLID185 is an eight noded structural solid element. In the case of equivalent 2D model, the mid surface of the entire foam filled panel is extracted (i.e., a rectangular area) and meshed with SHELL 181 elements. Finite element models of truss core panel filled with foam used for the 3D and equivalent 2D analysis are shown in Figure 6.5a and 6.5b respectively. Free vibration frequencies of the foam filled sand-

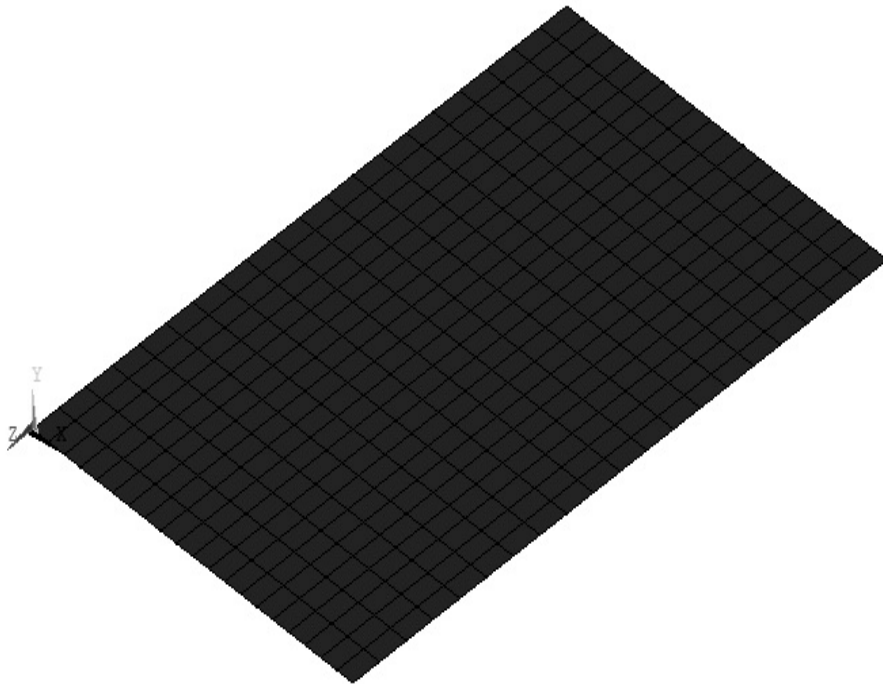
wich panel obtained from equivalent 2D finite element model are in good agreement with the frequencies calculated based on the 3D finite element model as seen in Table 6.1. Some of the free vibration mode shapes of the foam filled turss core sandwich panels obtained based on both the 3D and 2D finite element models are compared in Table 6.2 and found that there is no significant variation.

Table 6.1: Comparison of natural frequencies of foam filled truss core sandwich panel predicted by 3D and its equivalent 2D model.

Mode	Free vibration frequency (Hz)		
	3D Model	Equivalent 2D Model	absolute % error
1,1	134.04	134.51	0.3
2,1	209.15	206.14	1.4
1,2	272.42	280.21	2.8
3,1	291.41	288.38	0.2
2,2	330.21	338.15	1.0
4,1	372.04	372.22	0.04
3,2	405.20	410.33	1.2
5,1	450.47	452.82	0.5



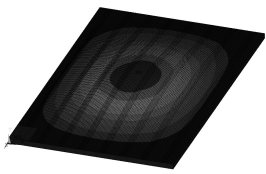
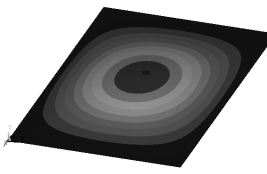
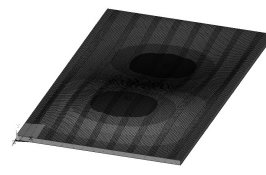
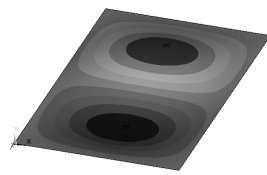
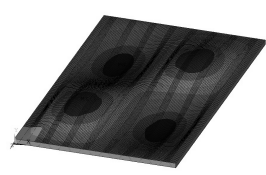
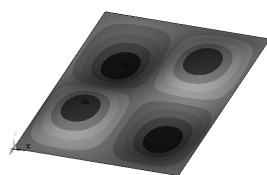
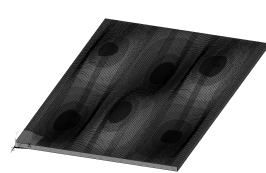
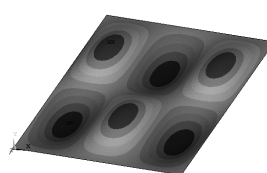
(a)



(b)
100

Figure 6.5: (a) 3D Finite element model, (b) Equivalent 2D finite element model

Table 6.2: Comparison of free vibration modes predicted by 3D and 2D equivalent finite element models

Mode	3D FE model	Equivalent 2D FE model
(1,1)		
(1,2)		
(2,2)		
(3,2)		

6.4 The effect of Filling Foam on Free Vibration Behavior of Truss Core Sandwich Panel

Influence of filling foam in empty spaces of CCCC (C-refers clamped boundary condition) truss core sandwich panel on free vibration response characteristics is presented in this section. Polyurethane foam with Young's modulus $E = 17 \times 10^5$ Pa, Poisson's ratio $\gamma = 0.4$ and density $\rho = 30 \text{ kg/m}^3$ (Harne *et al.*, 2012) is filled in the empty space

of the panel. Square panel with a side of 1.5 m having ten identical units is considered. To estimate the elastic properties for rectangular or cellular and triangular core, it is considered that f/p varies from $0 \leq f/p \leq 0.5$ for truss cores. In that, the ratio $f/p = 0$ relates to a triangular truss core, and $f/p = 0.5$ corresponds to a cellular truss core. In order to maintain the equal weight for all cases, same cross sectional area is considered and the dimensions of the sandwich panels with out foam are calculated accordingly and given in Table 6.3. Further, mass of panel with out foam filling is obtained. Now, in order to keep same mass for sandwich panel filled with foam, thickness of face sheet associated with the foam filled sandwich panel is modified as 1.4 mm, 1.2 mm and 1 mm for cellular, trapezoidal and triangular core sandwich panel respectively. Influence of filling foam on free vibration behavior is shown in Table 6.4. From Table

Table 6.3: Dimension of cellular core, trapezoidal core and triangular core in mm

Type of core	parameter			
	p	d	f	$t = t_c$
Cellular core	75	32.4	37.5	1.53
Trapezoidal core	75	32.4	22	1.42
Triangular core	75	32.4	0	1.19

6.4, it is clear that triangular core sandwich panel has high natural frequencies due to its high transverse shear stiffness compared to cellular core and trapezoidal core sandwich panel. Also from Table 6.4, it is clear that effect of filling foam increases natural frequencies in all types of core due to contribution of PUF in transverse shear stiffness.

Table 6.4: Influence of foam filling on free vibration behavior of truss core sandwich panel

S. No	Natural frequency (Hz)					
	Cellular core		Trapezoidal core		Triangular core	
	With-out foam	With foam	With-out foam	With foam	Without foam	With foam
1	130.34	131.34	126.20	127.61	157.35	161.46
2	144.04	147.24	144.49	148.49	294.15	300.22
3	166.89	173.60	171.54	179.70	296.60	306.15
4	194.03	204.72	202.81	215.52	408.64	419.75
5	222.79	237.79	235.58	253.12	480.87	483.96
6	251.54	271.25	268.55	291.20	486.03	509.10
7	279.71	304.47	301.27	310.39	574.39	583.47
8	307.05	329.97	308.75	323.28	577.88	600.80
9	329.56	337.17	319.32	329.26	693.45	692.89
10	333.55	339.69	333.64	348.86	708.18	740.74

6.5 The effect of Filling Foam on Vibro-Acoustic Response and Transmission Loss Characteristics

Influence of filling foam in empty spaces of truss core sandwich panel on dynamic and acoustic response characteristics is presented in this section. In order to investigate the forced vibration response of sandwich panel, it is excited with a force of 1 N at chosen point. The excitation location chosen in the present analysis is (1.05 m, 1.05 m) from the lower left corner of the plate. The excitation point has been chosen based on a condition that it should not be a vibration nodal point for any modes in the chosen excitation frequency range. The excitation frequency range is chosen as 0-630 Hz based on the coincidence frequency of the panel analysed. Based on the convergence study the panel is meshed with 40×40 elements for all the cases analysed. It is also ensured that the chosen mesh size satisfies the six elements per wave length requirement for the numerical vibro-acoustics analysis. Harne *et al.* (2012) considered a damping ratio of 0.145 for polyurethane foam for their structural acoustic studies on sandwich structures. In the present work, a damping ratio of 0.01 is assumed for truss core sandwich panel made up of Aluminium and a damping ratio of 0.155 is considered for foam filled

aluminium truss core sandwich panel. It is assumed that the foam, core and face sheet of the panel are held together rigidly and there is no relative motion between them. So the effective damping ratio of 0.155, which is sum of damping ratio of Aluminium and PUF, is considered for the response studies on PUF filled sandwich panel.

Figure 6.6 and Figure 6.7 shows the forced vibration response of truss core sandwich panel with and with out foam respectively. From Figure 6.6, it is clear that resonant amplitude of all type of sandwich panel are in same level irrespective of nature of core. Similarly from Figure 6.7, one can observe that resonant amplitudes are reduced significantly due to the enhanced damping provided by PUF filling.

The effect of core topology of truss core sandwich panel is shown in Figure 6.8. From Figure 6.8, it is clear that triangular core has reduced number of radiation modes in the interested frequency range due to its high shear stiffness of the triangular core sandwich panel. Also from Figure 6.8, it is clear that triangular core sandwich panel has lower sound power level compared to other two cases till its first resonance frequency.

Influence of foam filling on sound power radiated associated with cellular core, trapezoidal core and triangular core sandwich panels are shown in Figure 6.9, 6.10 and 6.11 respectively. From Figure 6.9, 6.10 and 6.11, it is very clear that sound power level is reduced significantly in all resonance amplitudes for foam filled sandwich panel. This is attributed to the high damping property of poly urethane foam.

The effect of foam filling on sound power radiated in all the frequency bands is significant as seen in Figure 6.12, which shows influence of foam filling on sound levels in octave bands. The effect of foam filling on over all sound power level is given in Table 6.5. From Table 6.5, it is very clear that foam filling reduces the over all sound power level significantly around 12 dB in each case. Sound pressure radiated at 100 Hz and 600 Hz are analysed to investigate the effect of foam filling on sound radiation directivity pattern. The results given in Figure 6.13 indicates that foam filling reduces the amplitude of sound pressure radiation significantly.

The effect of core topology on sound transmission loss characteristics of truss core sandwich panel is shown in Figure 6.14. From Figure 6.14, it is seen that in triangular core sandwich panel, there are not many sudden dips in the excitation frequency range whereas for cellular core and trapezoidal core many dips in transmission loss curve occur. It is attributed to the shear stiffness properties of the core geometry. The effect of foam filling is shown in Figure 6.15, 6.16 and 6.17 for cellular, trapezoidal and triangular core respectively. From the Figures 6.15, 6.16 and 6.17 one can say, the effect of filling foam is significant by avoiding the sudden dips at resonance frequencies also there is nearly 20 decibel is reduced at resonance.

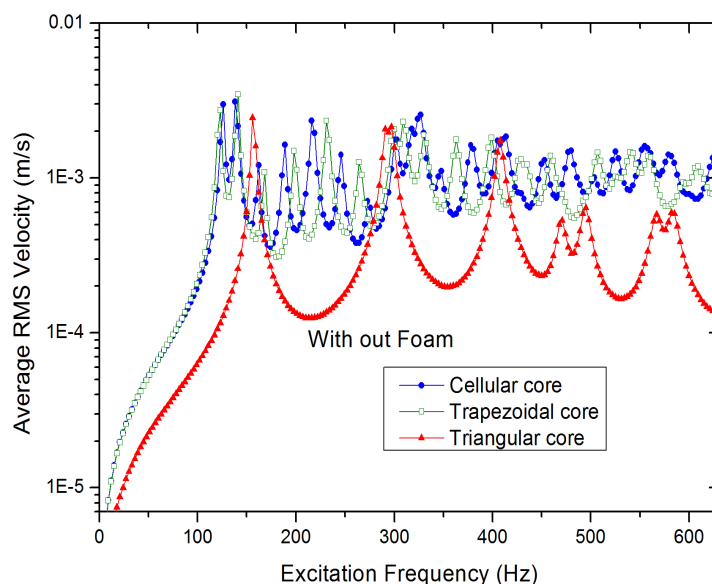


Figure 6.6: The effect of core topology of truss core sandwich panel with out foam on average rms velocity

Table 6.5: The effect of filling foam on over all sound power level

Influence	Sound Power Level (dB)		
	Cellular core	Trapezoidal core	Triangular core
Without Foam	106.65	105.52	106.43
With Foam	94.65	93.67	93.99
Reduction in SPL	12	11.85	12.44

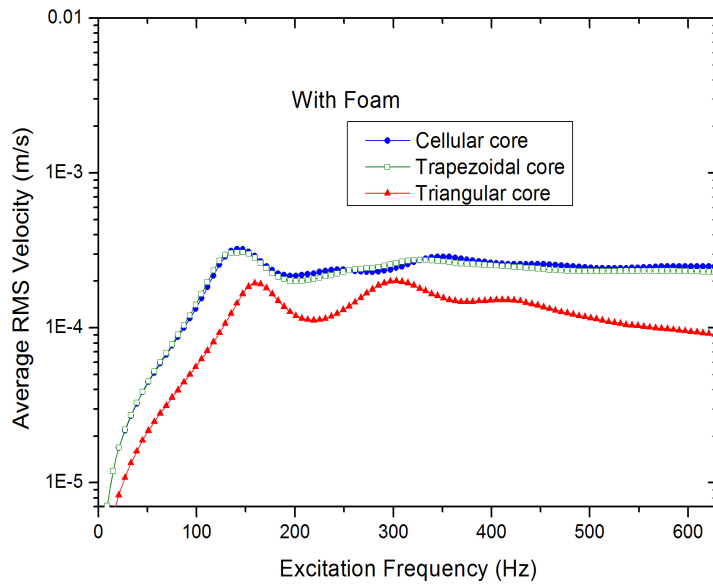


Figure 6.7: The effect of core topology of truss core sandwich panel filled with foam on average rms velocity

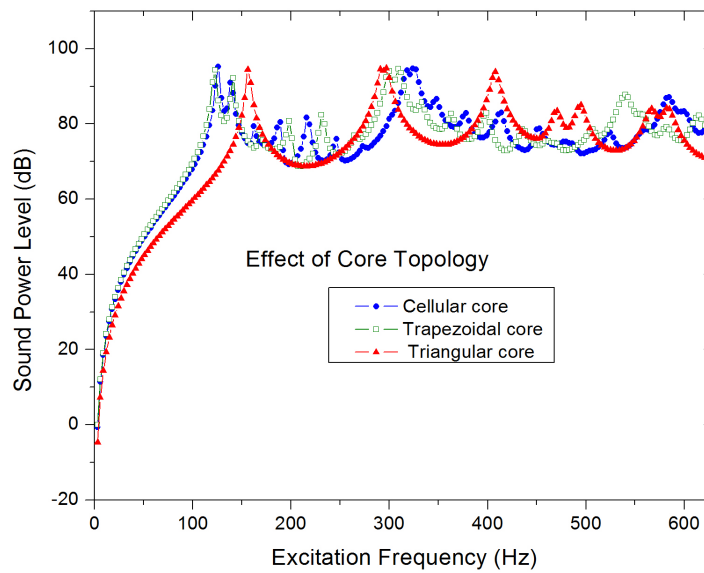


Figure 6.8: The effect of core topology on sound power radiated

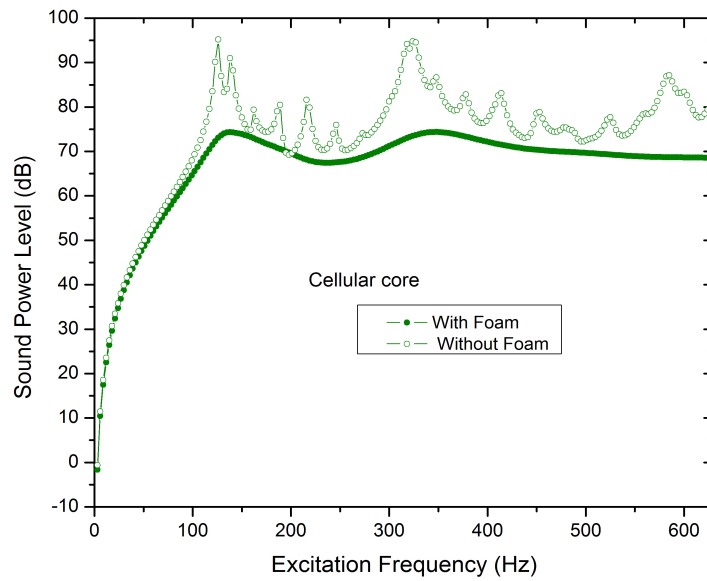


Figure 6.9: The effect of foam filling on sound power radiated of cellular core sandwich panel

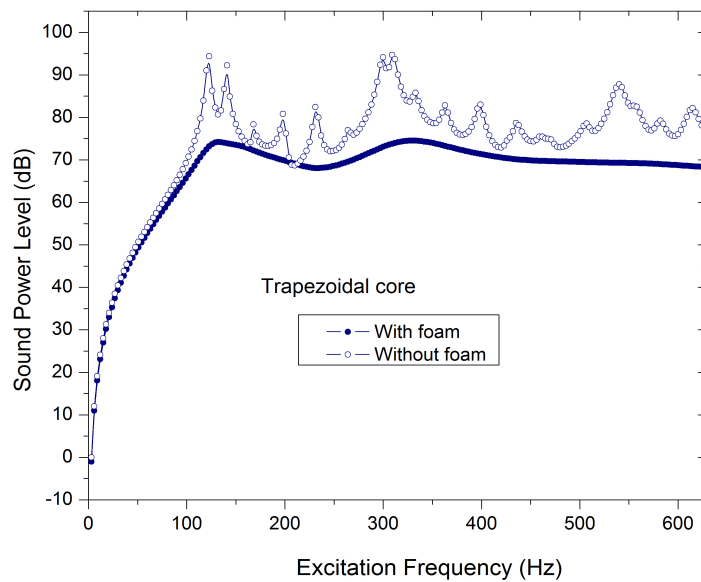


Figure 6.10: The effect of foam filling on sound power radiated of trapezoidal core sandwich panel

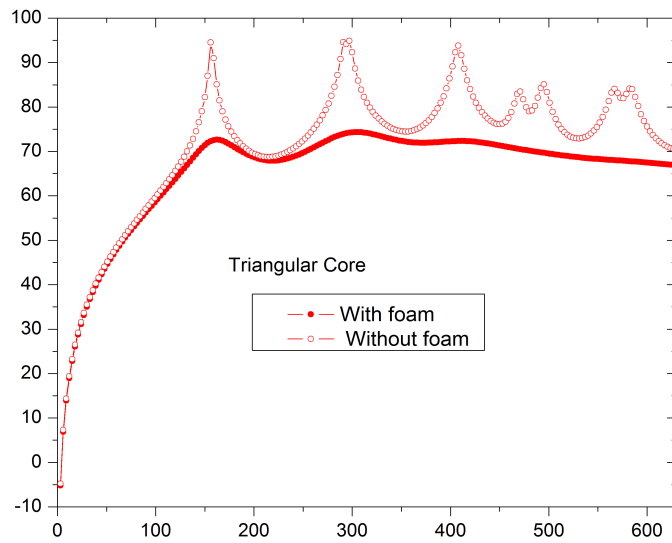


Figure 6.11: The effect of foam filling on sound power radiated of triangular core sandwich panel

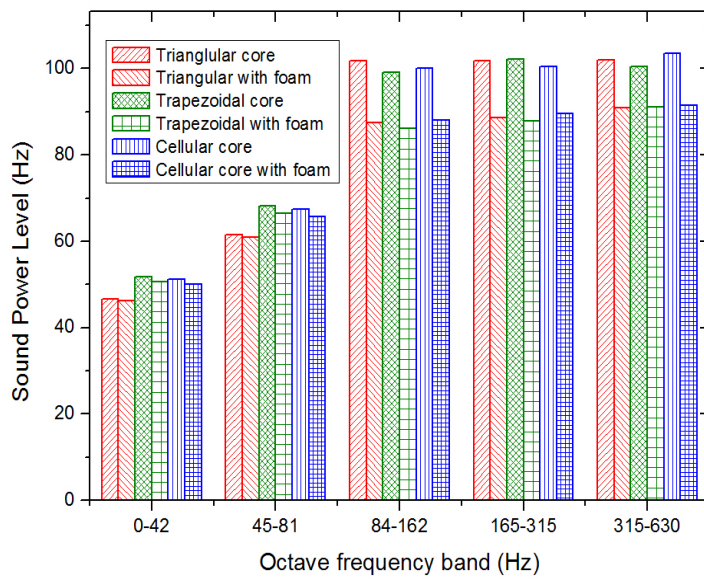
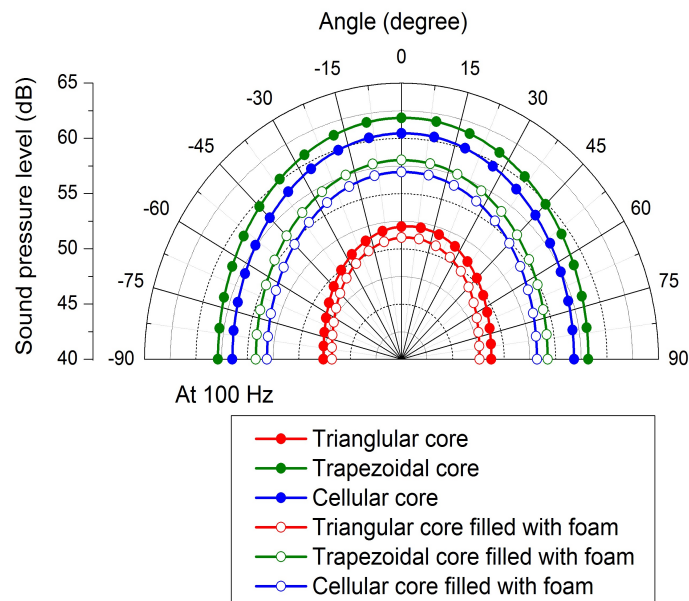
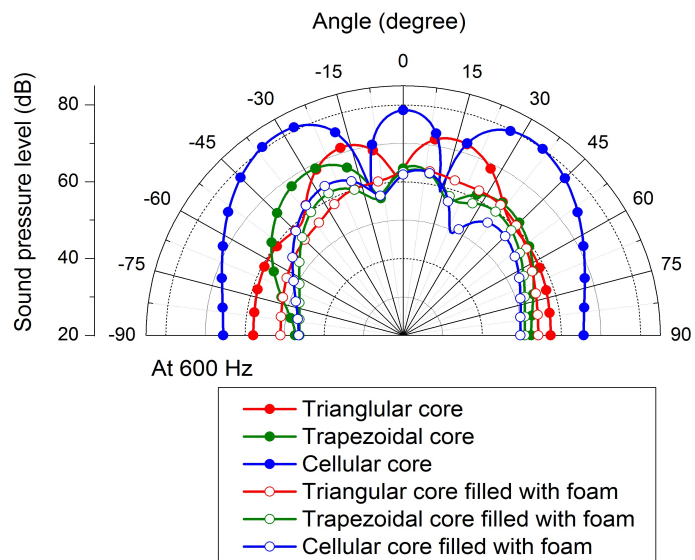


Figure 6.12: The effect of foam filling on sound power radiated in octave frequency bands



(a)



(b)

Figure 6.13: (a) Sound Pressure Level at 100 Hz, (b) Sound Pressure Level at 600 Hz

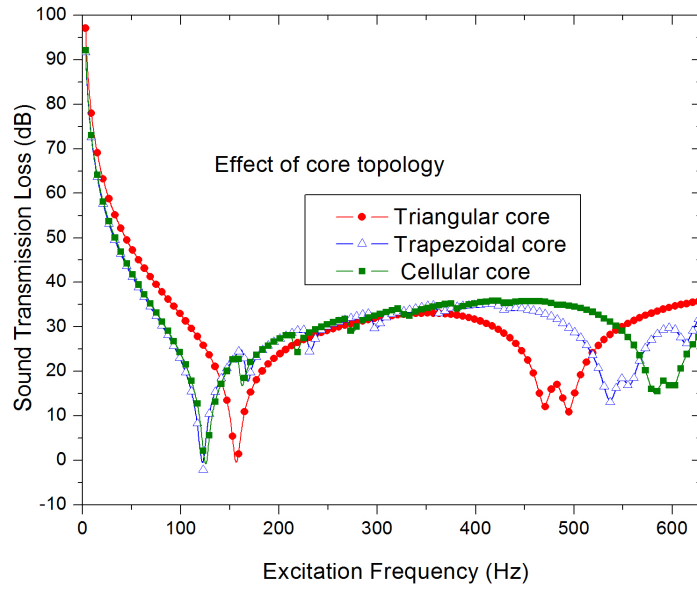


Figure 6.14: The effect of core topology on STL of truss core sandwich panel

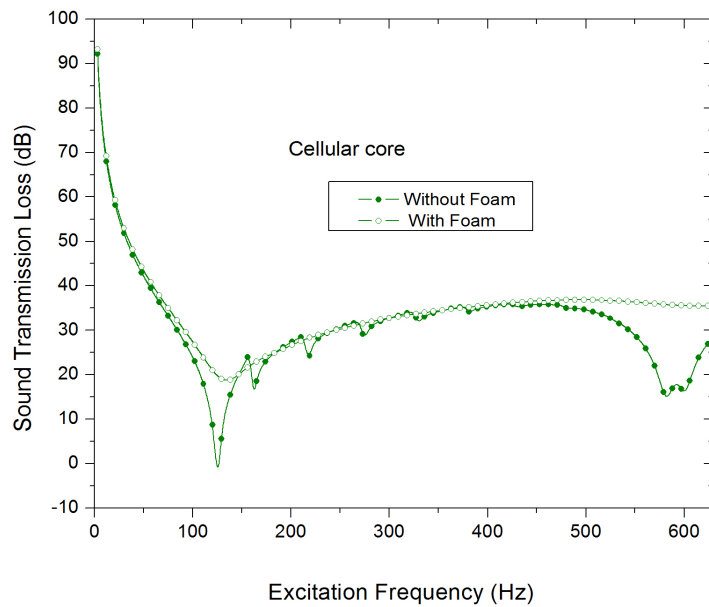


Figure 6.15: The effect of foam filling on STL of cellular core sandwich panel

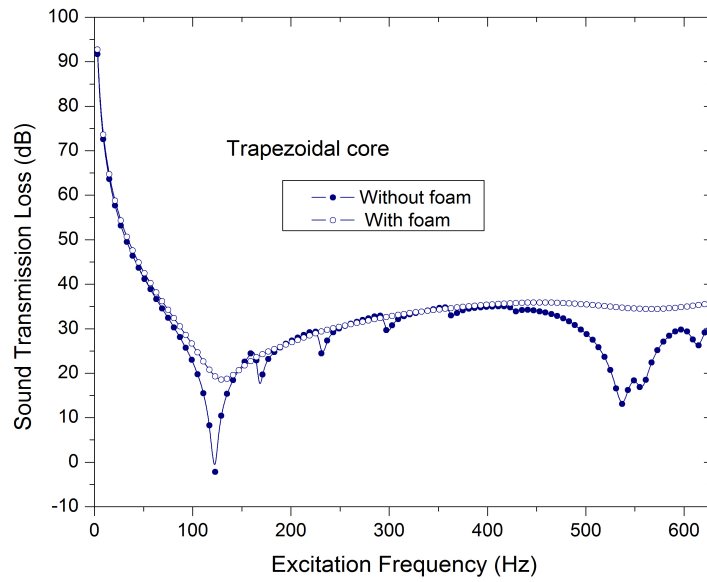


Figure 6.16: The effect of foam filling on STL of trapezoidal core sandwich panel

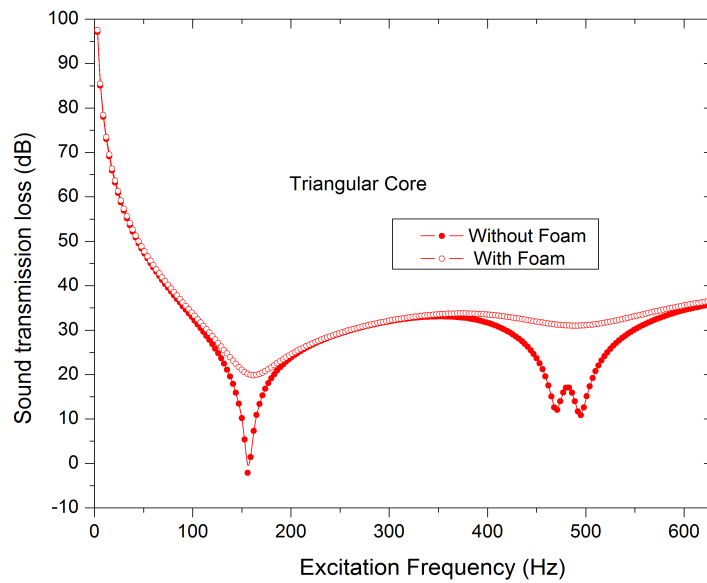


Figure 6.17: The effect of foam filling on STL of triangular core sandwich panel

6.6 Closure

In this chapter, the effect of polyurethane foam (PUF) filling in empty space of truss core sandwich panel on vibro-acoustic response and sound transmission loss characteristics is studied. Initially, the equivalent elastic properties of foam filled truss core sandwich panel is calculated. Further the free vibration response of truss core sandwich panel is compared with the foam filled truss core sandwich panel. It is observed that PUF filling slightly increases natural frequencies of truss core sandwich panel. Next in order, the foam filled sandwich panel is excited with point force and pressure to predict the vibro-acoustic response and sound transmission loss behavior respectively. It is observed that the effect of core topology on SPL is significant only in particular frequency zones. However, the effect of core topology on overall SPL is not significant. It is observed that, the resonant amplitude of vibration and consequent sound radiation responses is significantly reduced by the effect of PUF filling. Similarly, sudden dips in the sound transmission loss curve also reduced to a significant level due to the PUF filling. Octave band analysis carried out on sound power radiated also indicates that PUF filling reduces the sound power level significantly in all the frequency bands. It is very clear that, if truss core sandwich panel is filled with polyurethane foam, it would avoid high transmission noises at resonance i.e., around 20 dB of noise can be reduced in all core type of truss core sandwich panel.

CHAPTER 7

SUMMARY AND CONCLUSIONS

7.1 Summary

Detailed numerical investigation is carried out to analyse vibration, acoustic response and sound transmission loss characteristics of sandwich panels with different types of core is presented. Main objective of the present work is to reduce the noise level by controlling important geometric parameters of the panel without compromising on stiffness and mass requirement. The numerical approach followed in the present work is based on the 2D equivalent model which reduces processing time and computational effort associated with the actual geometrically complex sandwich panels. The forced vibration response due to time-varying mechanical harmonic excitation obtained using finite element method is given as an input to Rayleigh integral to obtain the acoustic response characteristics. The numerical approach is validated by comparing its results with results available in literature which are based on experimental and analytical approaches. However, a separate experimental investigation is carried out to validate the free and forced vibration response of a honeycomb core sandwich panel with the results based on 2D equivalent model.

7.2 Conclusions

7.2.1 The Effect of Geometrical Parameters of Honeycomb Core Sandwich Panel

From the studies carried out on the effect of core geometry on vibro-acoustic and sound transmission loss characteristics of honeycomb core sandwich panel, it is found that

- The effect of face sheet thickness on vibration and sound radiation characteristics are significant.
- In due consideration to space constraints, the desirable sound transmission loss can be achieved in lower core height honeycomb core sandwich panel.
- One can select cell size as the parameter to reduce the weight without affecting the sound and vibration characteristics.

7.2.2 The Effect of Inherent Material Damping of Honeycomb Core Sandwich Panel with Composite Facings

From the studies carried out on the effect of core geometry on vibro-acoustic and sound transmission loss characteristics of honeycomb core sandwich panel with FRP facings, it is found that

- Aluminium honeycomb core sandwich panel has lesser sound power level in high frequencies compared to Epoxy/Graphite FRP when effective stiffness alone is considered.
- Resonance amplitude of V_{rms} and SPL of Epoxy/Graphite FRP is higher compared to Aluminium honeycomb core sandwich panel without considering the damping effect of Epoxy/Graphite FRP honeycomb core sandwich panel.
- Sound transmission loss below the first resonance frequency for Epoxy/Graphite FRP is high compared to Aluminium honeycomb core sandwich panel.
- Resonance amplitude of V_{rms} and SPL of Epoxy/Graphite FRP is lower compared to Aluminium honeycomb core sandwich panel when the damping effect of Epoxy/Graphite FRP honeycomb core sandwich panel is considered.

- In the octave band analysis, the sound power level of Epoxy/Graphite FRP is less compared to aluminium honeycomb core sandwich panel in all the frequency range due to the material inherent damping.
- It is very clear that the aluminium honeycomb core sandwich panel can be replaced in to Epoxy/Graphite FRP [(0/90/c/90/0)] without losing the acoustic comfort. If these Epoxy/Graphite FRP [(0/90/c/90/0)] honeycomb core sandwich panels are used it would avoid high transmission noises at resonance and also nearly 40% of the weight can be reduced compared to aluminium honeycomb core sandwich panel.

7.2.3 The Effect of Core Topology of Truss Core Sandwich Panel

From the studies carried out on effect of core topology on vibro-acoustic response and sound transmission loss characteristics of truss core sandwich panel, it is found that

- The triangular core sandwich panel will be suitable among the different core topologies of truss core sandwich panel for better acoustic comfort due to the increased transverse shear stiffness and reduced radiation modes in the interested frequency zone.
- The effect of core topology on SPL is only significant in particular frequency zones. When overall SPL is considered, the effect of core topology is not significant.

7.2.4 The Effect of Filling Polyurethane Foam in Truss Core Sandwich Panel

From the studies carried out on effect of filling polyurethane foam on vibro-acoustic response and sound transmission loss characteristics of truss core sandwich panel, it is found that

- Resonance amplitude of SPL of foam filled sandwich panels are efficiently reduced.
- Sudden dips at resonance frequencies are significantly reduced.
- In the octave band analysis, the effect of foam filling is significant in all frequency zones.

- It is very clear that, if truss core sandwich panel is filled with polyurethane foam, it would avoid high transmission noises at resonance i.e., around 20 dB of noise can be reduced in all core type of truss core sandwich panel analysed.

The distinct results obtained in the present work using 2D FEM model can be used in the design of aerospace structures where acoustic comfort is required.

7.3 Scope for Future Research

The present work focuses on the flat surface sandwich panel in atmospheric conditions.

In future this work can be extended to carry out under thermal loads.

- The vibro-acoustic behaviour of honeycomb core filled with polyurethane foam under thermal loads.
- Vibro-acoustic behaviour of the sandwich panels under thermal loads to be analysed.
- Vibro-acoustic behaviour of Curved sandwich panel filled with foam should be analysed.

REFERENCES

- Assaf, S.** and **M. Guerich** (2008). Numerical prediction of noise transmission loss through viscoelastically damped sandwich plates. *Journal of Sandwich Structures & Materials*, **10**(5), 359–384.
- Aydincak, I.** (2007). *Investigation of Design and Analyses Principles of Honeycomb Structures*. Ph.D. thesis, Middle East Technical University.
- Bartolozzi, G., N. Baldanzini,** and **M. Pierini** (2014). Equivalent properties for corrugated cores of sandwich structures: A general analytical method. *Composite Structures*, **108**, 736–746.
- Bartolozzi, G., M. Pierini, U. Orrenius,** and **N. Baldanzini** (2013). An equivalent material formulation for sinusoidal corrugated cores of structural sandwich panels. *Composite Structures*, **100**, 173–185.
- Bilasse, M., L. Azrar,** and **E. Daya** (2011). Complex modes based numerical analysis of viscoelastic sandwich plates vibrations. *Computers & Structures*, **89**(7), 539–555.
- Bilasse, M.** and **D. Oguamanam** (2013). Forced harmonic response of sandwich plates with viscoelastic core using reduced-order model. *Composite Structures*, **105**, 311–318.
- Boorle, R. K.** (2014). *Bending, Vibration and Vibro-Acoustic Analysis of Composite Sandwich Plates with Corrugated Core*. Ph.D. thesis, University of Michigan-Dearborn.
- Boudjemai, A., R. Amri, A. Mankour, H. Salem, M. Bouanane,** and **D. Boutchicha** (2012). Modal analysis and testing of hexagonal honeycomb plates used for satellite structural design. *Materials & Design*, **35**, 266–275.
- Buannic, N., P. Cartraud,** and **T. Quesnel** (2003). Homogenization of corrugated core sandwich panels. *Composite Structures*, **59**(3), 299–312.
- Burlayenko, V.** and **T. Sadowski** (2010). Effective elastic properties of foam-filled honeycomb cores of sandwich panels. *Composite Structures*, **92**(12), 2890–2900.
- Carlsson, L. A., T. Nordstrand,** and **B. Westerlind** (2001). On the elastic stiffnesses of corrugated core sandwich. *Journal of Sandwich Structures and Materials*, **3**(4), 253–267.
- Chandra, N., S. Raja,** and **K. N. Gopal** (2014). Vibro-acoustic response and sound transmission loss analysis of functionally graded plates. *Journal of Sound and Vibration*, **333**(22), 5786–5802.

- Chen, D. and L. Yang** (2011). Analysis of equivalent elastic modulus of asymmetrical honeycomb. *Composite Structures*, **93**(2), 767–773.
- Cheng, Q., H. Lee, and C. Lu** (2006). A numerical analysis approach for evaluating elastic constants of sandwich structures with various cores. *Composite Structures*, **74**(2), 226–236.
- D’Alessandro, V., G. Petrone, F. Franco, and S. De Rosa** (2013). A review of the vibroacoustics of sandwich panels: Models and experiments. *Journal of Sandwich Structures and Materials*, **15**(5), 541–582.
- Daneshjou, K., A. Nouri, and R. Talebitooti** (2008). Analytical model of sound transmission through laminated composite cylindrical shells considering transverse shear deformation. *Applied mathematics and Mechanics*, **29**(9), 1165–1177.
- Daneshjou, K., H. Ramezani, and R. Talebitooti** (2011). Wave transmission through laminated composite double-walled cylindrical shell lined with porous materials. *Applied Mathematics and Mechanics*, **32**(6), 701–718.
- Daneshjou, K., R. Talebitooti, and M. Kornokar** (2017). Vibroacoustic study on a multilayered functionally graded cylindrical shell with poroelastic core and bonded-unbonded configuration. *Journal of Sound and Vibration*.
- Daneshjou, K., R. Talebitooti, and A. Nouri** (2009). Acoustic transmission through cylindrical shells treated with fld mechanisms. *Journal of Mechanics*, **25**(03), 299–306.
- Daneshjou, K., R. Talebitooti, and A. Tarkashvand** (2016). Analysis of sound transmission loss through thick-walled cylindrical shell using three-dimensional elasticity theory. *International Journal of Mechanical Sciences*, **106**, 286–296.
- De Gaetano, G., F. Cosco, C. Maletta, C. Garre, S. Donders, and D. Mundo**, Innovative concept modelling of sandwich beam-like structures. *In Proceedings of the 11th International Conference on Vibration Problems*. 2013.
- Franco, F., K. A. Cunefare, and M. Ruzzene** (2007). Structural-acoustic optimization of sandwich panels. *Journal of Vibration and Acoustics*, **129**(3), 330–340.
- Fung, T.-C., K. Tan, and T. Lok** (1996). Shear stiffness dgy for c-core sandwich panels. *Journal of Structural Engineering*, **122**(8), 958–966.
- Fung, T.-C., K.-H. Tan, and T.-S. Lok** (1994). Elastic constants for z-core sandwich panels. *Journal of Structural Engineering*, **120**(10), 3046–3055.
- Ghugal, Y. M. and A. S. Sayyad** (2011). Free vibration of thick orthotropic plates using trigonometric shear deformation theory. *Latin American Journal of Solids and Structures*, **8**(3), 229–243.

- Griese, D., J. D. Summers, and L. Thompson** (2015). The effect of honeycomb core geometry on the sound transmission performance of sandwich panels. *Journal of Vibration and Acoustics*, **137**(2), 021011.
- Hao, L., L. Geng, M. Shangjun, and L. Wenbin**, Dynamic analysis of the spacecraft structure on orbit made up of honeycomb sandwich plates. *In Computer Science and Automation Engineering (CSAE), 2011 IEEE International Conference on*, volume 1. IEEE, 2011.
- Harne, R. L., C. Blanc, M. C. Remillieux, and R. A. Burdisso** (2012). Structural-acoustic aspects in the modeling of sandwich structures and computation of equivalent elasticity parameters. *Thin-Walled Structures*, **56**, 1–8.
- Ichchou, M., O. Bareille, and J. Berthaut** (2008). Identification of effective sandwich structural properties via an inverse wave approach. *Engineering Structures*, **30**(10), 2591–2604.
- Jeyaraj, P., C. Padmanabhan, and N. Ganesan** (2011). Vibro-acoustic behavior of a multilayered viscoelastic sandwich plate under a thermal environment. *Journal of Sandwich Structures and Materials*, 1099636211400129.
- Jiang, D., D. Zhang, Q. Fei, and S. Wu** (2014). An approach on identification of equivalent properties of honeycomb core using experimental modal data. *Finite Elements in Analysis and Design*, **90**, 84–92.
- Kanematsu, H. H., Y. Hirano, and H. Iyama** (1988). Bending and vibration of cfrp-faced rectangular sandwich plates. *Composite Structures*, **10**(2), 145–163.
- Kant, T. and K. Swaminathan** (2001). Analytical solutions for free vibration of laminated composite and sandwich plates based on a higher-order refined theory. *Composite Structures*, **53**(1), 73–85.
- Kirkup, S.** (1994). Computational solution of the acoustic field surrounding a baffled panel by the rayleigh integral method. *Applied mathematical modelling*, **18**(7), 403–407.
- Kulkarni, S. and S. Kapuria** (2008). Free vibration analysis of composite and sandwich plates using an improved discrete kirchhoff quadrilateral element based on third-order zigzag theory. *Computational Mechanics*, **42**(6), 803–824.
- Laura, P. and R. Duran** (1975). A note on forced vibrations of a clamped rectangular plate. *Journal of Sound and Vibration*, **42**(1), 129–135.
- Lee, C. and K. Kondo**, Noise transmission loss of sandwich plates with viscoelastic core. *In 40th Structures, Structural Dynamics, and Materials Conference and Exhibit*. 1999.

- Lee, L.** and **Y. Fan** (1996). Bending and vibration analysis of composite sandwich plates. *Computers & structures*, **60**(1), 103–112.
- Li, D., Y. Liu,** and **X. Zhang** (2013). A layerwise/solid-element method of the linear static and free vibration analysis for the composite sandwich plates. *Composites Part B: Engineering*, **52**, 187–198.
- Li, D., R. Wang, R. Qian, Y. Liu,** and **G. Qing** (2016). Static response and free vibration analysis of the composite sandwich structures with multi-layer cores. *International Journal of Mechanical Sciences*, **111**, 101–115.
- Li, S.** and **X. Li** (2008). The effects of distributed masses on acoustic radiation behavior of plates. *Applied Acoustics*, **69**(3), 272–279.
- Libove, C.** and **S. Batdorf** (1948). A general small-deflection theory for flat sandwich plates. Technical report, DTIC Document.
- Libove, C.** and **R. E. Hubka** (1951). Elastic constants for corrugated-core sandwich plates.
- Liew, K., L. Peng,** and **S. Kitipornchai** (2006). Buckling analysis of corrugated plates using a mesh-free galerkin method based on the first-order shear deformation theory. *Computational Mechanics*, **38**(1), 61–75.
- Liu, Q.** and **Y. Zhao** (2001). Prediction of natural frequencies of a sandwich panel using thick plate theory. *Journal of sandwich structures and materials*, **3**(4), 289–309.
- Liu, Q.** and **Y. Zhao** (2007). Effect of soft honeycomb core on flexural vibration of sandwich panel using low order and high order shear deformation models. *Journal of Sandwich Structures & Materials*, **9**(1), 95–108.
- Lok, T.** and **Q. Cheng** (2000a). Free vibration of clamped orthotropic sandwich panel. *Journal of Sound and Vibration*, **229**(2), 311–327.
- Lok, T.-S.** and **Q.-H. Cheng** (2000b). Elastic stiffness properties and behavior of truss-core sandwich panel. *Journal of Structural Engineering*, **126**(5), 552–559.
- Lok, T.-S.** and **Q.-H. Cheng** (2001). Free and forced vibration of simply supported, orthotropic sandwich panel. *Computers & Structures*, **79**(3), 301–312.
- Malek, S.** and **L. Gibson** (2015). Effective elastic properties of periodic hexagonal honeycombs. *Mechanics of Materials*, **91**, 226–240.
- Mellert, V., I. Baumann, N. Freese,** and **R. Weber** (2008). Impact of sound and vibration on health, travel comfort and performance of flight attendants and pilots. *Aerospace Science and Technology*, **12**(1), 18–25.
- Molla, M. A., R. Talebitooti,** and **M. Shojaeefard** (). Sea and analytical model of sound transmission loss through sandwiches shells lined with poroelastic materials.

- Mukhopadhyay, T. and S. Adhikari** (2016a). Effective in-plane elastic properties of auxetic honeycombs with spatial irregularity. *Mechanics of Materials*, **95**, 204–222.
- Mukhopadhyay, T. and S. Adhikari** (2016b). Equivalent in-plane elastic properties of irregular honeycombs: An analytical approach. *International Journal of Solids and Structures*, **91**, 169–184.
- Natarajan, S., M. Haboussi, and G. Manickam** (2014). Application of higher-order structural theory to bending and free vibration analysis of sandwich plates with cnt reinforced composite facesheets. *Composite Structures*, **113**, 197–207.
- Nayak, A., S. Moy, and R. Sheno** (2002). Free vibration analysis of composite sandwich plates based on reddy's higher-order theory. *Composites Part B: Engineering*, **33**(7), 505–519.
- Ng, C. and C. Hui** (2008). Low frequency sound insulation using stiffness control with honeycomb panels. *Applied Acoustics*, **69**(4), 293–301.
- Noor, A. K., S. L. Venneri, D. B. Paul, and M. A. Hopkins** (2000). Structures technology for future aerospace systems. *Computers & Structures*, **74**(5), 507–519.
- Nordstrand, T., L. A. Carlsson, and H. G. Allen** (1994). Transverse shear stiffness of structural core sandwich. *Composite structures*, **27**(3), 317–329.
- Oh, I. K.** (2008). Damping characteristics of cylindrical laminates with viscoelastic layer considering temperature-and frequency-dependence. *Journal of Thermal Stresses*, **32**(1-2), 1–20.
- Paik, J. K., A. K. Thayamballi, and G. S. Kim** (1999). The strength characteristics of aluminum honeycomb sandwich panels. *Thin-walled structures*, **35**(3), 205–231.
- Petrone, G., V. D Alessandro, F. Franco, and S. De Rosa** (2014a). Numerical and experimental investigations on the acoustic power radiated by aluminium foam sandwich panels. *Composite Structures*, **118**, 170–177.
- Petrone, G., V. DAlessandro, F. Franco, B. Mace, and S. De Rosa** (2014b). Modal characterisation of recyclable foam sandwich panels. *Composite Structures*, **113**, 362–368.
- Petrone, G., S. Rao, S. De Rosa, B. Mace, F. Franco, and D. Bhattacharyya** (2013). Initial experimental investigations on natural fibre reinforced honeycomb core panels. *Composites Part B: Engineering*, **55**, 400–406.
- Qiu, C., Z. Guan, S. Jiang, and Z. Li** (2017). A method of determining effective elastic properties of honeycomb cores based on equal strain energy. *Chinese Journal of Aeronautics*.

- Qiu, K., Z. Wang, and W. Zhang** (2016). The effective elastic properties of flexible hexagonal honeycomb cores with consideration for geometric nonlinearity. *Aerospace Science and Technology*, **58**, 258–266.
- Ruzzene, M.** (2004). Vibration and sound radiation of sandwich beams with honeycomb truss core. *Journal of Sound and Vibration*, **277**(4), 741–763.
- Samanta, A. and M. Mukhopadhyay** (1999). Finite element static and dynamic analyses of folded plates. *Engineering Structures*, **21**(3), 277–287.
- Sargianis, J. and J. Suhr** (2012a). Core material effect on wave number and vibrational damping characteristics in carbon fiber sandwich composites. *Composites Science and Technology*, **72**(13), 1493–1499.
- Sargianis, J. and J. Suhr** (2012b). Effect of core thickness on wave number and damping properties in sandwich composites. *Composites Science and Technology*, **72**(6), 724–730.
- Shi, G. and P. Tong** (1995). Equivalent transverse shear stiffness of honeycomb cores. *International Journal of Solids and Structures*, **32**(10), 1383–1393.
- Shojaeefard, M. H., R. Talebitooti, R. Ahmadi, and M. R. Gheibi** (2014a). Sound transmission across orthotropic cylindrical shells using third-order shear deformation theory. *Latin American Journal of Solids and Structures*, **11**(11), 2039–2072.
- Shojaeefard, M. H., R. Talebitooti, R. Ahmadi, and B. Ranjbar** (2014b). A study on acoustic behavior of poroelastic media bonded between laminated composite panels. *Latin American Journal of Solids and Structures*, **11**(13), 2379–2407.
- Sorohan, Ş., M. Sandu, A. Sandu, and D. M. Constantinescu** (2016). Finite element models used to determine the equivalent in-plane properties of honeycombs. *Materials Today: Proceedings*, **3**(4), 1161–1166.
- Sudhagar, P. E., A. A. Babu, V. Rajamohan, and P. Jeyaraj** (2015). Structural optimization of rotating tapered laminated thick composite plates with ply drop-offs. *International Journal of Mechanics and Materials in Design*, 1–40.
- Sui, N., X. Yan, T.-Y. Huang, J. Xu, F.-G. Yuan, and Y. Jing** (2015). A lightweight yet sound-proof honeycomb acoustic metamaterial. *Applied Physics Letters*, **106**(17), 171905.
- Talebitooti, R., R. Ahmadi, and M. Shojaeefard** (2015). Three-dimensional wave propagation on orthotropic cylindrical shells with arbitrary thickness considering state space method. *Composite Structures*, **132**, 239–254.
- Talebitooti, R., K. Daneshjou, and M. Kornokar** (2016a). Three dimensional sound transmission through poroelastic cylindrical shells in the presence of subsonic flow. *Journal of Sound and Vibration*, **363**, 380–406.

- Talebitooti, R., M. Zarastvand, and M. Gheibi** (2016b). Acoustic transmission through laminated composite cylindrical shell employing third order shear deformation theory in the presence of subsonic flow. *Composite Structures*, **157**, 95–110.
- Tang, W., H. Zheng, and C. Ng** (1998). Low frequency sound transmission through close-fitting finite sandwich panels. *Applied Acoustics*, **55**(1), 13–30.
- Thamburaj, P. and J. Sun** (1999). Effect of material anisotropy on the sound and vibration transmission loss of sandwich aircraft structures. *Journal of Sandwich Structures and Materials*, **1**(1), 76–92.
- Van Tooren, M. and L. Krakkers**, Multi-disciplinary design of aircraft fuselage structures. In *45th AIAA Aerospace Sciences Meeting and Exhibit*. 2007.
- Wang, T., S. Li, and S. R. Nutt** (2009). Optimal design of acoustical sandwich panels with a genetic algorithm. *Applied Acoustics*, **70**(3), 416–425.
- Wang, T., S. Li, S. Rajaram, and S. R. Nutt** (2010). Predicting the sound transmission loss of sandwich panels by statistical energy analysis approach. *Journal of Vibration and Acoustics*, **132**(1), 011004.
- Wang, T., V. Sokolinsky, S. Rajaram, and S. R. Nutt** (2008). Consistent higher-order free vibration analysis of composite sandwich plates. *Composite Structures*, **82**(4), 609–621.
- Wen-chao, H. and N. Chung-fai** (1998). Sound insulation improvement using honeycomb sandwich panels. *Applied Acoustics*, **53**(1), 163–177.
- Wennberg, D., P. Wennhage, and S. Stichel** (2011). Orthotropic models of corrugated sheets in finite element analysis. *ISRN Mechanical Engineering*, **2011**.
- Wennhage, P.** (2003). Weight optimization of large scale sandwich structures with acoustic and mechanical constraints. *Journal of Sandwich Structures and Materials*, **5**(3), 253–266.
- Xia, Y., M. Friswell, and E. S. Flores** (2012). Equivalent models of corrugated panels. *International Journal of Solids and Structures*, **49**(13), 1453–1462.
- Ye, Z., V. L. Berdichevsky, and W. Yu** (2014). An equivalent classical plate model of corrugated structures. *International journal of solids and structures*, **51**(11), 2073–2083.
- Zhang, Q. and M. Sainsbury** (2000). The galerkin element method applied to the vibration of rectangular damped sandwich plates. *Computers & Structures*, **74**(6), 717–730.
- Zhou, R. and M. J. Crocker** (2010). Sound transmission loss of foam-filled honeycomb sandwich panels using statistical energy analysis and theoretical and measured dynamic properties. *Journal of Sound and Vibration*, **329**(6), 673–686.

CURRICULUM VITAE

1. Name: **M P Arunkumar**
2. Date of Birth: 04/07/1985
3. Permanent Address: No. 10, E. B Colony,
Amoor Road, Walajpet
Vellore district
Tamilnadu
Pincode-632513
4. Educational Qualification:
 - 2007 **Bachelor of Engineering**

Institution:	Crescent Engineering College, Chennai, Tamilnadu, India
Specialization:	Mechanical Engineering
 - 2011 **Master of Engineering**

Institution:	Anna University, Coimbatore, Tamil Nadu, India
Specialization:	Manufacturing Engineering
 - 2017 **Doctor of Philosophy**

Institution:	National Institute of Technology Karnataka Surathkal, Karnataka, India
Registration Date:	06/01/2014
Thesis Submission Date:	13/07/2017
Viva-Voice Date:	2/05/2018

List of Publications based on PhD Research Work

Sl. No	Title of the Paper	Authors (In the same order as in the paper, underline the Research Scholars name)	Name of the Journal / Conference / Symposium, Vol., No., Pages	Month & Year of Publication	Category *
1	Effect of core topology on vibro-acoustic characteristics of truss core sandwich panel	M P Arunkumar, Jeyaraj Pitchaimani, K V Gangadharan and M C Leninbabu	Procedia Engineering, Vol.144, Page 1397-1402. DOI: 10.1016/j.proeng.2016.05.170	May, 2016	3
2	Sound transmission loss characteristics of sandwich aircraft panels: Influence of nature of core	M P Arunkumar, Jeyaraj Pitchaimani, K V Gangadharan and M C Leninbabu	Journal of Sandwich Structures and Materials, Vol.19, No 1, Page 26-48. (Impact Factor: 2.933)	June, 2016	1
3	Influence of nature of core on vibro acoustic behavior of sandwich aerospace structures	M P Arunkumar, Jeyaraj Pitchaimani, K V Gangadharan and M C Leninbabu	Aerospace Science and Technology, Vol.56, No 3, Page 155-167. (Impact Factor: 2.151)	July, 2016	1
4	Sound radiation and transmission loss characteristics of a honeycomb sandwich panel with composite facings: Effect of inherent material damping	M P Arunkumar, M Jagadeesh, Jeyaraj Pitchaimani, K V Gangadharan and M C Leninbabu	Journal of Sound and Vibration, Vol.383, Page 221-232. (Impact Factor: 2.955)	August 2016,	1
5	Bending and Free Vibration Analysis of Foam Filled Truss Core Sandwich Panel	M P Arunkumar, Jeyaraj Pitchaimani, K V Gangadharan and M C Leninbabu	Journal of Sandwich Structures and Materials, DOI: 10.1177/1099636216670612, 1-22. (Impact Factor: 2.933)	December 2016,	1
6	Vibro-acoustic response and sound transmission loss characteristics of truss core sandwich panel filled with foam	M P Arunkumar, Jeyaraj Pitchaimani, K V Gangadharan and M C Leninbabu	Aerospace Science and Technology, Vol.78, Page 1-11. (Impact Factor: 2.151)	March 2018	1
7	An Approach to Predict Acoustic Response Characteristics of Honeycomb Core Sandwich Structure Using Equivalent 2D Mode	M P Arunkumar, Jeyaraj Pitchaimani, K V Gangadharan and M C Leninbabu	Journal of Sound and Vibration, (Impact Factor: 2.955)	Under Review	2

* Category: 1 : Journal paper, full paper reviewed
 2 : Journal paper, Abstract reviewed
 3 : Conference/Symposium paper, full paper reviewed
 4 : Conference/Symposium paper, abstract reviewed
 5 : others (including papers in Workshops, NITK Research Bulletins, Short notes etc.)
 (If the paper has been accepted for publication but yet to be published, the supporting documents must be attached.)

Research Scholar

Research Guides

Name & Signature, with Date

Name & Signature, with Date